ORNL-6696

ORNL--6696

DE92 008406

# Advanced Neutron Source (ANS) Project Progress Report FY 1991

**Principal Authors**

D. L. Selby R. M. Harrington
*Oak Ridge National Laboratory*

P. B. Thompson
*Engineering Division*
*Martin Marietta Energy Systems, Inc.*

**Editor**
J. H. Campbell
*Oak Ridge National Laboratory*

**Electronic Publishers**
L. W. Davis
S. C. Lyttle
*Oak Ridge National Laboratory*

Date Published—January 1992

Prepared by the
Oak Ridge National Laboratory
Oak Ridge, Tennessee 37831
managed by
Martin Marietta Energy Systems, Inc.
for the
U.S. DEPARTMENT OF ENERGY
under Contract No. DE-AC05-84OR21400

## Contributing Authors


D. J. Alexander
R. G. Alsmiller
J. L. Anderson
R. E. Battle
N. C. J. Chen
G. L. Copeland
B. Damiano
D. K. Felde
M. L. Gildner
J. E. Hardy
W. R. Hendrich
R. A. Lillie
A. W. Longest
C. R. Luttrell
J. A. March-Leuba
L. N. McCold
B. H. Montgomery
D. G. Morris
J. A. Mullens
R. E. Pawel
W. E. Ruggles
W. K. Sartory
H. B. Shapira
M. Siman Tov
W. F. Swinson
R. P. Taleyarkhan
C. D. West
B. A. Worley
G. T. Yahr
G. L. Yoder, Jr.
*Oak Ridge National Laboratory*

R. M. Beckers
R. S. Booth
R. A. Brown
J. E. Cleaves
J. T. Cleveland
K. K. Chipley
T. J. McManamy
G. R. McNutt
F. J. Peretz
C. C. Queen
T. L. Ryan
K. D. St. Onge
*Engineering Division, Martin Marietta Energy Systems, Inc.*

R. C. Birtcher
G. L. Hofman
J. Rest
J. L. Snelgrove
H. R. Thresh
T. C. Wiencek
*Argonne National Laboratory*

C. D. Fletcher
S. N. Jahshan
J. M. Ryskamp
R. C. Thayer
C. A. Wemple
*Idaho National Engineering Laboratory*

M. Ibn-Khayat
*University of Tennessee*

R. R. Fullwood
*Brookhaven National Laboratory*

W. E. Meek
H. N. Goldstein
P. J. Shipper
P. T. Talarico
*Gilbert/Commonwealth, Inc.*

G. K. Carlough
*DRS*

# CONTENTS

# LIST OF FIGURES

# LIST OF TABLES

# ACRONYMS

| | |
|---|---|
| A/E | Architect/Engineer |
| AEC | Atomic Energy Commission |
| AHP | Analytical Hierarchy Process |
| ALARA | As Low As Reasonably Achievable |
| ANL | Argonne National Laboratory |
| ANS | Advanced Neutron Source |
| ANSR | Advanced Neutron Source Reactor |
| ASME | American Society of Mechanical Engineers |
| B&W | Babcock and Wilcox Company |
| BNL | Brookhaven National Laboratory |
| BOP | Balance of Plant |
| CDR | Conceptual Design Report |
| CERCA | Compagnie pour l'Etude et la Realisation de Combustibles Atomiques |
| CFD | Computational Fluid Dynamics |
| CHF | Critical Heat Flux |
| CPBT | Core Pressure Boundary Tube |
| CSAR | Conceptual Safety Analysis Report |
| CSAU | Code Scaling Applicability and Uncertainty |
| DAS | Data Acquisition System |
| DOE | Department of Energy |
| DRS | Hundley Kling Gmitter |
| EIS | Environmental Impact Statement |
| ER | Environmental Report |
| ES&H | Environmental, Safety, and Health |
| FCI | Fuel-Coolant-Interaction |
| FIM-AP | Field-Ion-Microscope Atom Probe |
| FMECAs | Failure-Modes Effects and Criticality Analyses |
| HEDL | Hanford Engineering and Development Laboratory |
| HFIR | High Flux Isotope Reactor |
| I&C | Instrumentation and Control |
| IB | Incipient Boiling |
| ILL | Institut Laue Langevin |
| INEL | Idaho National Engineering Laboratory |
| JAERI | Japan Atomic Energy Research Institute |
| LANL | Los Alamos National Laboratory |
| LOCA | Loss-of-Coolant Accident |
| MCCI | Molten-Core-Concrete-Interactions |
| NIST | National Institute of Standards and Technology |
| NPR-HWR | New Production Reactor–Heavy-Water Reactor |
| NRC | Nuclear Regulatory Commission |
| NSCANS | National Steering Committee for the Advanced Neutron Source |
| NSRR | Nuclear Safety Research Reactor |

| | |
|---|---|
| ORNL | Oak Ridge National Laboratory |
| ORR | Oak Ridge Reservation |
| PCDAS | Plant Control and Data Acquisition System |
| PDR | Plant Design Requirement |
| PGAA | Prompt-Gamma Activation Analysis |
| PIR | Phenomena Identification and Ranking |
| PRA | Probabilistic Risk Assessment |
| PRSS | Primary Reactor Shutdown System |
| QA | Quality Assurance |
| R&D | Research and Development |
| RSCS | Reactor Secondary Cooling System |
| SCADA | Supervision Control and Data Acquisition Systems |
| SDD | System Design Description |
| SRSS | Secondary Reactor Shutdown System |
| TEM | Transmission Electron Microscopy |
| THTL | Thermal-Hydraulic Test Loop |
| TVA | Tennessee Valley Authority |
| UCN | Ultra-Cold Neutron |
| VCN | Very-Cold Neutron |
| WBS | Work Breakdown Structure |

# FOREWORD

The Advanced Neutron Source (ANS), now in conceptual design at Oak Ridge National Laboratory (ORNL), is being designed as a user-oriented neutron research laboratory centered around the most intense, continuous beams of thermal and subthermal neutrons in the world—an order of magnitude more intense than beams available from the most advanced existing reactors. While no commitment to build has been made as yet by the Department of Energy, the department is supporting design studies of the ANS in recognition of the fact that the nation's current research reactors are approaching the end of their design lives.

Primarily a research facility, the ANS will accommodate more than 1000 academic, industrial, and government researchers each year. They will conduct basic research in all branches of science, as well as applied research, leading to a better understanding of new materials, including high temperature superconductors, plastics, and thin films. Some 48 neutron beam stations will be set up in the ANS beam rooms and the neutron guide hall for neutron scattering and for fundamental and nuclear physics research. There will also be extensive facilities for materials irradiation, isotope production, and analytical chemistry.

The ANS will permit faster simulation of long-term irradiation effects on the properties of engineering materials for fusion and fission reactors than is currently possible and will produce isotopes for cancer therapy, heart disease diagnosis, osteoporosis treatment, aircraft radiography, and research. ANS production capacity for transuranics—isotopes heavier than uranium—will be at least as great as that at the High Flux Isotope Reactor at ORNL, which is the Western world's only source of such elements and which the ANS is planned to replace. These isotopes are used for a wide variety of medical, analytical, research, and engineering purposes.

The ANS will be built around a new research reactor of approximately 330 MW fission power, producing an unprecedented peak thermal flux of $>8 \times 10^{19}$ $n \cdot m^{-2} \cdot s^{-1}$. An initial complement of state-of-the-art instruments and support facilities will be provided as part of the project. Interested groups will be invited to share in designing, building, and operating other instruments as participating research teams once detailed design gets under way.

This year, the project has welcomed the Architectural/Engineering firm of Gilbert/Commonwealth, Inc., of Reading, Pennsylvania, as part of the conceptual-design team. We are now in full gear to finish the conceptual-design report in mid-1992, which will position us to request a construction line-item in FY 1994.

Colin D. West
ANS Project Director

# 1 PROJECT MANAGEMENT

The Advanced Neutron Source (ANS) effort was greatly enhanced by the addition of an Architect/Engineer (A/E) to the conceptual design team. The company selected was Gilbert/Commonwealth, Inc., and they elected to collaborate with other organizations having relevant specialized knowledge and experience: Air Products, Atomic Energy of Canada Limited, DRS, and the University of Tennessee. This strong collaboration is responsible for the Balance of Plant (BOP), and they have already made substantial contributions to the overall design of the buildings-and-site layout (Fig. 1.1) as well as to the primary-cooling system.

There are some significant technical achievements during this period, which are described more fully later in this report. One that should be highlighted here is the multidisciplinary Reactor Systems Design Team effort, a sustained attack over a period of many months on issues relating to reactor-system safety and to core design. The effort resulted in a primary-cooling circuit concept that appears to be resistant in that the core integrity is preserved, to a failure of any single component, anywhere in the loop, including the aluminum core pressure boundary tube (CPBT). As a part of the same series of trade-off studies and evaluations, it became apparent that a small reduction in the operating power from 362 MW(f) to 330 MW(f) would permit a significant increase in the fuel-cycle length from 17 d to 21 d while still meeting the primary technical objective of a five- to ten-fold increase in useful flux over existing facilities. The project's National Steering Committee, NSCANS, endorsed this trade-off.

Another major step forward is the preparation of draft System Design Description (SDD) documents that define and establish the requirements, descriptions, operating modes, and set points for the systems, structures, and components comprising the ANS facility. The set of SDDs is derived from the project's work breakdown structure (WBS) to ensure that all systems are identified and documented.

The project was again replanned during this year, in response to the realities of the FY 1991 budget and the guidance received from the Department of Energy (DOE) on the schedule and future funding. The schedule still calls for a design-and-construction line item beginning in FY 1994, but the preliminary design-only line item now seems unlikely to materialize. This will put more design work off until 1994 and will delay the expected project completion date by up to one year. Figure 1.2 shows the present proposed budget and review schedule.

Under the umbrella of an existing agreement covering various areas of neutron scattering, a statement of intent to collaborate on design, analysis, and research and development (R&D) work for the ANS was made between the Japanese Atomic Energy Research Institute (JAERI) and Oak Ridge National Laboratory (ORNL). Japanese researchers had already joined in the work of the project, and results from experiments at JAERI

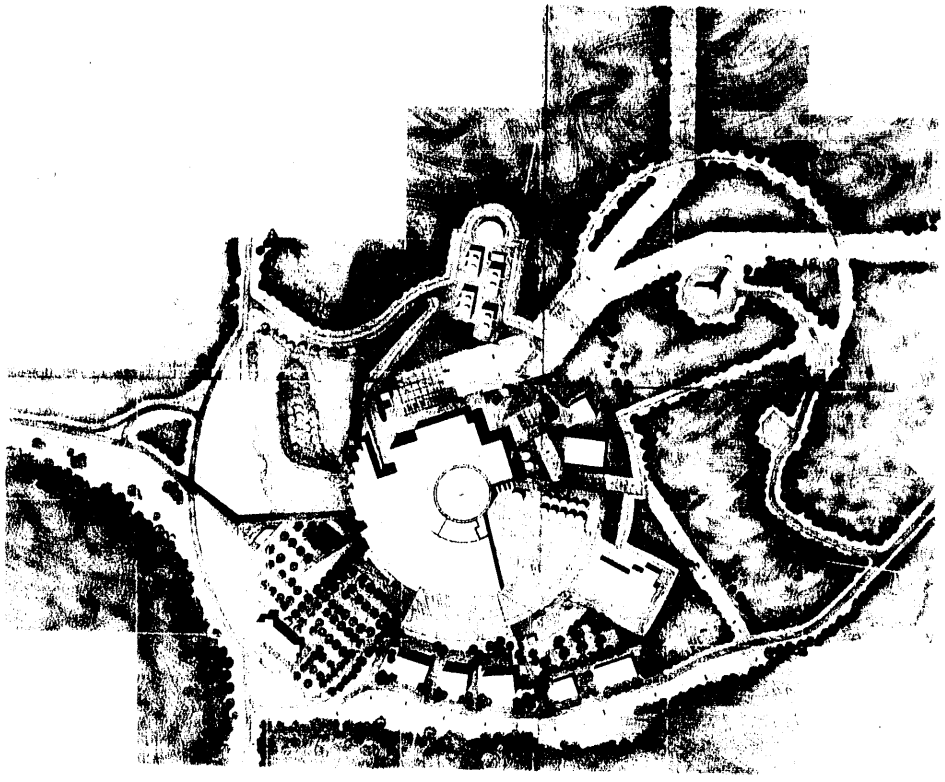

**Fig. 1.1. DRS proposed ANS site layout.**

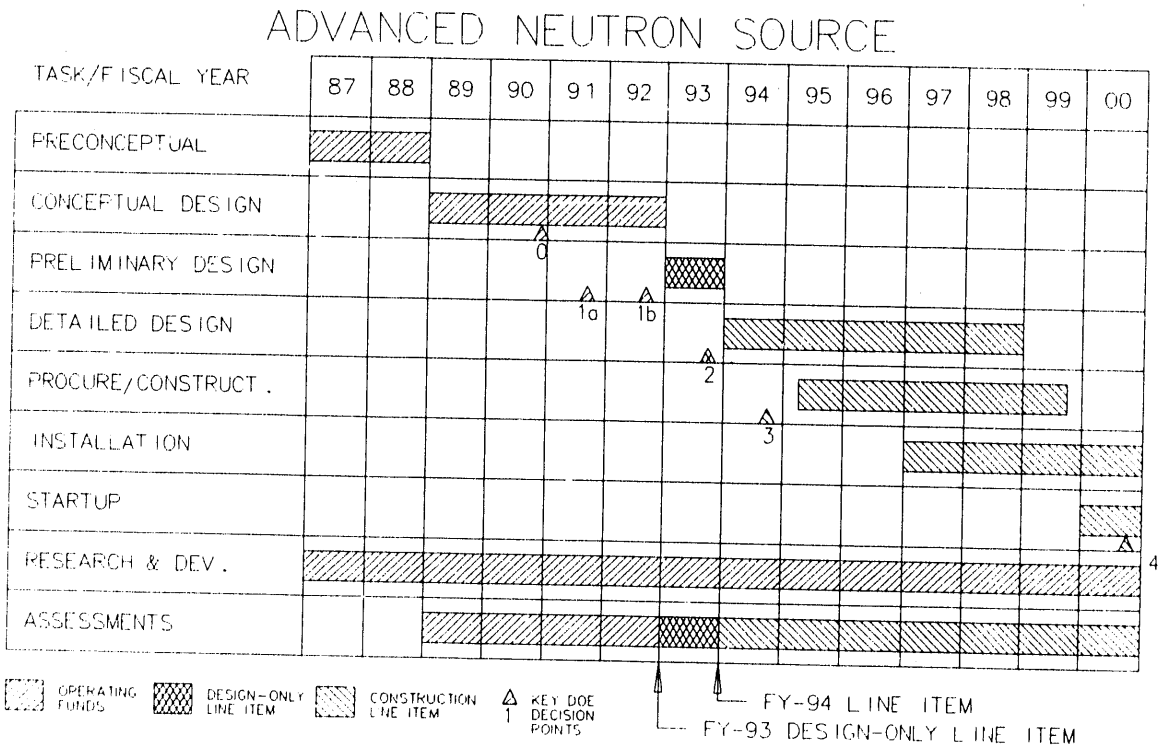


**Fig. 1.2. Project budget and review schedule.**

Oarai on fission-product release have been incorporated into our severe-accident-analysis work.

Moving most of the computer codes used for reactor physics and safety analysis from the large mainframe computers to workstations reduced the cost of the calculations performed this year by about $500K. The major codes involved include RELAP5, the Monte Carlo Code MCNP, Venture, and PDQ. Our experience has been that they typically run on the workstations at about 40% of the mainframe speed and that the cost of the workstation is recouped in less than two months. This has allowed us to do quite extensive trade-off and optimization studies within existing budgets.

## 1.1 ANS PROJECT QUALITY PROGRAM

### 1.1.1 Program Development

During the past year, the project's quality program has continued to evolve. The *ANS Project Quality Assurance Plan* was revised to expand our program of controls over research, technical development, and design software. The initial issue of the *ANS Project Procedures Manual* was made to participants.

A project self-assessment of applicable procedural coverage revealed that many activities were covered by procedures at the laboratory and at supporting division levels. However, some of these procedures were found to lack sufficient detail to control the activity appropriately. Therefore, a Project Procedure Development Plan was prepared. Several of the identified supplemental project procedures have been drafted and internally reviewed and are being validated through trial use prior to project-wide approval and issuance.

A methodology has been created to address the issue of a graded approach to quality requirements on a WBS task/subtask level of implementation. The methodology creates a matrix of the task/subtask constituent activities with associated quality program element and a listing of applicable implementing procedures.

A series of organizational changes within the ORNL Quality Department resulted in the ANS Project's quality manager reporting directly to the ORNL quality manager. This elevated reporting level has provided greater visibility, commensurate with the importance of the project's quality program. The project quality assurance staff was enhanced with the addition of another quality assurance (QA) specialist, bringing additional experience in quality programs focused on reactor design, construction, and operation.

### 1.1.2 Program Monitoring

The project quality assurance staff reviewed and approved the documented quality programs of the major project subcontractors. Review and approval of the remaining support contractors is planned prior to issuance of the project Conceptual Design Report (CDR).

An audit of cold-source-neutronics and reactor-physics analyses activities conducted by the ORNL Engineering Physics and Mathematics Division identified no technical deficiencies impacting analyses, and some procedural issues that were revealed are being corrected.

# RESEARCH AND DEVELOPMENT 2

Thirteen R&D tasks have been identified as essential to the ANS Project. These R&D tasks are required to address feasibility issues, to provide some of the data needed for the preparation of the CDR, to produce the data necessary to make a rational decision when alternative design concepts are identified, and to examine and demonstrate the applicability of technological advances. This chapter summarizes progress on these tasks for the reporting period and includes activities performed by Argonne National Laboratory (ANL), Babcock and Wilcox (B&W), Brookhaven National Laboratory (BNL), Idaho National Engineering Laboratory (INEL), Martin Marietta Engineering, the Massachusetts Institute of Technology, the National Institute of Standards and Technology (NIST), ORNL, Science Applications International Corporation, the University of Tennessee, and the University of Virginia.

## 2.1 REACTOR CORE DEVELOPMENT

The reactor core development task provides the neutronics and thermal-hydraulics support needed to support the conceptual core design.

### 2.1.1 Development of Analysis Techniques

This task includes the development of analysis techniques and involves software and the basic data necessary to perform numerical analyses of the reactor core performance. Three major activities—neutronics review, MCNP[1] model development, and treatment of uncertainties—are highlighted below.

#### 2.1.1.1 Neutronics Review

An external review was conducted of the neutronics methods used in the ANS Project and the analysis results. This review covered work performed at both INEL and ORNL. The four-member review committee had the following findings.

#### 2.1.1.2 MCNP Model Development

A very important task was to develop an approach for obtaining heat loads for the various components in the reactor core and the reflector region. It was determined that data from ENDF-VI were necessary to appropriately account for the fission-product energy deposition. The results of this work, which was performed at INEL, is discussed in Sect. 2.11.1 of this report.

#### 2.1.1.3 Treatment of Uncertainties

ANS reactor (ANSR) uncertainty analysis is being conducted to determine the maximum operating power limits of the reactor, while simultaneously accounting for uncertainties and providing safety margins compatible with an acceptable quantified confidence level. The Monte Carlo technique, combined with more effective

sampling techniques (such as Latin Hypercube), was chosen as the best approach to achieve this objective. The ANS steady-state thermal-hydraulic code was modified and integrated with a sampling code to provide a maximum power level probability distribution that allows selection of a power level consistent with a given confidence level.

Of the many parameters involved, eleven have been identified through an initial sensitivity study as significant, and uncertainty distributions were developed for each. A data base of applicable experimental data was compiled and evaluated against selected candidate thermal-hydraulic correlations. In addition, thermophysical property correlations for heavy water and light water were developed and their errors quantified.

### 2.1.2 Support to Design

The main changes in core parameters this year are the selection of a slightly lower power level [330 MW(f) vs 362 MW(f)] and an increase in the core life from 14 to 17 d. The physical dimensions of the core are unchanged from the conceptual design described in last year's progress report and less than 1 kg of extra fuel is needed. Calculations showed that the reduced power level could be compensated to some extent by lowering the coolant pressure and, therefore, the CPBT thickness. Also, the peak flux is not reduced very much by the relatively small fuel addition involved in raising the core life to 17 d. The core can still meet the minimum goal of five times the Institut Laue Langevin (ILL) peak thermal flux (Fig. 2.1). When account is taken of the larger beam tubes on ANS, the useful flux gain for many experiments is a factor of ten or more (Fig. 2.2). On this basis, NSCANS endorsed the design changes, accepting a slightly lower flux in return for the longer core life.

Analysis of beam-tube and cold-source worth was also performed. It was determined that approximately 1 to 2 kg of fuel would likely need to be added to the core to compensate for the

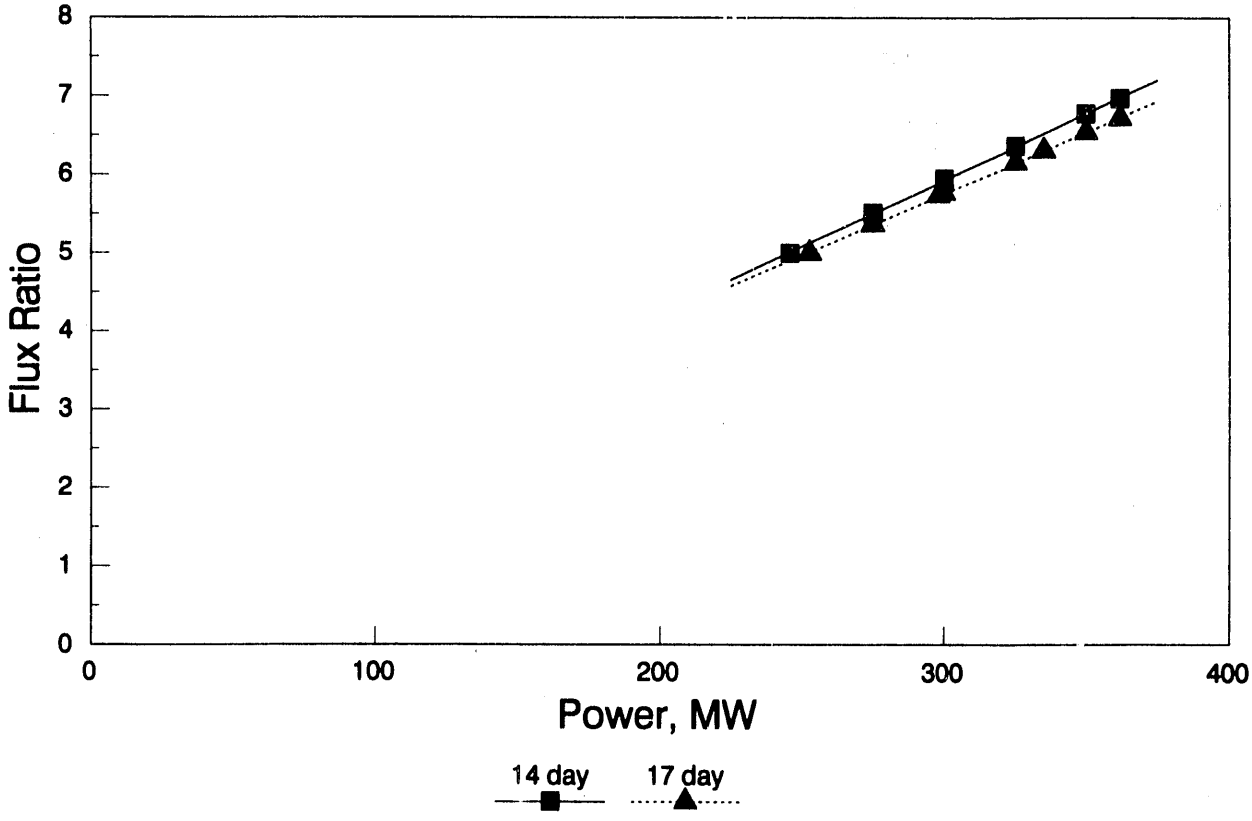


**Fig. 2.1. Power vs ANS/ILL thermal neutron flux ratio.**

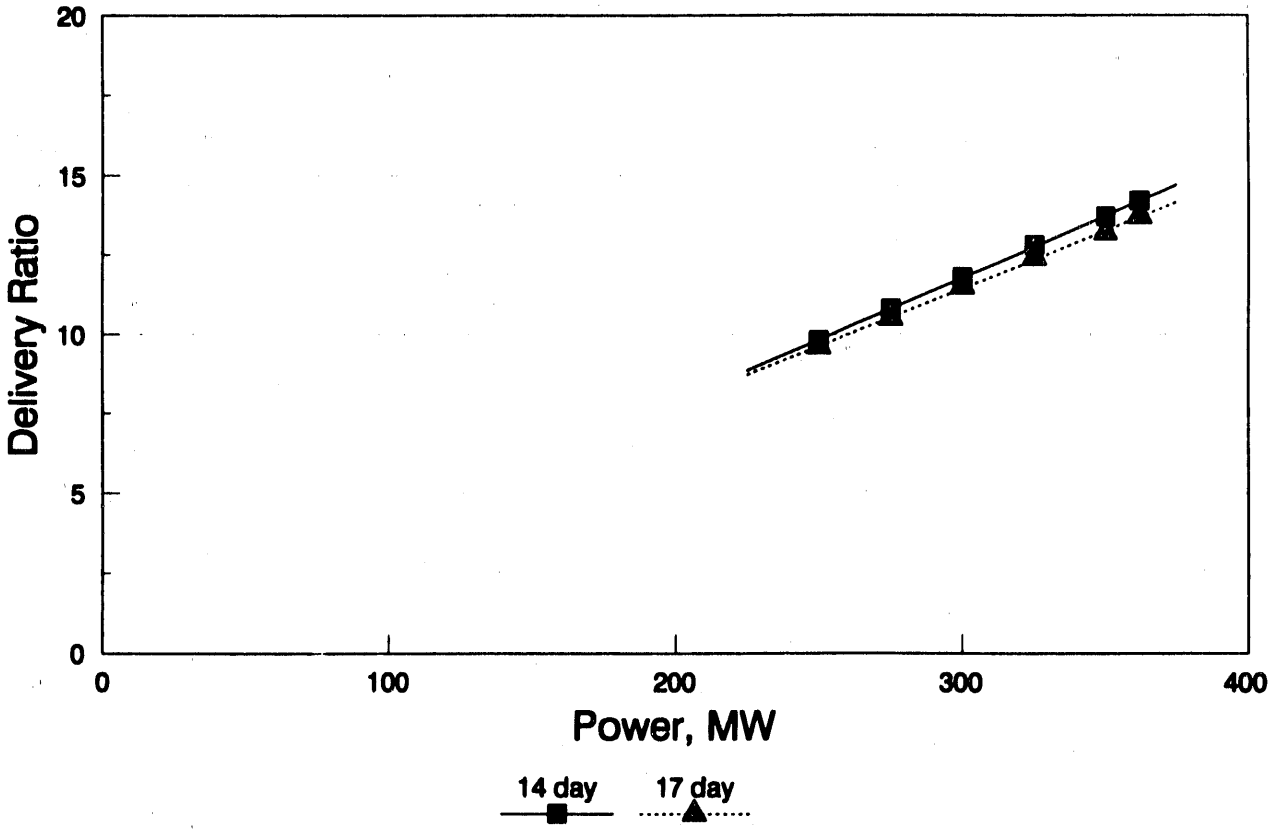


**Fig. 2.2. Power vs ANS/ILL neutron delivery ratio (peak thermal neutron flux × area of each beam tube).**

negative reactivity effects of these components and to maintain a 17-d core life.

## 2.2 FUEL DEVELOPMENT

The reference fuel for the ANS continues to be the $U_3Si_2$/Al mixture. Most of the work performed during this reporting period to support the fuel development was associated with irradiation of fuel capsules, fuel performance modeling, and fuel fabrication. These activities are discussed in Sects. 2.2.1, 2.2.2, and 2.2.3.

### 2.2.1 Irradiation of Fuel Capsules

Several problems were encountered in the fuel irradiation task during the report period. The first ANS target capsule completed irradiation testing in the High Flux Isotope Reactor (HFIR) facility on September 7, 1990. However, the capsule remained in the HFIR pool until mid-February as the hot cell was shut down while work to bring it into environmental safety and health compliance was underway. Once the capsule was delivered to the hot cell, additional problems were encountered that delayed evaluation of the capsule specimens. Polishing problems were then encountered that prevented immediate evaluation of the fuel particles.

At the end of the reporting period, the polishing problems appeared to be resolved by changing polishing compounds. The fuel was apparently being overetched beyond recognition by the carrier in a new polishing compound. At the time of this report, metallographic examination of one sample was performed, indicating similar characteristics to previous irradiations, and metallographic preparation of additional samples was continuing.

Enough information was obtained from the evaluation of the first fuel capsule to approve the fabrication and plan for the second fuel capsule.

However, because of these [illegible] appears that the second capsule irradiation will be delayed about 6 to 9 months from the [illegible] schedule.

### 2.2.2 Fuel Performance Code Modeling

The DART[2] thermal conductivity model was improved during the report period to account for a better representation of the dependence of the thermal conductivity on both the unirradiated and the irradiation-induced porosity. The original model smeared the irradiation-induced porosity throughout the meat, which results in a stronger dependence than was physically reasonable. The new approach for determining the thermal conductivity agrees favorably with measured data as shown in Fig. 2.3.

Significant efforts were also applied to the development of the fuel swelling model during this report period. It had been determined that the swelling in irradiated $U_3Si_2$ was based on the formation of a new grain-boundary surface area at about the position of the observed knee in the swelling data curve. The increase in slope of the swelling curve subsequent to the knee was attributed to the enhanced rate of growth of grain-boundary bubbles as compared to those resident in the bulk material. However, this theory was found to be in conflict with data obtained this year from tests that indicated that $U_3Si_2$ goes amorphous during ion irradiation. In addition, neutron-scattering analysis of irradiated $U_3Si_2$ indicated three distinct scattering components: purely crystalline, defected crystalline, and amorphous. Given the uncertainties in our understanding of the phenomena, mechanisms were explored that could give rise to the knee in the swelling curve in

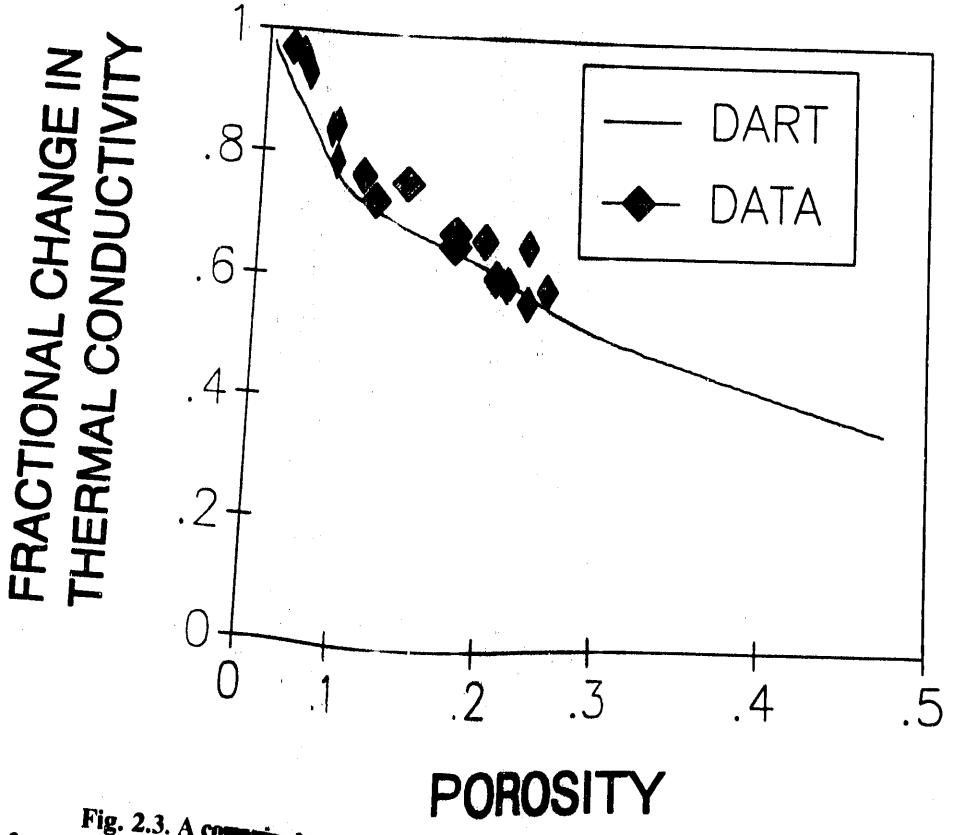


**Fig. 2.3. A comparison of the DART-calculated thermal conductivity for $U_3Si$ fuel as a function of irradiation-induced porosity compared to measured values in irradiated and subsequently annealed bulk $U_3Si$.**

amorphous as well as in crystalline material. At the end of the reporting period, this issue had not been resolved.

### 2.2.3 Fabrication Development

Development of fabrication techniques for the $U_3Si_2$ fuel plates continued at both ANL and B&W. Efforts during the early part of the year concentrated on studying the factors that control the fabrication of a uniformly loaded compact with $U_3Si_2$ fuel. Using tungsten aluminum powder to simulate the fuel, various techniques for loading the powder into the compact were examined. A process that used a spread-pouring technique without a funnel was developed after about 40 runs. This approach yielded acceptable compacts.

In an attempt to understand the effects of the particle size distribution and the cladding alloy on the quality of a $U_3Si_2$ fuel plate, B&W, NUKEM GmbH and CERCA archive full-size fuel plates were x-rayed and analyzed for fuel loading. Observations seem to support the conclusion that the initial fuel distribution in the fuel compact is the most important factor in determining the fuel distribution in the final fuel plate.

Initially fabricated $U_3Si_2$ fuel plates exhibited very poor fuel homogeneity, and there was some concern that some physical characteristic of the $U_3Si_2$ fuel might prohibit achieving fuel homogeneity approaching that obtained in the fabrication of $U_3O_8$ fuel plates. However, near the end of the reporting period, B&W rolled a set of HFIR-like fuel plates containing $U_3Si_2$ at the same volume fraction as the $U_3O_8$ in standard HFIR plates. B&W reported that these plates looked good but that more analysis would be necessary to reach definite conclusions. At the end of the reporting period, B&W was proceeding to make similar plates containing axial tapers.

## 2.3. CORROSION LOOP TESTS AND ANALYSES

The characterization of the many corrosion processes typical of 6061 Al fuel cladding in the core of the ANS has continued. The Corrosion Test Loop Facility, described in previous reports, [3-7] permits the exposure of aluminum alloy specimens to representative thermal-hydraulic conditions. In addition, the coolant path in the test loop is designed with main features similar to those in the reactor's primary-coolant system.

In the past year, we have conducted experiments designed primarily to extend our data base describing the film growth kinetics. These experiments have been useful in investigating the applicability of improved correlations for film growth. The preliminary correlation[8,9] described the film growth rates in terms of the local coolant temperatures and heat flux and was very sensitive to variations in the coolant velocity. As a result, it was somewhat restricted in its use and, furthermore, limited by the inability of the present Corrosion Test Loop geometry to provide the necessary range of these parameters. Effort is now directed to the development of a correlation in terms of specimen-coolant interface temperatures and heat flux. Such correlations seem much less sensitive to coolant velocity and thus permit variance of this parameter in order to enlarge the range of other system thermal-hydraulic parameters experimentally available in the present apparatus.

### 2.3.1 Summary of Results: FY 1991 Update

In our experiments, we continued to observe the sensitivity of the film growth rates on 6061 Al specimens to factors other than the specimen or film temperatures. We found earlier that the temperature of the coolant at the inlet to the test section, representative of the coolant water temperature in the 304-L stainless steel sections of the test loop, was an independent contributor to the film growth characteristics. This unexpected effect was associated with the extent of the Fe-rich layer on the outer surface of the product film that was hypothesized to act as a diffusion barrier.

The pH of the coolant water has also been observed to exert a significant effect on film growth over the range $4.5 \leq pH \leq 6$. CTEST No. 26 (see below), conducted at pH 4.5, exhibited much less film growth than would be anticipated

for the same thermal-hydraulic conditions at our standard pH of 5.0. This small increase in the coolant acidity also increased the intensity of the Fe-rich layer. Such experiments appear to confirm the importance of this layer on overall film growth: for conditions that favor its appearance, the primary aluminum corrosion product films (boehmite, $Al_2O_3 \cdot H_2O$) grow relatively slowly; furthermore, the overall growth kinetics are often altered, possibly because of the increased effectiveness of the diffusion barrier as it thickens during exposure.

The mechanism for the formation of this barrier layer remains speculative. However, based on observations of its features and behavior, we feel that it is a result of mass transport of metal-oxide species from the stainless steel components in the loop. If these species, predominantly Fe and Cr, exhibit a typical retrograde solubility at coolant pH levels of 5 and below, then a driving force will exist to provide transport from the cooler parts of the loop to the hotter aluminum specimen. Because of the local heat flux, the temperature at the specimen-coolant interface will be substantially higher than that of the bulk coolant. The experimental observations concerning the effect of coolant temperatures, coolant chemistry, coolant velocity, and heat flux are in qualitative agreement with this mechanism. The implication of these results is that this sort of mass transport is likely to occur in the reactor primary-coolant system and that layer growth on the fuel cladding will be similarly affected.

During FY 1991, we completed seven experiments on 6061 Al specimens in the ANS Corrosion Test Loop. Table 2.1 presents the test schedule for this report period, including a listing of the average values for the important experimental variables for the three reference positions on each specimen (these positions are located symmetrically about the specimen midpoint, 50.8 mm apart). The extent of the Fe-rich layer is indicated, as well as a comparison of the observed film thicknesses with those predicted by the Griess Correlation.[10,11] The occurrence of spallation at position 6 (near the coolant exit end) is also noted. Given the sensitivity of the reaction to the particular water chemistry, the +/o/- suffix on the base pH value gives a qualitative assessment of the effective pH for the experiment relative to its nominal value. A brief summary of these tests is as follows:

(1) CTEST No. 22 was designed in part to offer a limited test of our idealized film growth model. Specifically, this was a test to see if the properties of the film that determine its rate of growth at a given thickness are reasonably independent of the manner by which it reached that thickness. Thus, 22A, 22B, and 22C were run consecutively, changing the heat flux after 20 and 36 d. The rate constants for film growth calculated for the second interval, 22B, agreed well with those predicted by the preliminary correlation,[8] or by Correlation II (discussed later in this text). Segment 22C resulted in a very low film growth rate. In other words, the film growth model appeared to be obeyed, and film thicknesses calculated for changing thermal-hydraulic conditions would be expected to be valid.

(2) CTEST No. 23 achieved high interface temperatures at relatively low heat fluxes by reducing the coolant velocity. The rate constants observed in this experiment were consequently not within the range of parameters described accurately by the preliminary correlation, but rather by Correlation II, which was based on different variables.

(3) CTEST Nos. 24 and 25 were conducted under thermal-hydraulic conditions chosen to reinforce our correlation development and data base. Unfortunately, both of these experiments exhibited anomalous results—high film growth rates coupled with the absence of Fe-rich layers. These unexpected results are thought to have been because of faulty coolant water chemistry brought about either by undetected problems in the in-line pH and conductivity meters or by an inadvertent coolant pH excursion that had occurred prior to CTEST No. 24.

(4) CTEST No. 26 was our first test conducted with a pH 4.5 coolant in combination with a coolant inlet temperature of 49°C. Given the unexpected outcome of the previous two tests, these conditions were chosen on the basis of our mass transport model to favor the formation of the Fe-rich layer. Very slow film growth rates were observed for this experiment, and these were consistent with the reappearance of the Fe-rich

**Table 2.1. Corrosion test loop: completed tests and parameters**

| Test number | CT22A | CT22B | CT22C | CT23 | CT24 | CT25 | CT26[a] | CT27[a] | CT28[a] |
|---|---|---|---|---|---|---|---|---|---|
| Started | 6/12/90 | 7/2/90 | 7/20/90 | 10/5/90 | 1/8/91 | 2/12/91 | 5/1/91 | 6/7/91 | 7/17/91 |
| Completed | 7/2/90 | 7/20/90 | 7/31/90 | 10/26/90 | 1/24/91 | 2/19/91 | 5/20/91 | 6/28/91 | 7/23/91 |
| Total time (days) | 20 | 16 | 11 | 21 | 16 | 7 | 20 | 21 | 6 |
| pH | 5.0(+) | 5.0(o) | 5.0(o) | 5.0(o) | 5.0(o) | 5.0(o) | 4.5(o) | 5.0(o) | 5.0(o) |
| Conductivity (μS/m) | 250–400 | 450 | 450 | 400 | 300 | 300 | 1800 | 550 | 440 |
| Inlet temp (C) | 49 | 49 | 49 | 49 | 49 | 49 | 49 | 49 | 49 |
| Velocity (m/s) | 25.6 | 25.7 | 25.7 | 9.0 | 35.6 | 22.3 | 25.6 | 25.6 | 23.6 |
| Power (kW) | 22.2 | 44.6 | 22.2 | 20.5 | 52.6 | 43.2 | 44.5 | 45.0 | 52.5 |
| Heat flux | | | | | | | | | |
| Avg ($MW/m^2$) | 6.2 | 12.4 | 6.2 | 5.7 | 14.7 | 12.1 | 12.4 | 12.6 | 14.7 |
| Pos 2 | 6.2 | 12.3 | 6.2 | 5.6 | 14.0 | 11.7 | 12.3 | 12.1 | 14.0 |
| Pos 4 | 6.2 | 12.4 | 6.2 | 5.7 | 14.7 | 11.9 | 12.4 | 12.5 | 14.6 |
| Pos 6 | 6.2 | 12.6 | 6.2 | 5.9 | 15.3 | 12.6 | 12.5 | 13.2 | 15.4 |
| Coolant T (C) | | | | | | | | | |
| Pos 2 | 51 | 54 | 51 | 55 | 53 | 54 | 53 | 53 | 55 |
| Pos 4 | 56 | 62 | 56 | 66 | 60 | 63 | 62 | 62 | 66 |
| Pos 6 | 60 | 71 | 60 | 77 | 68 | 73 | 70 | 70 | 77 |
| Interface T (C) | | | | | | | | | |
| Pos 2 | 95 | 136 | 95 | 144 | 126 | 142 | 137 | 135 | 154 |
| Pos 4 | 99 | 142 | 99 | 152 | 134 | 149 | 143 | 142 | 164 |
| Pos 6 | 102 | 149 | 102 | 162 | 142 | 160 | 149 | 152 | 176 |
| Fe-rich layer? | | | Heavy | Heavy | None? | None? | Heavy | Medium | Light |
| Oxide product (>/< Griess) | Same | Less | Less? | Less | Same | More | Less | Less | Same |
| Spall at Pos 6? | | | No | No | Yes | Yes | No | No | Yes |

[a]Tear-sheet data.

barrier layer found upon disassembly of the specimen.

(5) CTEST Nos. 27 and 28 were tests to verify the loop's ability to reproduce conditions and results prior to CTEST No. 24, as well as to add to our data base. These experiments were generally successful, although some differences in the shape of the film growth rate curves and the calculated rate constants were observed.

### 2.3.2 Correlation Development

The main thrust of our investigation continues to be the growth behavior of boehmite ($Al_2O_3 \cdot H_2O$) films on 6061 Al surfaces exposed to conditions typical for fuel cladding in the ANS core. From these studies, we hope to develop a predictive capability by which the product film thickness at any point on the cladding surface can

be estimated if the thermal-hydraulic history of that point is known.

Our results have generally supported a semiempirical oxidation model that can be written as

$$dx/dt = k/x^n , \quad (1)$$

where

$dx/dt$ = rate of layer growth, μm/h ;
$k$ = rate constant, $\mu m^{1.351}/h$ ;
$x$ = layer thickness, μm ;
$n$ = constant, 0.351 .

If the rate constant can be expressed as a function of a given set of system parameters, this constitutes a correlation that can be used to determine film growth. In our preliminary correlation, five CTESTS involving coolant pH = 5, coolant inlet temperatures $T_{ci}$ = 39 to 49°C, and coolant velocity $V_c$ = 25.6 m/s were included such that

$$k = 6.992E5 \exp[-7592./(T_c+10\phi)] \ \mu m^{1.351}/h , \quad (2)$$

where

$T_c$ = local coolant temperature, K ;
$\phi$ = local heat flux, $MW/m^2$ .

An Arrhenius plot depicting this correlation is shown in Fig. 2.4. Since this correlation was first

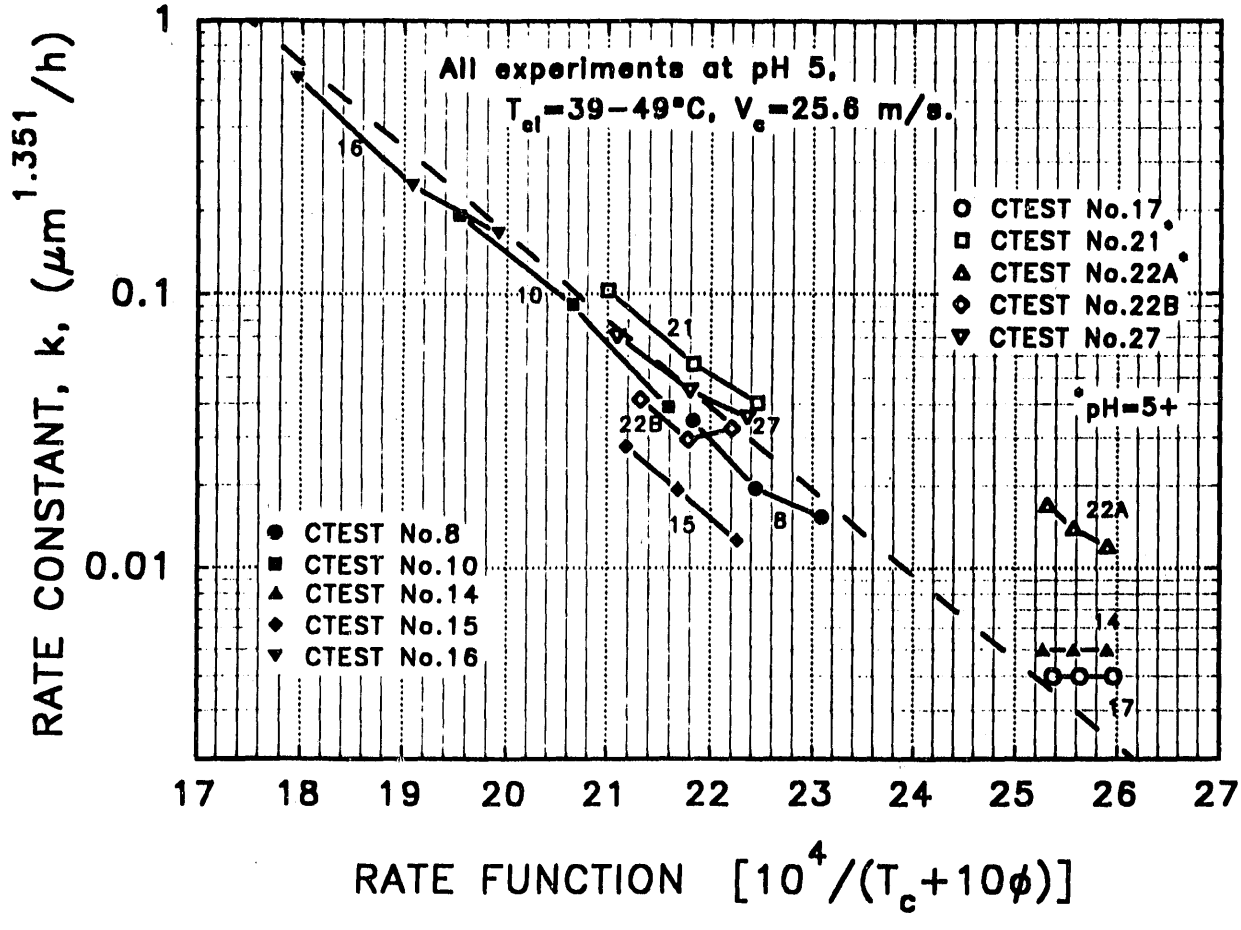


**Fig. 2.4. Corrosion test loop results showing grouping of rate constants according to Eq. (2), the preliminary correlation.**

presented, several more experiments that met the experimental criteria have been performed, and these are included in the figure as the open data points for CTESTS numbered higher than 16. The additional data tend to confirm the applicability of the correlation. It should be pointed out that in CTEST Nos. 21 and 22A, the average coolant pH was slightly above 5, possibly leading to the higher measured rates. The dashed line in the figure is Eq. (2) and yields conservative values for the film growth rate constants.

Rate correlations on the basis of interface temperature, $T_{x/c}$, and heat flux, ø, appear to be largely independent of coolant velocity, permitting the present test loop and test geometry to yield a wider range of correlation variables. The choice of these particular parameters is also intuitively more satisfactory. We have not yet attempted to optimize this form of correlation, but a recent working version, Correlation II, which stipulates only that the coolant pH = 5 and the coolant inlet temperature $T_{cl}$ = 39 to 49°C, is

$$k = 6.388E7 \exp[-9154./(T_{x/c} + 1.056ø)] \quad \mu m^{1.351}/h , \qquad (3)$$

where

$T_{x/c}$ = oxide-coolant interface temperature, K .

This correlation is presented, along with the applicable experimental data, in Fig. 2.5. Most outliers, with the possible exception of CTEST No. 28, can be explained qualitatively on the basis

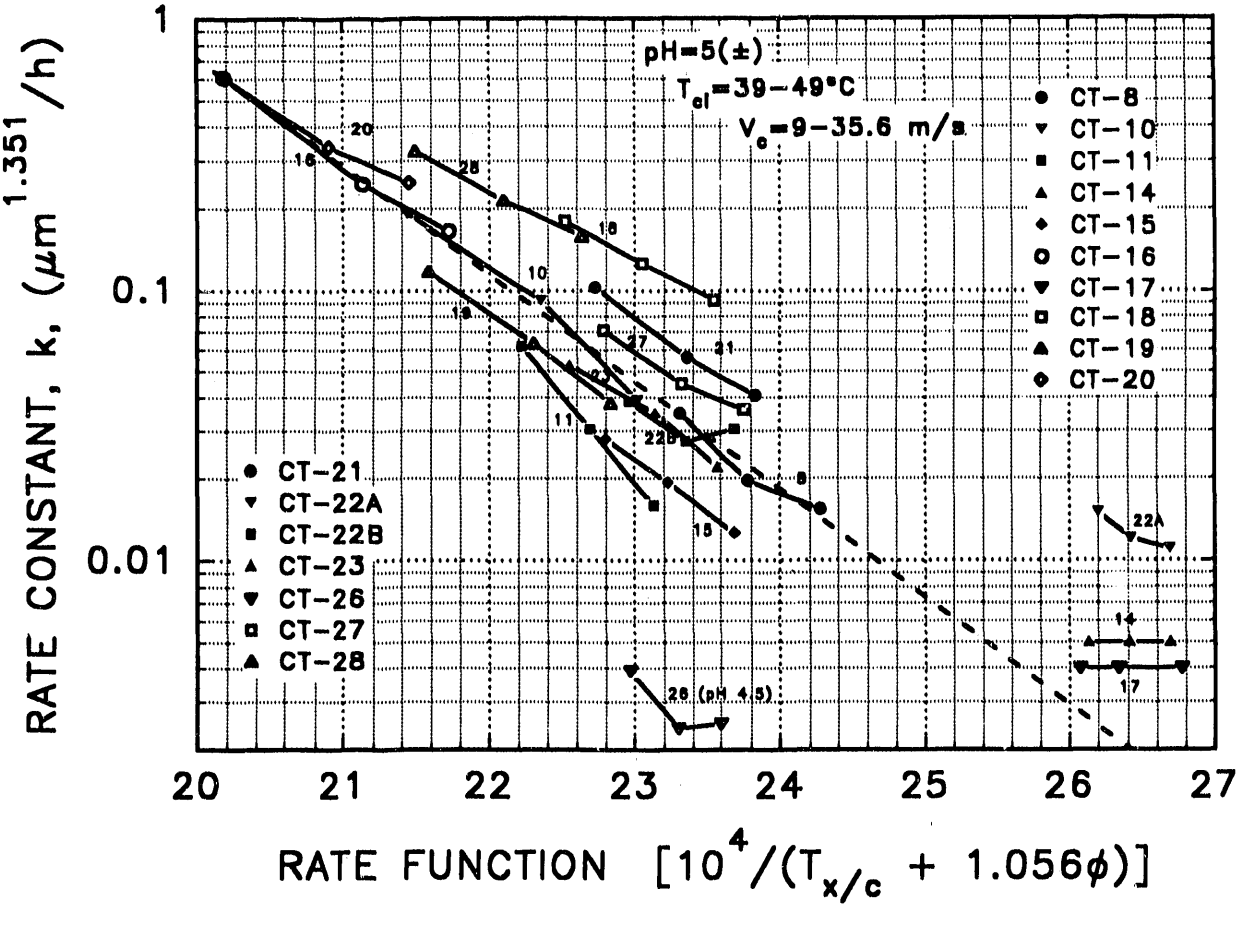


**Fig. 2.5. Corrosion test loop results showing grouping of rate constants according to Eq. (3), Correlation II.**

of observed pH variations during the experiment. Additionally, the rate constants from CTEST Nos. 26, 27, and 28 are all calculated from tear-sheet data; small corrections are generally required when the final data acquisition system (DAS) information is analyzed. The data from CTEST No. 26 are included in this plot only to show the large influence of a 0.5 unit change in the pH of the coolant.

### 2.3.3 Additional Testing

In support of the New Production Reactor-Heavy Water Reactor (NPR-HWR) Program, the ANS Corrosion Test Loop is being used to perform three long-term experiments on 8001 Al specimens under conditions pertinent to that reactor. These tests, started in late FY 1991, are scheduled for completion in the second quarter of FY 1992. Subsequently, additional tests with 8001 Al, and other aluminum alloys, are planned in order to evaluate their performance (relative to 6061 Al) for the ANS fuel cladding.

## 2.4 THERMAL-HYDRAULIC LOOP TESTS

The thermal-hydraulic performance of the ANS reactor will directly influence both normal and off-normal operational limits and behavior. Characterization of that behavior will require correlations and models that accurately predict the important thermal-hydraulic phenomena. This task will include the measurement and the analyses necessary to validate the correlations and models that, in turn, will be used to assess the capability for forced and natural convection under estimated hot channel conditions.

### 2.4.1 Test Loop

Several sets of experiments will be required to establish the thermal-hydraulic operating limits of the ANSR. Some of these tests will be performed in the ANS Thermal-Hydraulic Test Loop (THTL), which has recently been completed. The loop is designed to provide known thermal-hydraulic conditions in a test section that simulates a full-length aluminum coolant subchannel of the ANSR core. A photograph of the completed system is shown in Fig. 2.6. The loop is designed to provide coolant velocities up to 35 m/s through the test channel. Two power supplies operating in parallel will provide direct electrical-resistance heating of the test channel. A photograph of the test section assembly and associated electrical and hydraulic interfaces is shown in Fig. 2.7. The test channel (not visible) is enclosed inside the stainless steel pressure backing visible in the picture between the horizontal aluminum electrode assemblies. The cross-section of an extruded aluminum test channel design is shown in Fig. 2.8. The channel has the ANS prototypic 1.27-mm flow channel gap, with a reduced channel width in order to limit total power requirements to the test section. The reduced wall thickness at the radiused sides is designed to prevent heat flux peaking on the ends of the channel.

### 2.4.2 Thermal-Hydraulic Loop Schedule

At the end of this reporting period, the loop was undergoing final shakedown testing. Initial checkout of the test section hydraulic and electrical interfaces has been completed. The system has been successfully operated with low power levels to the test section. System fine-tuning and calibration of instruments is still in progress. Further testing at higher power levels and initial benchmark tests are expected to be completed early in the next fiscal year. Most of the first ten planned tests will benchmark the loop and test channel performance against existing data from the literature. The second series of tests is aimed at parametrically varying the coolant conditions around the ANS operating point. The third series is aimed at examining the low-flow critical heat flux (CHF)/flow instability behavior. This series of tests will include conditions representative of pony-motor flow regimes at both high pressure (loss-of-offsite power) and low pressure (loss-of-coolant accident). The fourth series of tests will examine the effects of oxide on the thermal limits, and the fifth series will

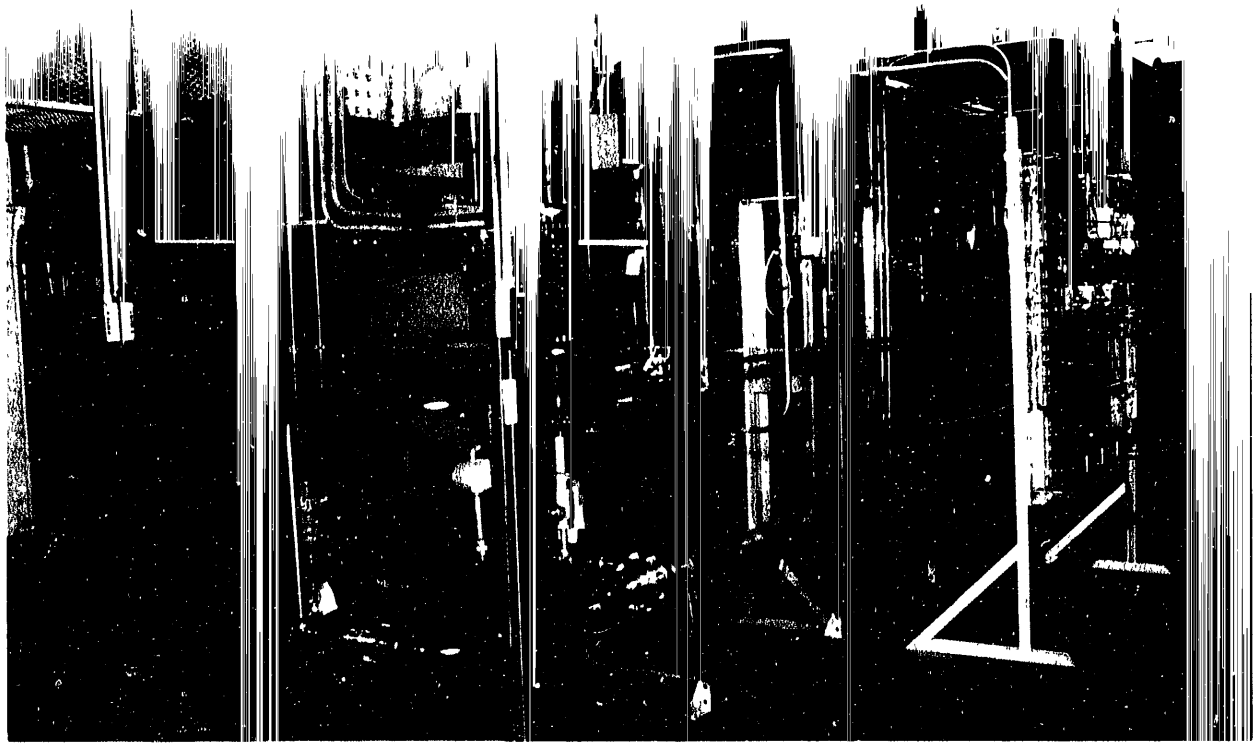

**Fig. 2.6. Thermal-hydraulic test loop.**

substitute $D_2O$ for $H_2O$ as the coolant to confirm the thermal-limit behavior.

## 2.5 REACTOR CONTROL AND SHUTDOWN CONCEPTS

During the reporting period, a number of issues were addressed and some changes were made in the control and shutdown concept. For the inner system, the hafnium thickness was reduced from 6 mm to 4 mm, and the number of rods was reduced from four to three. For the outer system, a decision was made to drive the rods hydraulically from above, which led to the need to use shorter rods because of space restrictions. These issues, along with other control and shutdown concept points of interest, are discussed in the remainder of this section.

### 2.5.1 Hafnium Thickness Requirement

In an attempt to reduce the weight and heat load of the inner control hafnium elements, the impact of reducing the hafnium thickness was examined. Hafnium thicknesses of 9 mm, 6 mm (reference case), 5 mm, 4 mm, 3 mm, 2 mm, and 1 mm were examined. It was determined that the reactivity value was not greatly improved by hafnium thicknesses greater than about 3 mm. After allowing for some additional margin for burnup and uncertainty, it was determined that a 4-mm hafnium thickness would be adopted. This

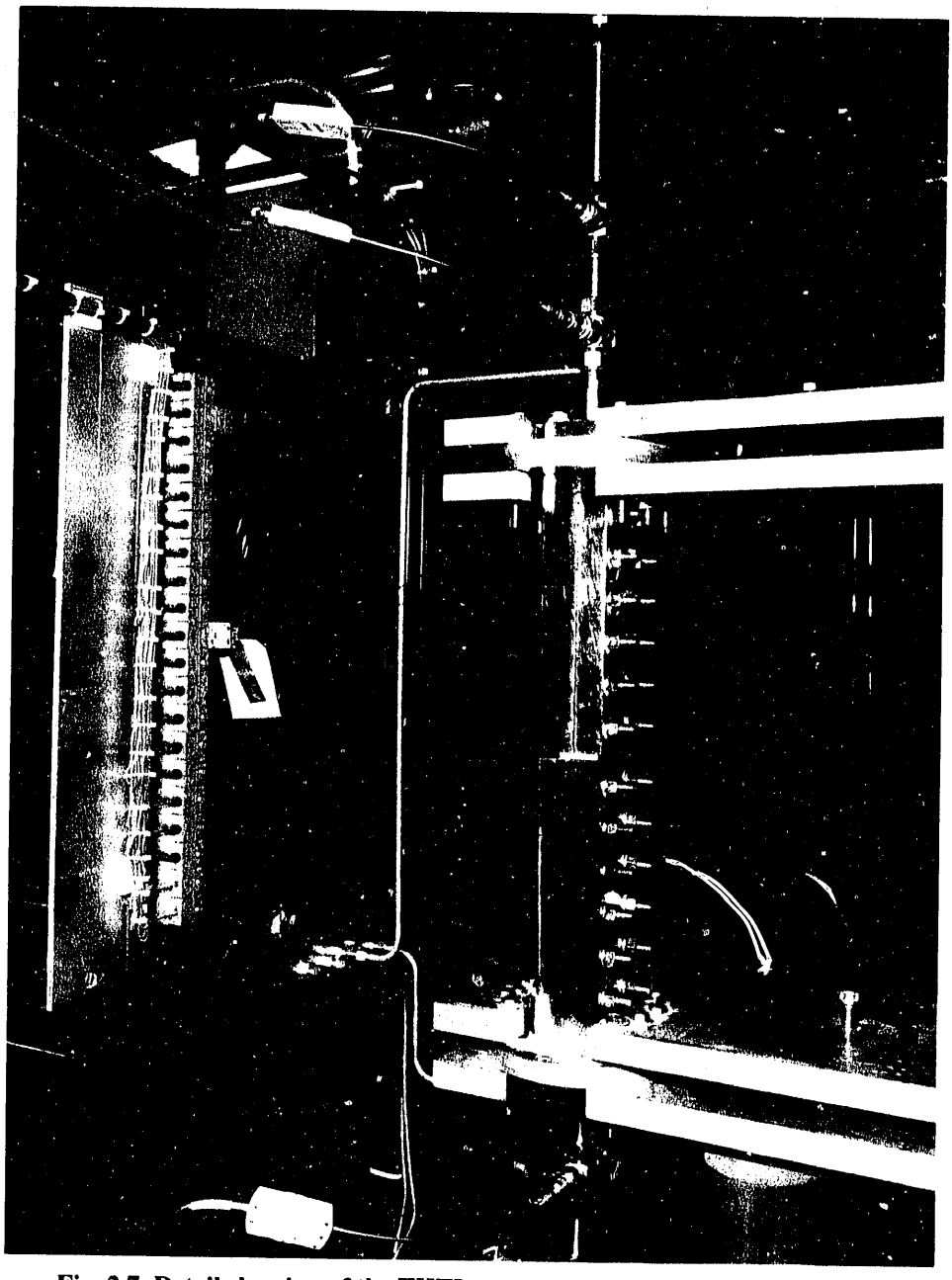

**Fig. 2.7. Detail showing of the THTL test section and electrode assembly.**

led to an approximately 30% decrease in the hafnium weight and also resulted in a reduction in the heat deposited in the rods. The net decrease in the hafnium rod worth was determined to be only 0.7% (±0.4%). This was considered to be acceptable, and the reference thickness for the hafnium section of the inner control rods was changed to 4 mm.

### 2.5.2 Three vs Four Rods

Early in FY 1991 it was recognized that we had a potential flow-induced vibration problem associated with the four rods of the control system. One proposed solution was to decrease the number of rods while increasing the size of the rods, making them more stable. A series of

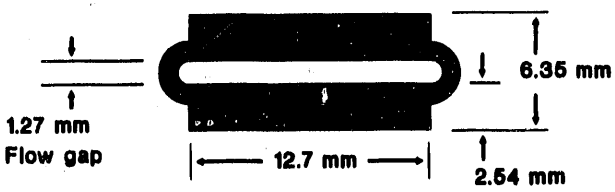


**Fig. 2.8. Cross section of the THTL test channel.**

calculations was performed to examine the reactivity differences of the proposed three 37-mm diam rods and the reference four 27-mm diam rods. The results indicated that (1) both systems provided approximately the same level of shutdown when all rods were inserted; (2) a single rod was worth slightly more in the three-rod system, meaning that for a single-rod ejection event the reactivity added to the system would be slightly larger for the three-rod case; and (3) since a rod is worth more in the three-rod system, the shutdown margin that can be obtained under the stuck-rod criteria is less for the three-rod system. Thus, it appeared that neutronically there was a disadvantage in going to the three-rod system. However, since a fast rod ejection in either the three- or the four-rod system is an event that cannot be tolerated, and since the shutdown margin requirement could be met by either system with a stuck rod, it was determined that there was essentially no functional difference between the three- and the four-rod system. As a result of this evaluation, and the need for a more mechanically stable rod geometry, the three-rod system was adopted as the reference concept. Note that in this evaluation the incremental worths of the two different systems were not examined. However, it was the staff's opinion that the relative differences would be on the same order as the differences reported for the full rod-worth, which was considered to be very minor.

### 2.5.3 Development of Outer-Rod Concept

The function of the secondary poison rod system is to provide a redundant shutdown of the reactor for those events with a high enough frequency that the combined probability of the event and of failure of the primary shutdown system results in unacceptable core damage probability. Early during the report period, it was recognized by the probabilistic risk assessments (PRA) that with the secondary system driven from the bottom close to the inner-rod system drives, there was a potential for a common mode failure of both systems that could preclude the secondary system from performing its primary function. As a result, a decision was made to drive the outer rods from above. Analysis of this layout indicated that eight shorter rods extending only to the core midplane could provide an adequate shutdown level.

Analysis was then performed to determine the tradeoff between reactivity and flux penalty because of the parked position of the rods and the speed with which negative reactivity could be supplied. Various drive systems were considered, along with other options such as fast injection of $He^3$ followed by gravity fall of the rods. Near the end of the report period, a decision was made to park the rods with their bottom end located approximately 400 mm above the top of the upper fuel element. In addition, a decision was made to use a hydraulic drive system for the purpose of additional diversity and compatibility with available space.

## 2.6 CRITICAL AND SUBCRITICAL EXPERIMENTS

This task was initiated and two significant accomplishments were made during the last half of the reporting period. The first was the development of a comprehensive list of desired tests and measurements. This list was based on a review of critical experiments performed for the ILL and HFIR facilities as well as consideration of unique tests determined to be necessary to validate the ANSR core performance. The second accomplishment was that initial contact was made with facilities believed to have the potential to perform these tests. Potential candidates included facilities both inside and outside the United States. The present plans call for the selection of the site to perform the experiments by the end of FY 1992.

The ANS critical experiments are planned for performance late in the development project and are considered to be confirmatory in nature. This is consistent with our belief that the present costs of performing this type of experiment preclude the use of such experiments as a development tool. However, it was also recognized that some experimental validation of analytical models is necessary in the short term to avoid potential significant surprises when eventually the critical experiments are performed. It was determined that this dilemma could be resolved by using the ANS analytical approaches to analyze the ILL critical experiments. At the end of the reporting period, work had been initiated to develop a three-dimensional (3-D) MCNP model of the ILL critical experiment geometry, and a series of calculations were planned to begin during the FY 1992 period.

## 2.7 MATERIAL DATA, STRUCTURAL TESTS, AND ANALYSIS

Long-term successful operation of the ANS requires research in several areas to ensure structural adequacy because of the extremely high neutron fluence and the high coolant-flow rates. Work during this report period has focused on three primary areas: (1) CPBT, (2) fuel elements, and (3) inner control elements. Progress in each of these areas is discussed in the following sections.

### 2.7.1 Core Pressure Boundary Tube

The CPBT concept employs a primary pressure containment that is of just sufficient diameter to envelop the reactor core and a small bypass flow section. This allows the surrounding reflector vessel, which contains the various guide tubes and beam tubes, to operate at a relatively low pressure.

#### 2.7.1.1 Code Case for 6061-T6 Aluminum

After careful consideration of candidate materials, 6061-T6 aluminum was selected as the reference CPBT structural material. Although it has been used in previous research reactors, 6061-T6 aluminum has not been included in the American Society of Mechanical Engineers *(ASME) Boiler and Pressure Vessel Code* for Class 1 nuclear construction. The project has formally requested the *ASME Boiler and Pressure Vessel Code* Committee to include 6061-T6 aluminum as an acceptable material for Class 1 components. That request must be considered and approved by a series of *Code* committees up through the Main Committee of the *ASME Boiler and Pressure Vessel Code* Committee. Allowable stress-intensity values and design-fatigue curves have been approved at the subgroup level. Current *Code* committee attention is directed at the relatively low ductility of 6061-T6 aluminum, especially after the extremely high neutron irradiation that the CPBT will be subjected to in service.

#### 2.7.1.2 Fracture Toughness of Irradiated 6061-T6 Aluminum

An extensive irradiation testing program and surveillance program is planned to determine more precisely the irradiation embrittlement of 6061-T6 aluminum. Two HFIR target capsule assemblies were fabricated and assembled this year for irradiation of 6061-T6 aluminum fracture-toughness specimens at conditions simulating those for the CPBT. The purpose of these experiments is to provide data for evaluation of fracture-toughness changes caused by irradiation at temperatures in the neighborhood of 95°C. Each capsule assembly occupies four HFIR target positions, and each contains sixteen 0.45 T compact fracture-toughness specimens; 15 small, flat tensile specimens; 30 transmission electron microscopy (TEM) specimens; and 30 field-ion-microscope-atom probe (FIM-AP) needle specimens, all in contact with reactor cooling water. The tensile, TEM, and FIM-AP specimens are included for correlation of tensile, microstructural, and fracture-toughness properties. In addition to the test specimens, each capsule assembly contains eight melt-material capsules for temperature monitoring and five neutron dosimetry capsules.

Irradiation of the first capsule assembly, HANSAL-T1, is in progress. The second cycle of its planned three-cycle irradiation was completed on September 17, 1991, and the third cycle was started on September 27, 1991. Exposure for the first two cycles, HFIR Cycle Nos. 299 and 300, was 3465 MWd, or approximately 41 d at 85 MW reactor power.

The first capsule assembly is being irradiated for three months, i.e., three cycles, to obtain early data at an approximate dose of $10^{26}$ neutrons/m$^2$. The second capsule assembly, HANSAL-T2, will be irradiated for two years to an approximate dose of $10^{27}$ neutrons/m$^2$ and will follow the first one.

#### 2.7.1.3 Fracture Analysis of CPBT

The CPBT will be carefully examined, using nondestructive techniques, to establish the maximum size flaw that could escape detection. Fracture-mechanics analyses will be performed on the CPBT to determine when the vessels should be removed from service to avoid the possibility of an undetected flaw resulting in failure. A maximum flaw size twice as large as could have escaped detection and the experimentally determined fracture toughness (stress-intensity factor) as a function of irradiation exposure will be used in the fracture-mechanics analysis.

### 2.7.2 Fuel Elements

The high-power density of the ANS results in several challenging structural problems in the two fuel elements. Each of the two fuel elements consist of a few hundred 1.27-mm thick aluminum-clad uranium silicide involute fuel plates held in concentric aluminum support cylinders. The involute shape allows the initial 1.27-mm gap between fuel plates to remain constant across the span of the plates when the fuel elements heat up. Careful analysis and experiment are required to ensure that the required high-coolant velocity does not cause hydraulic buckling of the fuel plates.

#### 2.7.2.1 Prediction of Hydraulic Buckling Velocity

A new methodology for the analysis of hydraulic buckling was developed based on the widely used commercial finite-element program, ABAQUS, for the involute fuel plates and a specially written user element adapted for use with ABAQUS for the fluid in the coolant channels. Predictions obtained using the new methodology did not agree with previous predictions. Corrections were made in the previous method[12] that resulted in agreement between the two methods within 1.4%.

The calculated hydraulic buckling velocity must be multiplied by 0.8 to account for the intermittent welds that attach the fuel plates to the support cylinders. In addition, a factor of safety of 1.5 is applied to obtain an allowable coolant velocity for use in design. The allowable coolant velocity is therefore 0.533 times the calculated hydraulic buckling velocity. Since the revised allowable coolant velocity is slightly below the current design target of 27.4 m/s, the use of combs at the leading edge of the fuel plates was investigated as a potential means of restoring the calculated velocity to a value above the design target. A comb is a ring that assures proper spacing between fuel plates at some intermediate location between the concentric aluminum cylinders that hold the fuel plates. Combs are, of course, an old idea, but a calculation seemed worthwhile at this time because the computational method currently under development lends itself to a detailed analysis of the effect of combs. It was found that one inlet comb, located 5/16 of the involute arc length from the outer sidewall, would raise the allowable coolant velocity for the lower fuel element from 25 m/s to 30 m/s.

#### 2.7.2.2 Experimental Validation of Analytical Hydraulic Buckling Predictions

Although in the past tests conducted on arrays of flat plates demonstrated instability at high velocities, such tests had never been done on arrays of involute plates. Benchmark tests of arrays of aluminum involute plates and proof tests of

complete dummy fuel elements are planned. However, the flow rates and pressures required to ensure that plate instability can be reached are fairly large for aluminum plates. The lower modulus of elasticity of plastic (epoxy) plates, compared to aluminum, reduces the critical velocity, so that modest flow rates and pressure can be used if epoxy is used to model the aluminum plates.

Tests have been done on a full-scale epoxy model of a portion of the upper fuel element. There were six flow channels and five active plates in the test section. Because of the boundary conditions involved, the three central plates best modeled the plate response expected in the ANSR as a function of coolant flow. Five strain gages were located along the plate length at the entrance, the quarter point, the half point, the three-quarter point, and the exit. Prior to the assembly of the test section, the gages were calibrated to signal the maximum plate deflection at the five positions noted. The four flow channels bounding the three active central plates each contained five static pressure taps located in the same cross-sectional planes as the strain gages.

Plate 6, which was the most central one, was the plate with the most deflection, and its response at the entrance, scaled for the aluminum prototype, is shown in Fig. 2.9. Several things are noted. The deflection of the plate because of coolant-flow velocity is negligible below a velocity of 40 m/s. The proposed coolant velocity for the ANSR is 27.4 m/s. The analysis predicted a critical velocity of 45.7 m/s. In this flow velocity range, the test showed an instability. In addition, the maximum deflection occurred at the entrance, which is where the analysis predicted. Additional tests are planned to validate the analyses further.

The pressure differences across the plates were essentially bounded by, and in some cases equaled, the dynamic or stagnation pressure.

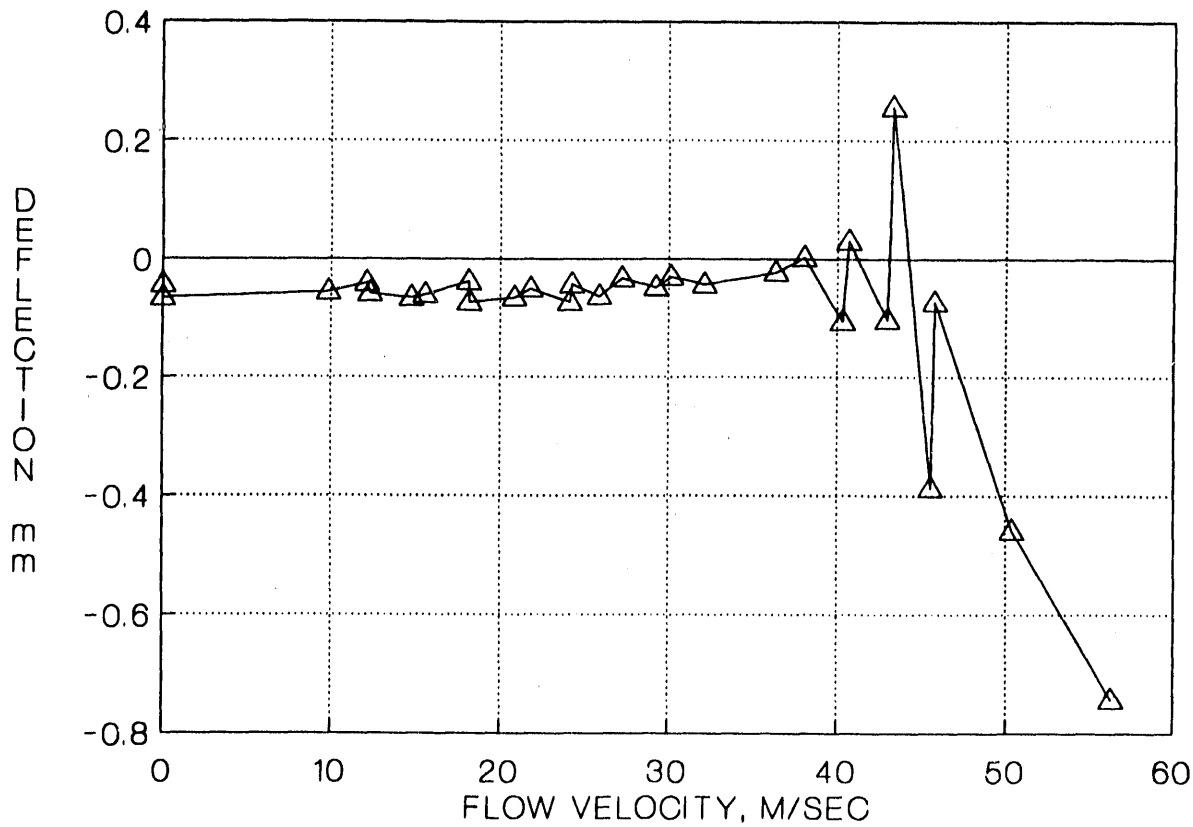


**Fig. 2.9. Plate deflection vs flow velocity for aluminum plates as scaled from epoxy test.**

Further, the pressure differences, when used to calculate the plate deflection, agreed reasonably well with the observed deflection. Thus, the dynamic pressure approach[13] can be used as a design tool to estimate the anticipated maximum plate deflection.

#### 2.7.2.3 Fuel-Plate Temperature Limits

Limits must be placed on the maximum temperature in the fuel plates to avoid various problems. High fuel-plate temperature will reduce the elastic modulus, increase the creep rate, and reduce the yield stress and the ultimate tensile strength of the aluminum. Since the operating temperature of the sidewalls differs from that of the fuel plates, there may also be a significant thermal stress in the plates during normal operation. It is important to choose fuel-plate temperature limits to ensure that all of these factors combined will not adversely impact the structural integrity of the fuel plates. Because the present ANS core is designed to operate as near as possible to the allowable coolant velocity, it is expected that the weakening of the plates at high temperature will be expressed first as a reduced buckling threshold.

To obtain a preliminary fuel-plate temperature limit, thermal-plastic behavior and thermal stress were incorporated into our hydraulic buckling analysis methodology. An upper-limit calculated fuel-plate temperature profile was obtained, and a sidewall temperature profile was estimated based on earlier HFIR work. A series of working temperature profiles was generated by simple proportional scaling of the upper-limit profile, which has a maximum temperature of 255°C.

When both plastic behavior and coolant velocity effects were included, it was found that operation at the presently estimated upper-limit calculated fuel-plate temperature profile would decrease the design margin about 19%. Although the present results do not identify an inflexible upper-temperature limit (and were not expected to do so), they do estimate the tradeoff in coolant velocity required to maintain the design margin at high temperatures. Note, however, that an upper limit temperature profile was used in these calculations.

#### 2.7.2.4 Fuel-Plate Thermal Deflection

Variations in the width of the gap between fuel plates will have an effect on their cooling. A detailed finite-element analysis of the hottest fuel plate was done to determine the deflected shape in both the upper and lower fuel element. A similar analysis of the coolest fuel plate will be done when the temperature profile is obtained. It will then be possible to predict the minimum gap that could be caused by temperature variations in the core.

### 2.7.3 Inner Control Element

The control elements are confined to a very small space inside the core and, as a result, have a large length-to-diameter ratio. Flow-induced vibrations of these long slender cylinders are a major concern because of the large unsupported length immersed in a turbulent flow condition and are being investigated. Buckling because of large axial scram accelerations is also being investigated.

#### 2.7.3.1 Flow-Induced Vibration

Investigations during the past year have reinforced the need for full-scale testing to ensure that axial-flow-induced vibrations will not cause problems in the control elements. This full-scale response test will be done in the Control Element Test Facility that is currently in the planning stages. Software to acquire and analyze transient, modal, and flow-induced vibration data from this test facility was acquired, and is being evaluated on smaller test articles.

An empirical correlation with published response tests was made to scope the flow-induced vibration problem associated with the current baseline configuration of the control elements. This empirical prediction indicates undesirable contact, that could lead to wear, is likely between the control elements and their supporting structure.

A series of dynamic models of the control elements, at three control element positions, was

developed. These simplified dynamic models were used as a basis for the empirically predicted displacements and were also used for parametric studies to guide the design process. From these parametric studies, it became evident that three control elements were superior to four, because the three-element configuration allowed each element to be larger in diameter and thus less susceptible to flow-induced vibrations. Based on the results of these parametric studies, other key design features were also improved, such as the support structure material thickness and the location and manner of support required for the control elements.

#### 2.7.3.2 Column Buckling

Studies have shown that buckling of the control elements is not a major concern during the acceleration portion of a scram. However, dampers or velocity control devices will likely be required during the deceleration phase to prevent buckling.

#### 2.7.3.3 Hafnium Temperature and Fluence Limits

Hafnium has been chosen as the neutron absorber for use in the control elements. Temperature and fluence limits for hafnium were determined on the basis of existing data for use in the preliminary design. The tensile strength of hafnium at temperatures as high as 371°C has been reported in the literature.[14] Other sources[15,16] give the tensile strength of hafnium at temperatures above 300°C. The strength at 371°C is only half the strength at room temperature. On the basis of the existing data, it seems reasonable to select 371°C as the maximum allowable temperature during the conceptual design stage of ANS.

A memo[17] from EG&G Idaho gives the best currently available information on fluence limits for hafnium. This 1984 memo recommends a fluence limit of $5.0 \times 10^{26}$ n/m$^2$ (E > 1 MeV) for the hafnium control rods in the Advanced Test Reactor. A paper[18] from EG&G Idaho that was presented at the International Symposium on Research Reactor Safety, Operations, and Modifications in 1989 indicates that the fluence limit they use for hafnium safety rod assemblies is still $5.0 \times 10^{26}$ n/m$^2$ (E > 1 MeV). They refer to a loss of ductility as the limiting factor.

#### 2.7.3.4 Irradiation-Induced Relaxation in Inconel X-750 Control-Rod Springs

The inner control rods depend on springs for scram. The possibility that irradiation-induced relaxation could reduce the load on the springs enough to adversely affect scram was evaluated. The available data in the open literature indicate that significant irradiation load relaxation would not occur in the control-rod scram springs at their expected locations.

## 2.8 COLD-SOURCE DEVELOPMENT

The cold-source development work has been divided into two major areas: (1) neutronics modeling and (2) mechanical and thermal modeling, including testing programs and thermal-hydraulics development.

### 2.8.1 Cold-Source Neutronics

The cold-source neutronics work for the report period focused on three major tasks: the evaluation of new ortho- and para-deuterium cross sections, the development of a 3-D Monte Carlo model, and examination of impact of cold-source design perturbations.

#### 2.8.1.1 New Cold-Source Cross Sections

A 39-energy-group liquid deuterium cross-section set was received from the University of Stuttgart. This cross-section set contained 25 thermal groups that spanned the energy range down to as low as 0.01 meV. These cross sections were used to evaluate the cold-source experiments performed in the Siloette swimming pool reactor at Grenoble, France. Results of this analysis were compared with measured data and with

evaluations performed using the previous deuterium cross-section set. It was determined that while over some energy ranges the agreement with measured data was not as good as previously obtained, it was improved over most of the energy range of interest. The decision was made to use these cross sections as the reference deuterium cross sections in future analyses.

#### 2.8.1.2 Cold-Source Monte Carlo Models

At INEL, a model of the ANS cold source was included in the 3-D MCNP (Monte Carlo) model of the reactor core and reflector tank. This model was used to determine the cold-source impact on core reactivity and on heat loads for several cold-source geometries. Evaluations indicated that the cold source would have <1% impact on the core reactivity, and the heat loads obtained were consistent with previous calculations and extrapolations of ILL-reported heat loads.

At ORNL, a 3-D MORSE (Monte Carlo) model was generated with a representative core boundary source. This model was developed to examine cold-neutron behavior in geometries that could not be modeled using the two-dimensional (2-D) discrete-ordinates code DORT. At the end of the report period, comparisons with previously calculated 2-D geometries had been performed to benchmark the 3-D Monte Carlo model. Results indicated that for the energy range of interest, the MORSE model generally predicted about a 10% higher neutron current in the cold-neutron guide tubes.

#### 2.8.1.3 Examination of Cold-Source Design Perturbations

A number of design perturbations were examined. Of particular importance was the determination that elimination of the 2-mm heavy-water layer between the cold source and the cold-neutron-guide vacuum tube could result in as much as a 20% increase in the cold-neutron flux seen by the guides. This was one of the driving forces that led to the examination of a horizontal cold-source geometry as discussed below.

### 2.8.2 Cold-Source Mechanical and Thermal Modeling

The first few months of FY 1991 were spent procuring equipment and performing the final assembly work on the ANS Cold Source Test Facility. The test facility consists of a pair of liquid nitrogen dewars; one is capable of holding an instrumented full-scale model of the cold-source moderator vessel, and the other is used to simulate the heat exchanger used to cool the moderator. Neutron and gamma heating of the moderator was simulated by passing electric current through several banks of heating wires inside the cold-source model.

Phase I tests in May and June were encouraging. Stable boiling of the liquid nitrogen in the model was observed at heat loads in excess of 15 kW, about 1.5 times the heat load expected in the ANS facility. No instabilities were observed, and higher heat loads might have been possible but were not attempted because the electric heaters were operating near their burnout point.

Discussions in July with Reactor Systems and Experiment Systems personnel led to the development of an alternate cold-source configuration, in which the cold source would be placed in a horizontal thimble instead of being inserted through a flange on the top of the reflector vessel (see Fig. 2.10). Project personnel agreed that the alternate concept (called a "horizontal" configuration) offers several attractive features, especially with regard to maintenance and to optimization of the cold-neutron flux but concluded there was insufficient time to evaluate the horizontal concept in FY 1991.

An external review of the cold-source program was held in September. The review committee consisted of three staff members from other laboratories and one engineer from an industrial gas company. Other participants included representatives from ANS Reactor Systems, ANS Experiment Systems, and Gilbert/Commonwealth.

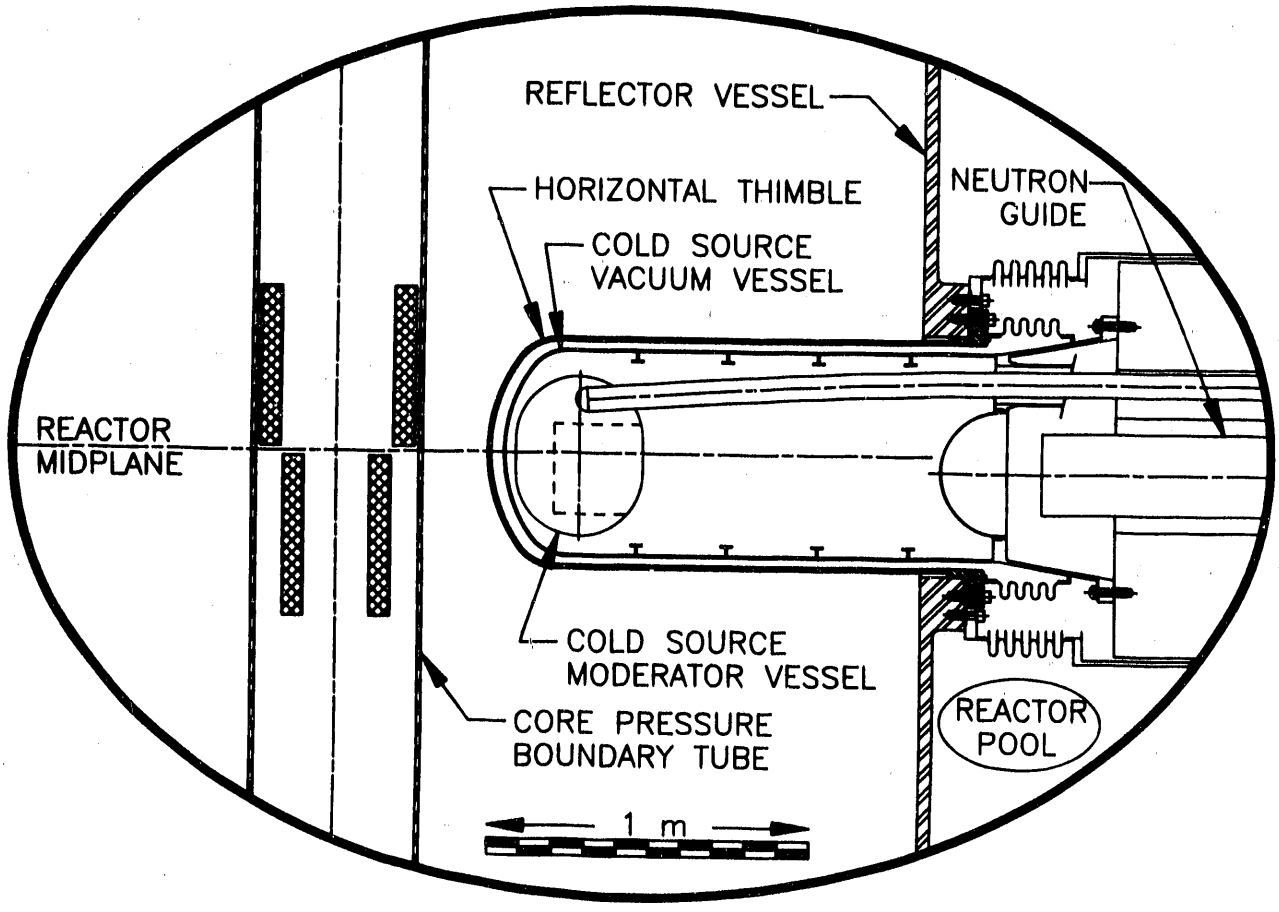


**Fig. 2.10. Horizontal cold-source thimble geometry.**

The review committee felt that the ANS staff was well qualified and that the progress made was consistent with the level of funding received. The committee's report and oral summary also made several recommendations to the project. A few of the more significant comments were:

1. Determine as accurately as possible the neutron and gamma heating loads at an early stage of the conceptual design, document the findings, and subject them to peer review. Validate the computer model used to estimate heat loads by comparing its calculated values for the ILL cold source to the measured values at that facility.
2. Pursue the "horizontal" cold source rather than a "vertical" cold source. Develop engineering solutions at an early stage of the design to the problems of rapid and accurate removal, replacement, and realignment of the cold sources, the shielding, the neutron guides, and the ancillary equipment.
3. Since the feasibility of the boiling moderator design for ANS heating rates is an open issue, subject to experimental verification, consider using a nonboiling mechanically pumped liquid deuterium system without extra vessel wall cooling. This option has a much greater probability of being properly scoped, analyzed, and budgeted in the available time.
4. Designing to prevent a deuterium-oxygen reaction within the system is a better approach than designing to contain a

reaction because the strength of assemblies necessary to contain a reaction would not be practical for this application. A helium envelope should surround all cryogenic vacuum in the system.

5. Minimization of deuterium inventory should be viewed as a goal but should not be overemphasized or viewed as the limiting goal.

The ANS cold-source development team began to consider the recommendations of the committee and came to these conclusions:

1. The committee's recommendation regarding the neutronics modeling was accepted.
2. It would be unwise to commit to a horizontal configuration and a mechanically pumped nonboiling deuterium system before considering the ramifications of choosing those configurations. A tentative plan was formulated to investigate these options and to make decisions in December 1991.
3. The committee's recommendations regarding deuterium inventory and safety were accepted, on the condition that the system can be designed so that the deflagration risks are acceptably low.

Thermal-hydraulic subcontract work at the University of Virginia progressed well during FY 1991. The 2-D two-phase computer model was completed and will be benchmarked in FY 1992 using light-water data from the extant literature.

## 2.9 BEAM TUBE, GUIDE, AND INSTRUMENT DEVELOPMENT

Significant progress has been made in the past year towards finalizing concepts for all aspects of experiment systems. Initial drafts of SDDs were issued covering beam transport, scattering instruments, nuclear and fundamental physics instruments, transplutonium production, materials irradiation, isotope production, analytical chemistry, instrument support, and computers and data handling. Evaluation of operational parameters, such as angular ranges and distances between axes, has led to realistic layouts for the beam-room and guide-hall instruments. These and the various irradiation facilities are close to final conceptual design and are discussed in Sect. 3.3, where a description will also be found of the revised layout of the very cold neutron (VCN) and ultracold neutron (UCN) facilities, consequent to the proposed change in the cold-source geometry from vertical to horizontal. The second-floor beam-room space originally allocated to UCN facilities, which would be freed by this new arrangement, offers an excellent position for the positron facility that is under study, following a request by NSCANS to include such an option in the conceptual design.

We have benefitted from close collaboration with the site planners and the A/E contractor in integrating needed support facilities for experiments into the building layouts and in allowing for future expansion of the experimental facilities, while maintaining high security for reactor operations (see Sects. 3.3 and 3.4). The result is a facility concept that will be very user friendly.

There has been an extensive study of how the ANS might operate as a user facility, including an assessment of how participating research teams would interact with the user program and what the consequences would be of permitting proprietary research. At the request of DOE, this study has been greatly expanded to consider the general question of nonfederal participation (industrial, state, and foreign) in the design, construction, and operation of the ANS.

Instrumental research has included (1) assessments of likely radiation levels at sample positions (more than 10 mSv/hr at 300 mm in unfavorable cases) and the consequences for automation and shielding and (2) instrumentation and control (I&C) studies of some innovative neutron multidetector design concepts. However, most effort has been concentrated on aspects of beam transport that have the most immediate impact on the overall conceptual design of the ANS. Detailed instrument layout studies have resulted in a new beam-tube layout. The reference beam-tube size of 200-mm high by 100-mm wide

has provided the basis for detailed design studies of the beam-tube/reactor interface, including such aspects as cooling and wall thickness and concepts for safety windows and shutters. (An example is given in Sect. 3.3.) Further neutron optics simulations are being carried out by the neutron scattering group at BNL. Equivalent mechanical design studies of the cold-guide/cold-source interface are now approaching conclusion.

### 2.9.1 Thermal Beam-Tube/Guide-Tube Combinations

The plan for the ground-floor beam room of the ANS calls for the installation of some short thermal guide sections at the ends of selected beam tubes to allow placement of more thermal instruments in the reactor hall. The highly successful supermirror development program, coordinated by the group at NIST, has shown that guides with critical angles at least three times that of natural nickel will be available, and the next stage has been to analyze the performance of beam-tube/guide-tube combinations. This has been undertaken by the neutron scattering group at ORNL. The problem was scoped by considering beam tubes 200-mm high and 5-m long in combination with supermirror guides also 200-mm high and either 5-m or 10-m long. For this analysis, a tube is a device with totally nonreflecting internal walls, and a guide is a device with walls that totally reflect all neutrons incident below the critical angle corresponding to their wavelength. The analysis was based on calculating acceptance diagrams, which define the spread in angular divergence as a function of position in the cross-section plane of a beam tube or guide.

A measure of the overall performance of the guide is the conductance, defined as the ratio of the total current at the exit to the total current at the entrance. This is given by the ratio of the exit and entrance acceptance diagram areas and is presented in Fig. 2.11 as a function of wavelength. A related measure is the gain, defined as the ratio of the total exit current to the exit current for a single tube of the same total length as the tube/guide combination. This is given by the ratio of the acceptance diagram area to the central, direct transmission area, and is shown in Fig. 2.12. In examining these figures, it should be remembered that instruments fed from a thermal source will usually operate at wavelengths shorter than 0.25 nm.

It is clear that the guide section should begin as close to the source as possible in order to approach full illumination. The work is being extended to study tube/guide combinations of fixed total length with the length of the guide section as a variable.

### 2.9.2 Cold-Neutron Guide Tubes

The optimal dimensions of the beam tubes were assessed by analyzing a wide variety of experiment classes that use thermal neutrons. A similar study to evaluate the optimal dimensions and coating materials for the cold-neutron guides is now nearing completion. The important experimental parameters for this purpose are the maximum horizontal and vertical divergence and the maximum useful beam size at the sample position. Of course, the desired beam size is directly related to the anticipated maximum sample size, and this can only be estimated on the basis of past experience.

There are some general considerations to keep in mind. Bigger guides are better, provided the experiment can use the full guide area, but oversized guides deliver neutrons outside the sample, requiring more shielding and creating potential (and probably actual) background problems. This is particularly true with straight guides, which are in use at NIST and are proposed for the ANS. Straight guides permit selection of the guide width independently of the length and transmit cool as well as cold neutrons, but they also allow streaming of unwanted radiation (fast neutrons and gamma rays). In general, there will be more than one instrument per guide. This can be achieved by stacking monochromators in series, with each instrument operating in a different spectral regime, or by splitting the guide into smaller sections so that each instrument sees a virgin spectrum. In the latter case, the proposed pair-wise spacing of ANS guides would dictate that any such split should be top-to-bottom, rather than left-to-right, so that a tall, narrow guide would be better than a short, wide one.

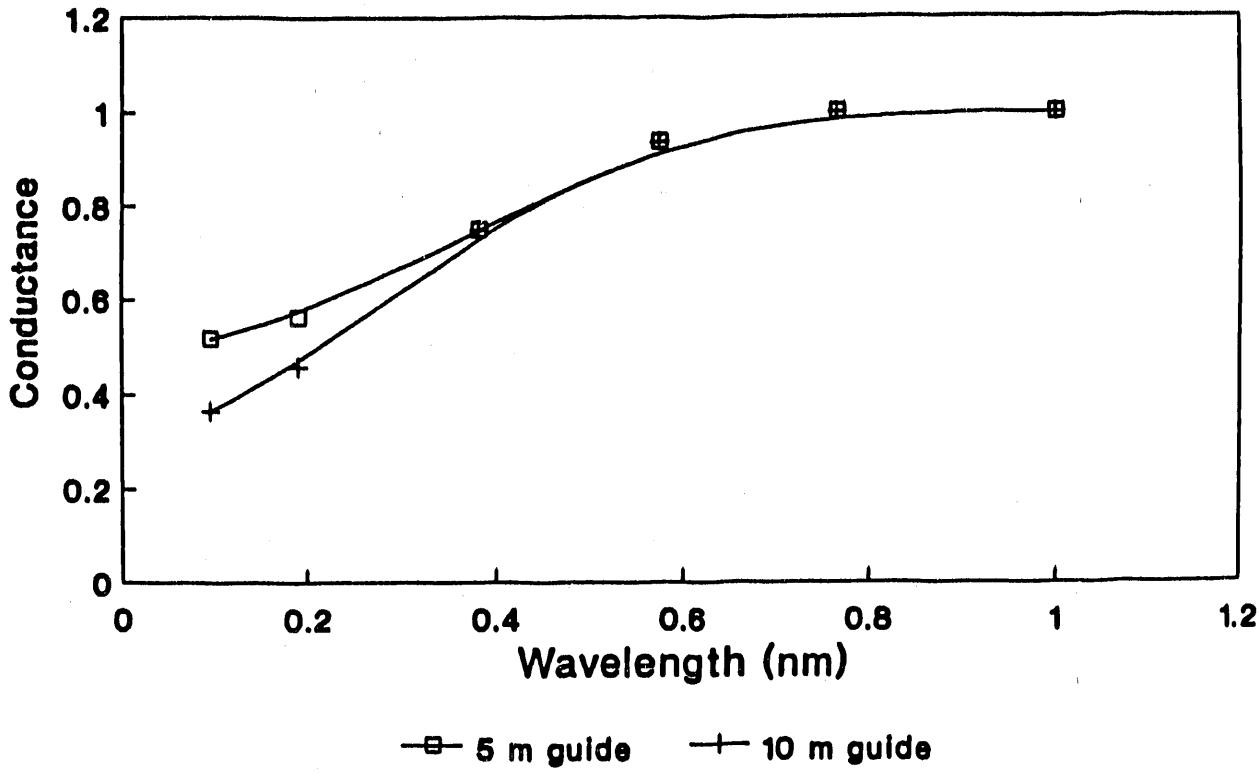


Fig. 2.11. Conductance for 5-m beam tube/guide tube combinations as a function of neutron wavelength.

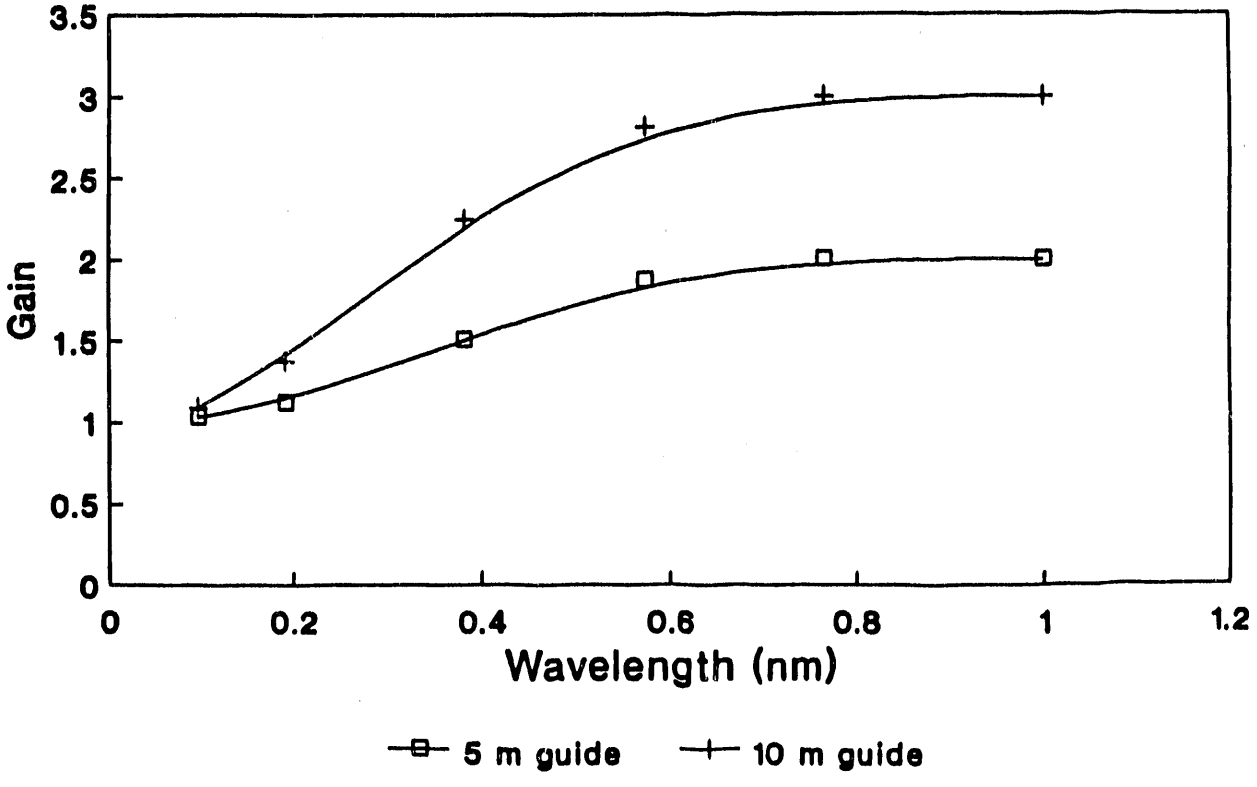


Fig. 2.12. Gain factors for 5-m beam tube/guide tube combinations as a function of neutron wavelength.

The potential use of focusing has an important bearing on guide dimensions. Focusing increases the flux on the sample at the cost of increased divergence. Vertically focusing monochromators are used routinely on instruments, such as 3-axes, and recent research has shown that horizontal focusing may also be used in certain 3-axes experiments. Instruments designed to measure incoherent scattering, such as time-of-flight spectrometers, and certain small-angle neutron scattering configurations will also gain by using converging guide sections to provide 2-D focusing.

Table 2.2 summarizes the conclusions of these studies for a limited set of instrument types. As expected, there is a wide variation in experimental requirements. A standard guide-geometry-based worst case presented here would be 200-mm high by 40-mm wide; for comparison, our reference design previously assumed 150 mm by 50 mm. The case for 200-mm height is sufficiently strong that it will be adopted as the new reference. The primary impact is on the cold-source geometry. Studies continue to define the best width, but a final choice in the range being considered (40 to 50 mm) will not impact any other aspects of the ANS conceptual design. Independent of detailed geometry, a mix of supermirror and nickel guide coatings should be installed to accommodate best the final instrument plan.

The NIST/State University of New York research on neutron fiber microguides is being closely followed. This development offers revolutionary opportunities especially at the depth profiling and prompt-gamma activation analysis (PGAA) stations. The current design for the PGAA stations uses beam benders to split the full guide into several sections followed by smaller straight guides (to equalize beam-intensity distributions). Highly curved microchannel guides would allow a single full guide to be split into multiple PGAA stations as desired.

## 2.10 HOT-SOURCE DEVELOPMENT

The hot-source development is a planned R&D activity that has not been initiated with present funding levels. In addition, since the R&D program work for FY 1992 is by necessity focused on support to the development of the CDR, no

**Table 2.2. Summary of guide requirements**

| Instrument | Source | Coating | | Height (mm) | Width (mm) |
|---|---|---|---|---|---|
| | | Sides | Top and bottom | | |
| HRPD | Th/cold | Ni | SM | 220/176 | 30 |
| SRPD | Th/cold | Ni | SM | 266/212 | 30 |
| Diffuse-crystal | Cold | Ni | SM | 106 | 30 |
| Diffuse-liquid | Hot | Not applicable | Not applicable | Not applicable | Not applicable |
| Single crystal-chemical | Th | SM | Ni | 143 | 10 |
| Single crystal-biology | Th/cold | Ni | Ni | 36/29 | 10 |
| Triple axis-thermal | Th | SM | SM | 218 | 40 |
| Triple axis-cold | Cold | SM | SM | 209 | 40 |
| SANS | Cold | Ni | Ni | 30 | 30 |

significant hot-source development activity is expected until FY 1993 or FY 1994.

## 2.11 NEUTRON TRANSPORT AND SHIELDING

There were two major accomplishments under this task for the reporting period: (1) resolution of inconsistencies in heat load calculations and (2) initiation of the evaluation of adequacy of spaces allocated for shielding purposes.

### 2.11.1 Component Heat Load Analysis

Early examination of the energy deposition due to all processes in the MCNP 3-D model of the ANS core and reflector components showed a discrepancy in the contribution of the total fission-product photon yield energy when compared with established data. An ORIGEN[19] calculation was performed to check the total fission-product photon yield from the fuel, and the results were in agreement with those obtained in the MCNP calculation. However, upon consulting with Los Alamos National Laboratory (LANL), INEL determined that for continuous operation or for times of under a few minutes after shutdown, ORIGEN (and MCNP) will underpredict the fission-product photon yield for the ANS model. This is because the fission-product photon yield is not available for a sufficient number of the isotopes in either the ENDF/B-IV or V data sets. Since the newer version (with ENDF/B-VI libraries) of CINDER-7[20] has not been released yet, the LANL code DKPOWR,[21] which is based on measured data and the 1979 ANSI/ANS 5.1 Decay Power Standard, was utilized to produce the fission-product photon yield, total energy, and spectrum. The fission rates from ORIGEN at each burnup step were input to DKPOWR as the core fission history. The results obtained indicated about a factor of two increase in the fission-product photon energy yield. These new values were found to be consistent with theoretical expectations.

### 2.11.2 Shielding Evaluations

Initial one-dimensional (1-D) shielding evaluations were performed for the bulk shield during this report period. Neutron and gamma sources at the reflector tank wall were used to drive a multigroup, coupled neutron and gamma 1-D model from the reflector tank through the light-water pool and bulk shield. Results indicated that with conventional shield materials, the space allocated for the bulk shield appears to be appropriate. It was, however, recognized that with the large number of beam-tube penetrations in the shield, more sophisticated analyses will be necessary to determine the adequacy of space available for local shielding requirements. Shield heat loads were also obtained from this analysis, but at the end of the reporting period the cooling requirements for the shield had not been established.

## 2.12 I&C RESEARCH AND DEVELOPMENT

The Plant Instrumentation, Control, and Data Systems and the Reactor Instrumentation and Control System are planned as an integrated digital system with hierarchical, distributed control with fault-tolerant architecture. A hybrid digital/analog protection system will be required to achieve the fast response necessary for critical parameters. Data networks will transfer information between systems for control, display, and recording. The proposed system architecture is shown in Fig. 2.13.

### 2.12.1 Reactor Protection System Concept

Reactor protection is accomplished by the rapid insertion of negative reactivity with control rods to shut down the fission process and to reduce heat generation in the fuel. Two independent reactivity control systems of different design principles are provided, and each system has multiple independent rods to provide

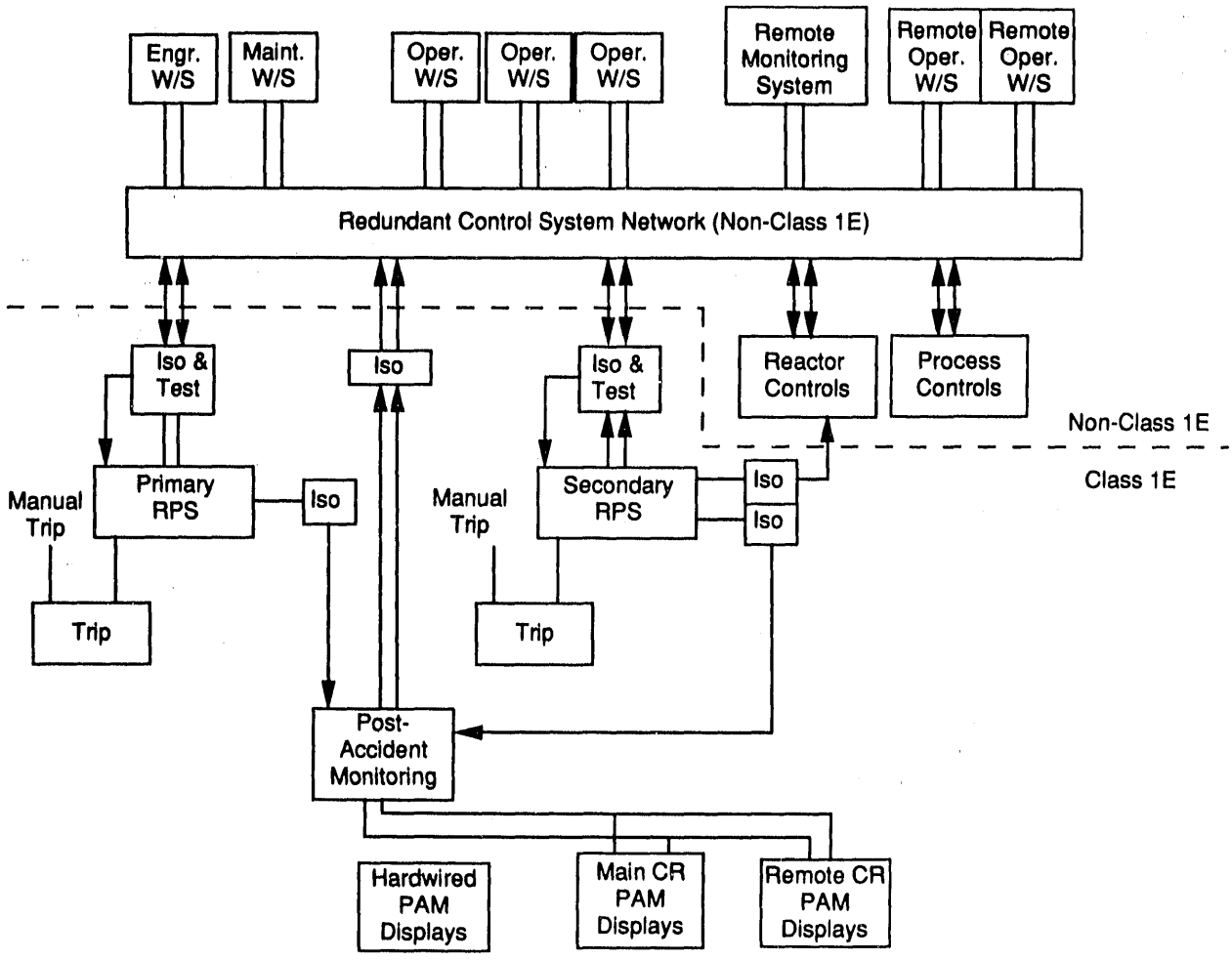


**Fig. 2.13. Proposed control system architecture.**

appropriate margin for malfunctions such as stuck rods or other single failures. Each reactivity control system has its own wiring, signal processing, logic, and actuating systems. In some cases, sensors may be shared between systems to minimize penetrations and access to the primary piping system. Each system has sufficient shutdown margin to keep the reactor in cold shutdown with adequate margin independently of the functioning of the other system, even with a single-rod failure to scram in the active system. Either system will be capable of dealing with any anticipated operational occurrences, even in the event of failure of the other system. The combination of both systems will have the capability of dealing with any design-basis event.

The primary and secondary shutdown systems each will have four independent channels of instrumentation to assure high reliability and availability. Coincidence logic is arranged in two out of four, so that agreement of any two channels is required to initiate protective action. Comprehensive on-line testing is employed to detect failures. If a failure occurs in one channel, that channel may be bypassed (placed in the untripped condition) until the failure is repaired. The remaining system thus will be in two-out-of-three coincidence logic, fulfilling both the reliability and availability goals until the system is restored to normal. The tentative scram parameters and set points are shown in Table 2.3. Other scram parameters under consideration are

**Table 2.3. Protection system parameters, set points, and uncertainties (tentative)**

| Parameter | Set point | Response | Accuracy |
|---|---|---|---|
| Power-equivalent-flux to primary-coolant flow ratio | >1.15 | 1–10 ms flux<br>200 ms flow | ±2% |
| Core thermal power | >115% | 2 s | ±2% |
| Primary-cooling sytem pressure (core outlet) | <80% | 30 ms | ±1% |
| Reactor inlet temperature | >110% | 2 s | ±1% |
| Rate-of-change of neutron flux | >20%/s | | ±5% |
| Very low primary-coolant flow rate (low-low flow) | <8%<br>(TBD) | 1 s | ±5% |
| Primary-coolant fission-product activity | >150% of background | 2 s | ±20% |

primary-coolant heavy-water leak, accumulator heavy-water levels, reflector tank cooling, cold-source parameters, other experiment parameters, and seismic activity.

The reactivity elements for the primary shutdown system consist of the three inner control-rod assemblies. These rods are located in the central core region and serve the combined functions of shim, regulation, safety, and shutdown. The control function of the primary control-rod system is eased by the presence of burnable poison. Each rod has an individual scram latch and accelerating spring to perform the safety and shutdown functions. In normal operation, with the latches engaged, the rods are driven altogether by a common two-phase ac drive motor for shimming action—that is, long term reactivity control over the full rod stroke. A unidirectional, air-operated turbine is used to provide fast insertion (negative reactivity) of the shim drive to enhance certain control functions. This turbine is incapable of withdrawing the rods and serves no safety function. A separate dc servomotor is used in a piggyback fashion to provide fast regulating motion of the rod assembly. The regulating stroke is positively limited by mechanical stops so that the total reactivity worth of the regulating system is limited to a safe value. Because the inner control rods are used for the combined functions of control and safety, they are always in a position of high incremental reactivity worth and therefore will have optimum response for rapid shutdown when needed. Calculations indicate that only 40 mm of motion is required to insert $1 of reactivity.

The reactivity elements for the secondary shutdown system consist of the eight outer control-rod assemblies. These rods are located in the reflector region and serve as safety and shutdown rods only. In normal operation, these rods will be fully withdrawn to minimize the flux perturbation between the core and the beam tubes. The outer rods are hydraulically actuated and are either fully inserted or fully withdrawn. No intermediate positioning is needed or provided. All outer rods must be fully withdrawn before permission is given to withdraw the inner rods. Conversely, all inner rods must be fully inserted before permission is given to withdraw the outer rods. The outer rods may be manifolded so that they operate in groups, to minimize the number of necessary penetrations of the reflector vessel.

The primary reactor coolant pumps will be tripped when low pressure is detected in the

primary-coolant system by the reactor protection system sensors. This is to protect the pumps from damage by cavitation and to mitigate the loss of coolant if the low pressure is the result of a loss-of-coolant accident.

### 2.12.2 Control System Concept

A principal objective of the ANS operation is to maintain the reactor continuously at the highest power level that is consistent with safety and the available coolant flow. A highly reliable, fault-tolerant control system is used not only to achieve high availability of the reactor but also to reduce challenges to the protection system by maintaining important plant parameters within appropriate limits. The control system has a number of contingency features to maintain acceptable, although off-normal, conditions in spite of certain control or plant component failures, thereby further reducing protection system challenges.

Core thermal power has been chosen as the basic control parameter, although it is used indirectly. Thermal power is derived by detecting the rate of coolant flow and its temperature rise as it passes through the core. The required speed of response is obtained by utilizing the accurate, but delayed, core thermal-power information to provide continual and automatic calibration of neutron flux measuring devices by adjusting the gains of the flux instruments. This arrangement permits fast action by the nuclear instrumentation and, at the same time, allows a high degree of accuracy regardless of the operating history of the core, the positions of the control rods or ionization chambers, or any other effects that may cause the nuclear signal to vary in a manner not proportional to the core thermal power. The power-equivalent flux obtained in this way is employed directly as the basic control parameter.

Signals from flow-measuring instruments are used (1) to ensure that the control system will limit automatically the maximum allowable operating power to a level consistent with the actual flow rate and (2) to set the neutron flux trip levels in the protection system channels automatically at appropriate values. This action permits the reactor to operate with less than full-rated coolant flow at a power level commensurate with the available flow. An example of this control function is shown in Fig 2.14.

The plant heat removal control system is a hierarchy of multiple levels and multiple loops using advanced digital techniques to maintain close control of plant parameters under a variety of operating conditions. The system is slave to the prime function of controlling the demanded reactor thermal power. The heat removal system functions to maintain the reactor coolant inlet temperature near the design temperature of 49°C.

The reactor power level control system depends on regulation of the primary-coolant system to maintain near-constant reactor inlet temperature. The primary-coolant flow rate is intended to be constant. Flow changes in the primary loop will be step-wise only, as a result of the starting or stopping of one or more constant-speed primary-coolant pumps. The normal operating condition is for three loops, with their associated pumps, to be in operation with the fourth loop valved out as an installed spare. To control the reactor inlet temperature, it is necessary to control the heat removal rate in the primary heat exchangers. Fast proportional control is achieved by regulation of the secondary-coolant flow rate with variable speed coolant pumps.

The cooling tower fans and a tower-to-basin bypass valve are adjusted to maintain constant off-tower water temperature as it reenters the basin. This assures near-constant secondary-coolant temperature to the primary heat exchanger. The ultimate cooling is adjusted by the number of fans in operation and the fan speeds to provide the correct amount of heat removal with the tower bypass valve closed. Each primary heat exchanger has a separate secondary-cooling loop with independent pumps, cooling towers, and control features. These functions will be performed under computer control with a minimum of operator intervention.

Primary-coolant pressure at the reactor outlet is regulated by letdown control valves. The desired letdown flow rate is regulated by adjusting the speed of the variable-speed pressurizer pumps. The charging flow enters the system near the reactor outlet on a common header. Each loop has a letdown control valve near the main heat

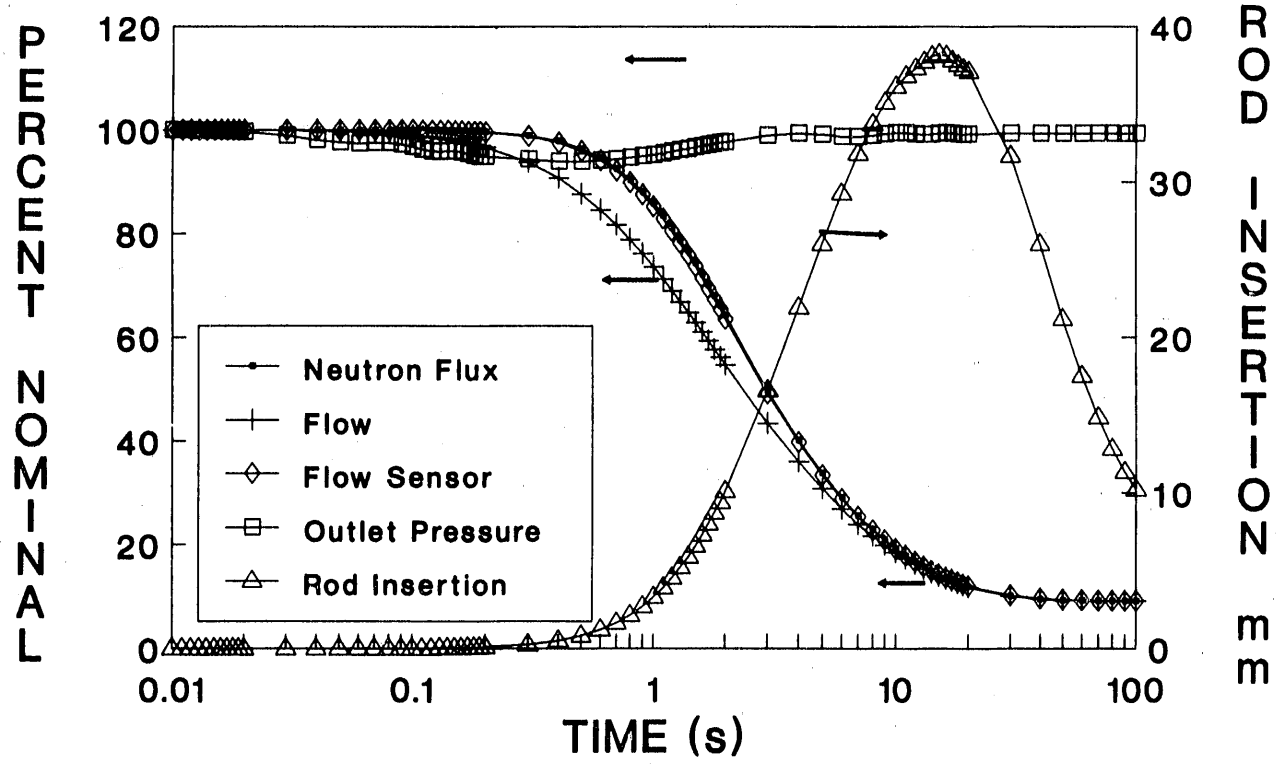


**Fig. 2.14. System response to loss of pumping power.**

exchanger for that loop, but a common validated pressure signal is used for all loops.

### 2.12.3 I&C Activities for FY 1991

Three major activities have dominated the I&C effort during FY 1991: (1) writing the draft system design description for the reactor I&C (SDD 33), (2) developing and analyzing control-rod concepts for the primary and secondary shutdown systems, and (3) supporting the safety analysis of different reactor options.

Chapter 1 of SDD 33, which is now drafted, documents the functions and requirements of the reactor I&C system. Chapter 2, which is also drafted, contains a description of the system conceptual implementation. SDD 33 thus contains a summary of the project R&D efforts in the reactor I&C area and provides documentation of the present concepts, a summary of which has been included in the previous sections.

A number of appendices in SDD 33 will detail the interfaces to other parts of the project, as well as the applicable codes, standards, and regulations. Missing from the current draft of SDD 33 are Chaps. 3 through 6 that deal with operation, system limitations, casualty events and recovery procedures, and maintenance.

A large effort has been devoted during FY 1991 to the development and analysis of the control-rod concepts. This is a continuing effort, with a final goal of defining a conceptual design for the reactivity control systems. This effort has resulted in a reference design that includes the three inner rods with their magnetic latch and the eight half-length hydraulic rods described in the previous sections. The requirements and performance of different options have been evaluated through a number of analyses; in particular, the need for a fast secondary scram was analyzed in the context of a $^{3}$He-based secondary scram system that was also studied.

I&C staff continue to support safety analysis efforts by analyzing different reactor design

options using transient dynamic models. Significant effort was devoted to the analysis of loss-of-coolant events, as they affected the design of the reactor cooling circuits (see Fig. 2.15). Based in part on these analyses, the reference cooling circuit was modified to include four independent cold legs with inertial flow diodes, and a double wall was added to the CPBT to minimize the probability, and the consequences, of failure.

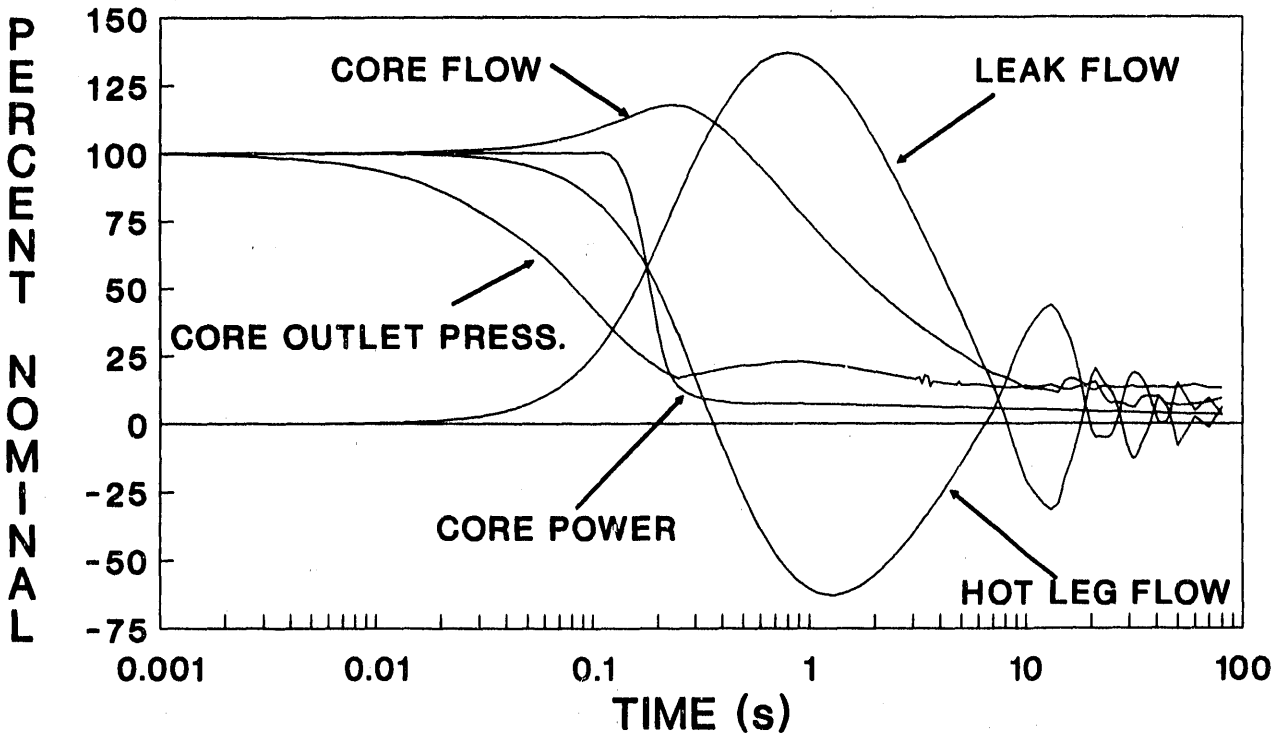


**Fig. 2.15. Reactor cooling circuit response to large core outlet break.**

# DESIGN 3

## 3.1 SYSTEMS INTEGRATION

### 3.1.1 Configuration Control

The principal focus of configuration control has been to ensure that requirements are identified and tracked throughout the design process. This process will ultimately control the functional and physical configuration of the ANS facility and systems.

An essential document employed in this process is the Systems Engineering Management Plan that defines the control documents for the project and the relationships between them and that calls for the preparation of a Configuration Management Plan as part of the conceptual design process. Key configuration control issues include the identification of basic project objectives along with design, environmental, and safety requirements. The flow of requirements into the design process is implemented by use of controlled documents. Top level requirements are incorporated into the Plant Design Requirements (PDRs) with system-level requirements incorporated into a set of SDDs.

### 3.1.2 Plant Design Requirements

This key document defines the overall plant-level requirements for the ANS facility, along with a set of consistent definitions for use in other documents, and controls the plant's baseline configuration. It is structured as a living document to which new material and modified material will be added throughout the life of the ANS. The authors of the various sections of the PDR are those persons responsible for each requirement. An example is the safety section written by the ANS safety manager.

Progress this year included an update of the initial issue covering fundamental research goals and necessary research facilities, fundamental reactor goals and features, and the overall plant-level safety goals. A second release in August of 1991[22] added a detailed table addressing ANS event categories and acceptance criteria. These include normal operations as well as anticipated, unlikely, and extremely unlikely events. Also incorporated in this revision is a tabulation of the ANS design-basis conditions and events and a detailed listing of the functions, responsibilities, and primary interface systems for each of the SDD documents. A third issue, planned for early in FY 1992 as part of the conceptual design documentation, will complete the safety classifications and will add scope relative to general design criteria and definition of plant-level design-basis events. This will include aspects of regulatory jurisdiction [e.g., DOE and the Nuclear Regulatory Commission (NRC)], quality groups, and seismic and wind classifications.

### 3.1.3 System Design Descriptions

The SDDs establish the requirements, descriptions, operating modes, and set points for

the systems, structures, and components comprising the ANS facility. The set of SDDs is derived from the project's WBS to assure that all systems are identified and documented. The process draws requirements from the PDR document and adds others at the system level. The author of each SDD is the responsible engineering designer for that system.

First drafts of the set of SDDs were released in May and July 1991, with emphasis in each document on the first chapter that deals with requirements. This first chapter defines specific functions as well as design and safety requirements. Other key features of these documents include the use of interface tables to identify the specific ties to other systems and requirements traceability. The interface tables address the aspect of requirements placed on a particular system by other systems, as well as requirements placed by the particular system on other systems. The requirements traceability table provides a means to identify the source of each requirement.

A subset of the SDD deals with those elements of the facility that have functional interfaces with more than one other system. These systems are documented by use of a set of Integrating System Design Descriptions, whose purpose is to identify the particular functions involved and to allocate specific functions and requirements to the appropriate hardware systems for incorporation into those systems' requirements documents. Examples of integrating systems include the reactor containment, reactor shutdown and cooling systems, overall plant control, environmental control and monitoring, and safeguards and security systems.

### 3.1.4 Document Control

Document control and records management are also key components in the configuration control process. A formal document control approach has been initiated through the use of a high-level project review board to approve formally controlled documents and procedures. This board is chaired by the ANS project director and includes each of the key managers on the project. Meetings are held on an as-needed basis and are the mechanism by which the PDR documents, the project's QA Plan, and various project-specific policies and procedures were approved and released for implementation.

## 3.2 REACTOR SYSTEMS

### 3.2.1 Reactor Assembly Configuration

Design changes to the reactor assembly configuration have continued throughout the year. A depiction of the reactor assembly as defined at the early stages of the conceptual design is indicated in Fig. 3.1.

### 3.2.2 Core Pressure Boundary Tube

Design activities have concentrated on the development of a concept for the CPBT that will meet all requirements, including satisfactory accommodation of all identified potential failure modes. The primary requirement governing the design of the CPBT is to provide an adequate flow of cooling water to the fuel element assembly under conditions where an individual component of the CPBT might fail. Analyses using dynamic system modeling indicate that failures of a single-walled CPBT downstream of the fuel element can be tolerated. However, a CPBT failure upstream of the fuel element must also be accommodated in a manner that would provide coolant flow through the fuel element assembly sufficient to permit shutdown of the reactor in a safe manner.

The configuration that resulted from these design studies is a concentric cylinder double-walled arrangement in which the outer wall acts as the pressure boundary during normal operations. A schematic diagram illustrating this concept is shown in Fig. 3.2. As indicated, the CPBT is configured so that it allows coolant to pass through a series of passages at the lower end to provide cooling in the annular space between the outer and inner walls. This annular flow path is designed with a flow restriction sufficient to

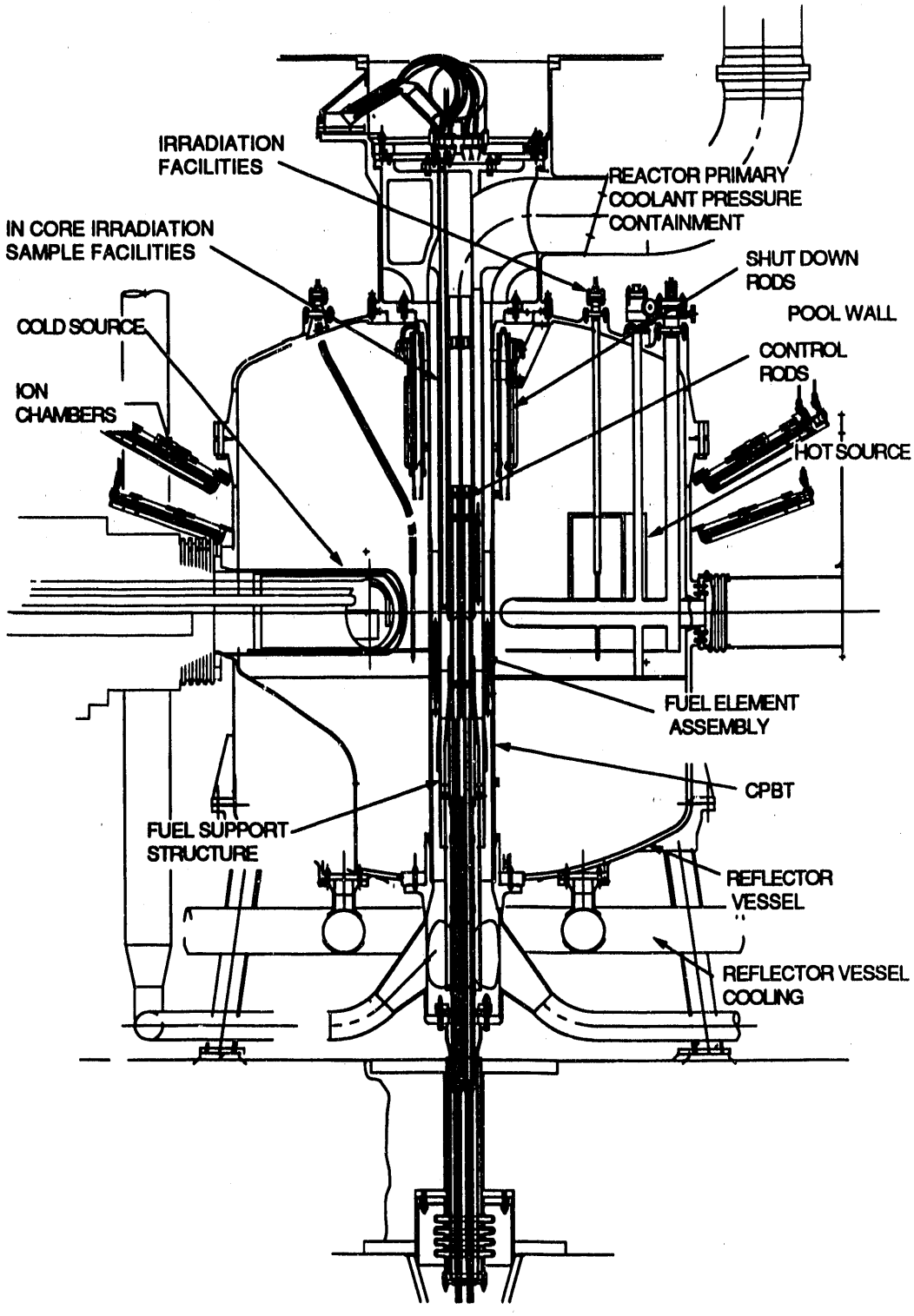


**Fig. 3.1. Reactor assembly showing internal components.**

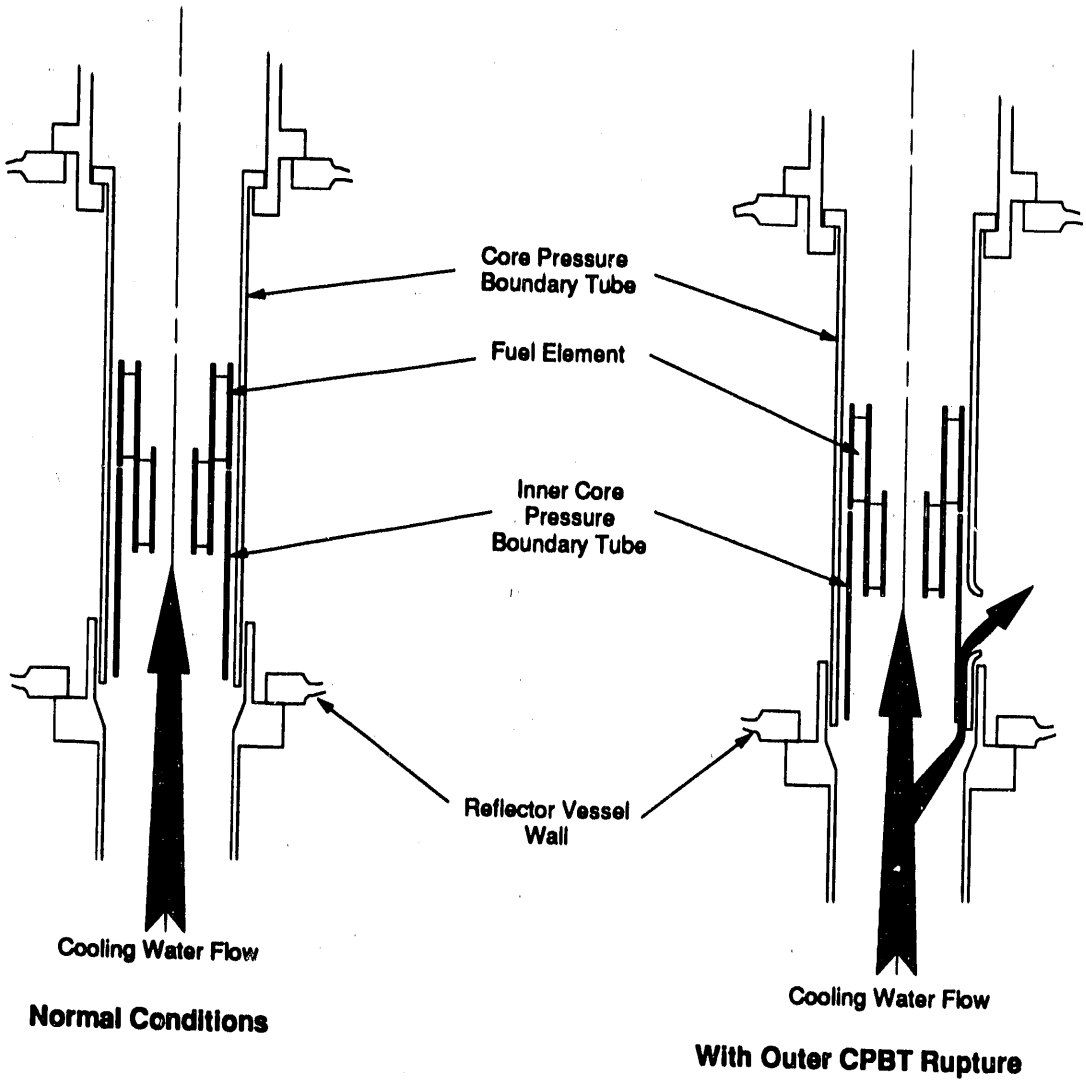


**Fig. 3.2. CPBT conceptual schematic.**

match the pressure drop across the fuel assembly. This flow restriction also results in the lower-inner wall operating under a compressive pressure load during normal operating conditions. This compressive pressure load acts to prohibit any potential flaw growth that could lead to failure of this component. Inspection verification that the inner CPBT wall is free of detectable flaws when initially installed, in conjunction with the compressive load operating condition, will assure that the integrity of this component of the CPBT is maintained during its defined operating life.

The flow passages in the lower-inner wall are sized to limit flow into the reflector vessel to less than that of a failed 200-mm pipe, which has been postulated as the maximum failure event upstream of the core. If there is a rupture of the outer (CPBT) wall, the pressure between the inner and outer wall will drop to an intermediate pressure depending on the severity of the break. The lower-inner CPBT wall would then be a flow restrictor, reducing the rate of loss of coolant to an acceptable value, and would be subjected to internal pressure loading. The inner wall is designed to be capable of withstanding this full pressure difference across the wall with margins consistent with off-normal operating conditions. This type of design is characterized, following the

practice in the Clinch River Breeder Reactor Project, as a "pressure vessel with an internal guard pipe."

The seals at the CPBT that interface with the primary-coolant system piping have continued to be an important factor in the design of the CPBT, the fuel assembly support, the reflector vessel, and the refueling and maintenance system. The CPBT conceptual configuration has a hard-seal bolted flange at the upper end and a labyrinth arrangement at the lower end to restrict the flow from the high-pressure primary-coolant system into the low-pressure reflector-coolant system. This configuration facilitates the removal and replacement of the CPBT and allows for thermal expansion of the CPBT. However, studies of positive seals to replace the labyrinth are continuing.

### 3.2.3 Reflector Vessel

Preliminary analyses using the *ASME Pressure Vessel Code* were performed to determine the reflector vessel wall thickness for two conditions: (1) internal pressure requirements associated with the heavy-water cooling systems for the reflector vessel and (2) an evacuated reflector vessel submerged under the light-water pool. These analyses identified the external pressure as the determining factor in wall thickness. The present vessel concept is based on a membrane wall thickness of about 18 mm. Conceptual designs have been defined for the reflector vessel's support structure, based on bolted joints to the reflector vessel with all fastener axes oriented vertically for access from above using tooling and equipment that can be manipulated in a vertical orientation. Calculations have also been made that define the weight of the vessel, the internal components, and the heavy-water inventory within the vessel to be approximately 40,000 kg.

### 3.2.4 Control Rods

The current configuration of the inner control-rod system is a refinement of earlier concepts using a spring-driven scram system with the springs located within the high-pressure heavy-water primary-coolant system. In these concepts, the springs are located below the core, which results in a smaller outside diam and a longer length for the initial acceleration spring.

Other designs were investigated where the springs were moved as far from the core as is practical. One concept used two scram acceleration springs, one above and one below the core. That design also included a means of replacing the upper spring without removing the control rods.

The outer shutdown rod system design has progressed through a series of major iterations. The rod assemblies no longer penetrate the bottom of the reflector vessel into the subpile room, and the design concept has changed from a magnetically latched system, similar to the inner control-rod scram system, to an arrangement depending on hydraulic pressure to keep the absorber in the withdrawn position. When this hydraulic pressure is interrupted, the absorber units are driven into a shutdown configuration by springs aided by gravity. There are eight shutdown assemblies located within the reflector vessel 400 mm above the top of the fuel element assembly. Each assembly is comprised of a hydraulic cylinder with a spring acting on a piston with a force acting in the downward direction. During operation, a flow of heavy water, through clearance around the piston and through bleed holes in the piston, lifts the piston against the spring force and also provides cooling of the piston and cylinder. A signal to scram would trigger a valve venting the pistons. The top side of the piston is open to the reflector heavy water in the reflector vessel so that any pressure excursion in the reflector vessel would tend to aid rather than impede the insertion of the rods. A schematic representation of the concept is shown in Fig. 3.3.

### 3.2.5 Refueling

The design work on this topic has concentrated on parallel development and comparison of a refueling machine concept and a stack-and-tunnel concept. At this time a revised

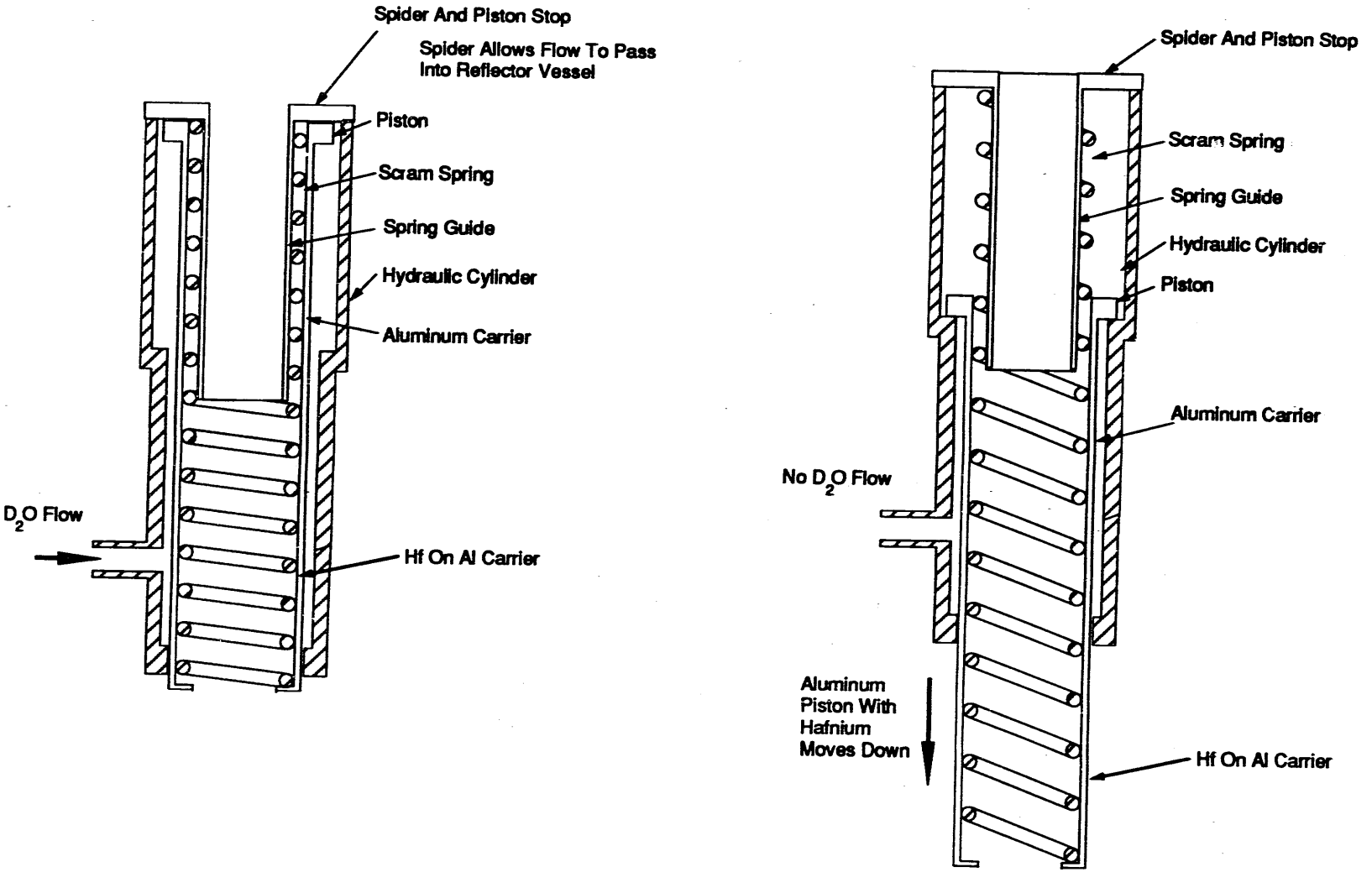


**Fig. 3.3. Outer shutdown rod hydraulic-actuation system schematic.**

stack-and-tunnel concept, as shown in Fig. 3.4, is the preferred choice. There are several important topics that still need to be addressed, including decay heat removal, maintenance access, and controls for the remote handling equipment.

A conceptual arrangement of hydraulically actuated bolt-turning devices coupled to remote tooling has been developed, providing a system to remove the materials irradiation capsules and provide access to the fuel elements. A poison-rod assembly has also been defined for use in handling the fuel during those periods when the fuel is being removed or installed in the reactor. This concept is shown in Fig. 3.5. The poison-rod device will be mechanically interlocked so that control-rod position, auxiliary absorber systems, and the structural interlock latches are in the correct position before any fuel element can be moved. This assembly contains a three-lobed array of absorber material that fits between the inner control-rod components within the central hole in the fuel element. Other items in this assembly provide for locking the entire assembly to the fuel element and for unlatching the fuel element from the CPBT and associated supporting structural components.

## 3.3 EXPERIMENT SYSTEMS

The first draft of the SDDs for all experiment systems elements was issued in May. This draft focused on Chap. 1, the Function and Design Requirements. Future revisions will include the systems' descriptions.

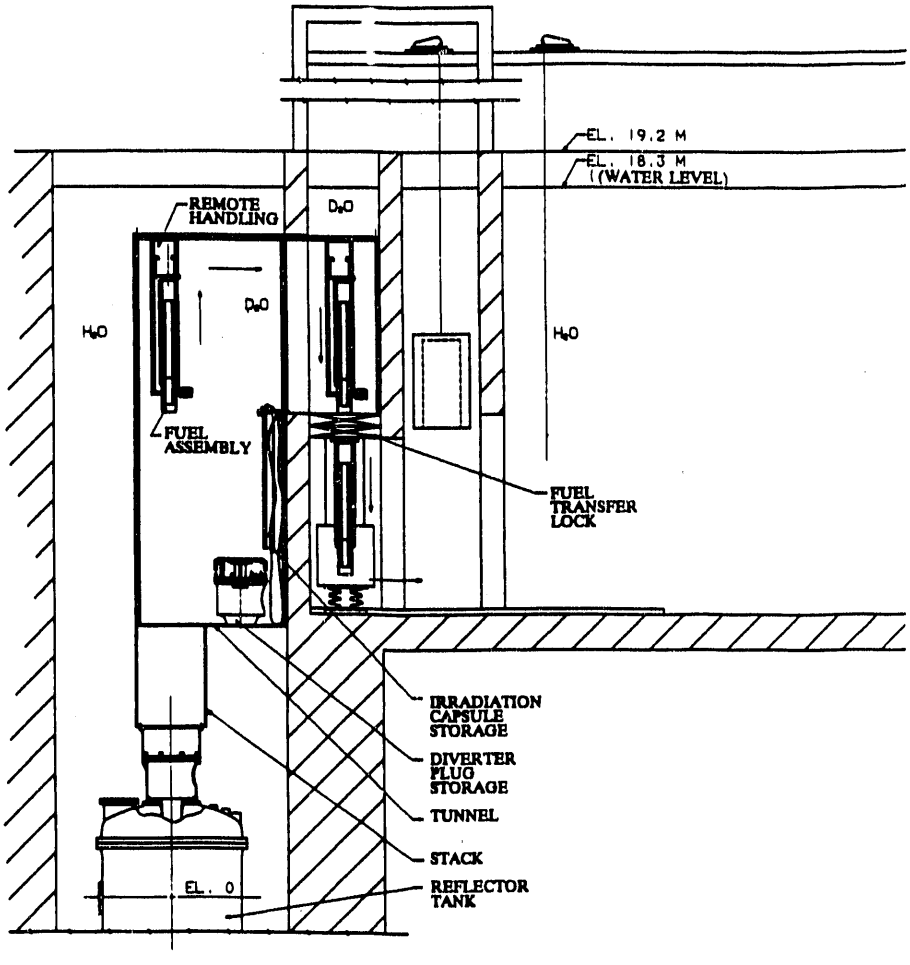


**Fig. 3.4. Refueling concept showing fuel assembly removal through a stack-tunnel concept.**

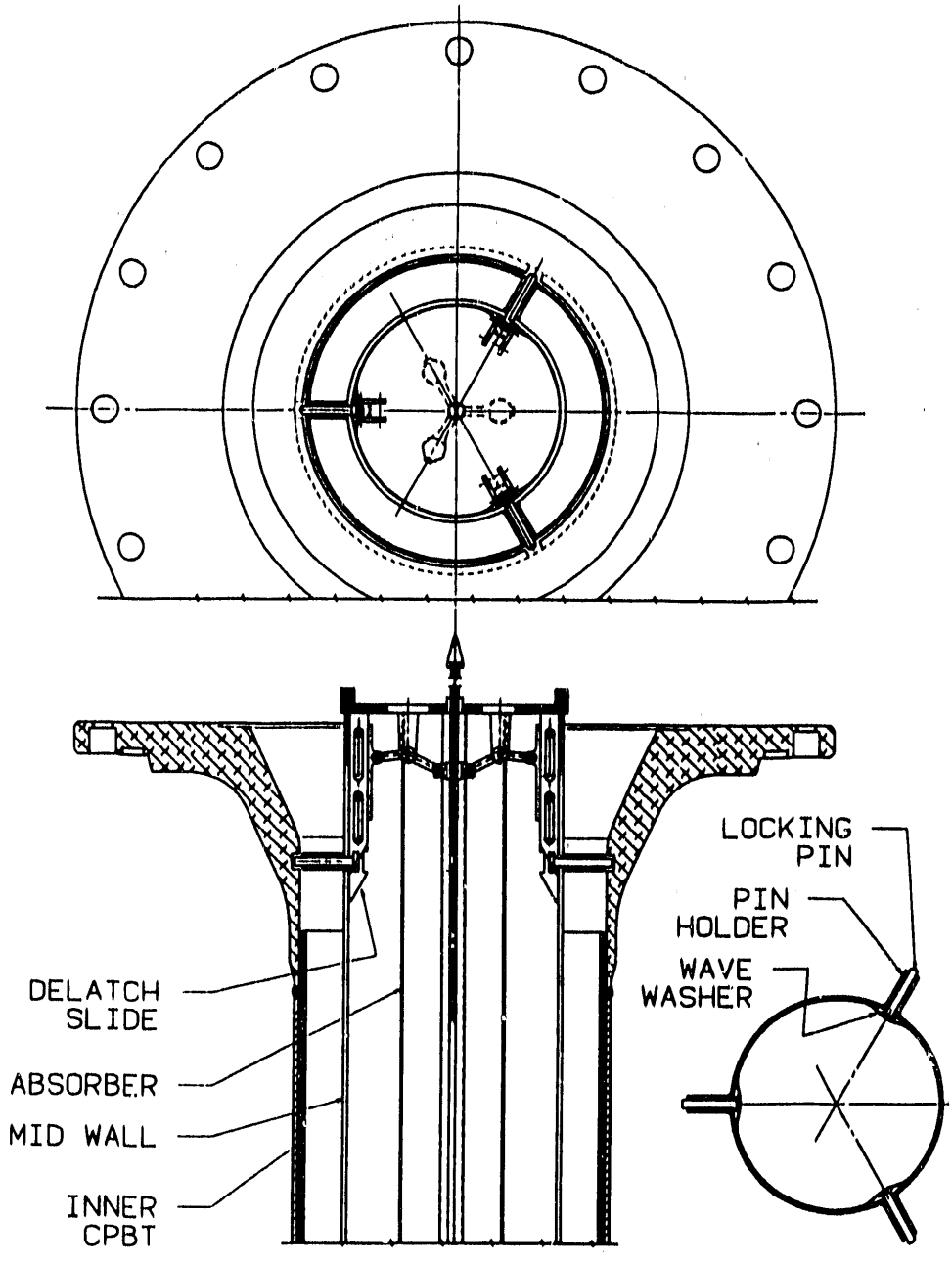


**Fig. 3.5. Poison-rod assembly concept for use in fuel element handling.**

### 3.3.1 Irradiation and Production Facilities

A workshop was held in December 1990 on the Materials Irradiation Facilities. The workshop panel felt that the project had done an excellent job in addressing the needs of the materials community. They did comment that the ANS cannot fulfill all of the research needs in this field and that other neutron source facilities will be needed.

The two slant-irradiation tubes will be moved to resolve an interference with the shutdown rods. This will be accomplished after the shutdown rod geometry and location are finalized.

There has been no change in the design for the transuranium production targets outside the lower fuel element.

Three hydraulic tubes will be dedicated to isotope production, and a fourth hydraulic tube could also be used if needed. The vertical holes for isotope production have been changed from seven at varying radii to four at the same radius. Different flux levels can be chosen by varying the axial location of the samples.

### 3.3.2 Analytical Chemistry Facilities

The in-tank analytical chemistry facilities for activation analysis were revised in response to input from the research community. The pneumatic tube systems were increased from three to five within the reflector tank (four 40 cc and one 2 cc), and two more were added in the light-water pool (120 cc and 40 cc). The location and orientation of the reflector tank tubes were also changed to place them in a region with relatively low gamma heating and the sample axis aligned normal to the heating gradient so that sample dose levels could be equalized by rotating the samples. A schematic diagram of the pneumatic and hydraulic tube systems is shown in Fig. 3.6. All pneumatic tube samples to and from NAAF-2, the analysis laboratory outside of containment, are routed through a transfer station for security. Samples coming from the reactor that must be analyzed rapidly are counted at NAAF-1, which will be located near the transfer station. The hydraulic tube will connect to a hot cell for loading and unloading samples.

### 3.3.3 Main Floor Beam Transport

Significant improvements in the beam transport and instrumentation layouts have been made as shown in Fig. 3.7. The beam-line locations have been selected based on the specified instrument set and the desired ranges of travel for detectors. This layout also incorporates supermirror thermal guides that improve the space utilization. This assumption is based on recent encouraging results from the R&D program. Conceptual designs for standard beam-tube plugs have been developed (Fig. 3.8) that allow for horizontal installation and removal.

The new layout includes one larger beam-tube penetration in the reflector tank and a biological shield that has been designed to allow for a future thermal guide-hall expansion with four thermal guides as shown in Fig 3.9. No changes in the reflector tank or biological shield penetration would be required for the expanded beam-guide system. This arrangement could also be adapted to an additional horizontal cold source (see below) and cold guides.

### 3.3.4 Horizontal Cold-Source Proposal

A recent proposal has been made to consider a horizontal cold-source configuration vs a vertical configuration. The potential advantage for users is an increased cold flux because of the elimination of a heavy-water gap and two structural walls between the $D_2$ cryostat and the guide system. In this configuration, the very cold guides would come out horizontally, and it is likely that the instruments would be located on the main beam floor as shown schematically in Fig. 3.10. Neutronic evaluations and a decision on whether this option should be adopted will be made early next year. Layout work on the second-floor instrument set is on hold until this decision is made. One second-floor addition that will be made is a positron experiment system.

### 3.3.5 Guide-Hall Layout

A realistic instrument set layout has been developed as shown in Fig. 3.11. This layout incorporates some minor beam-line changes, including splitting the analytical chemistry beams and adding a new station by splitting the beam used for the L12 physics experiment station, using the transmitted as well as the reflected polarized beams. The layout includes space allowance for shielding and expected detector travel ranges.

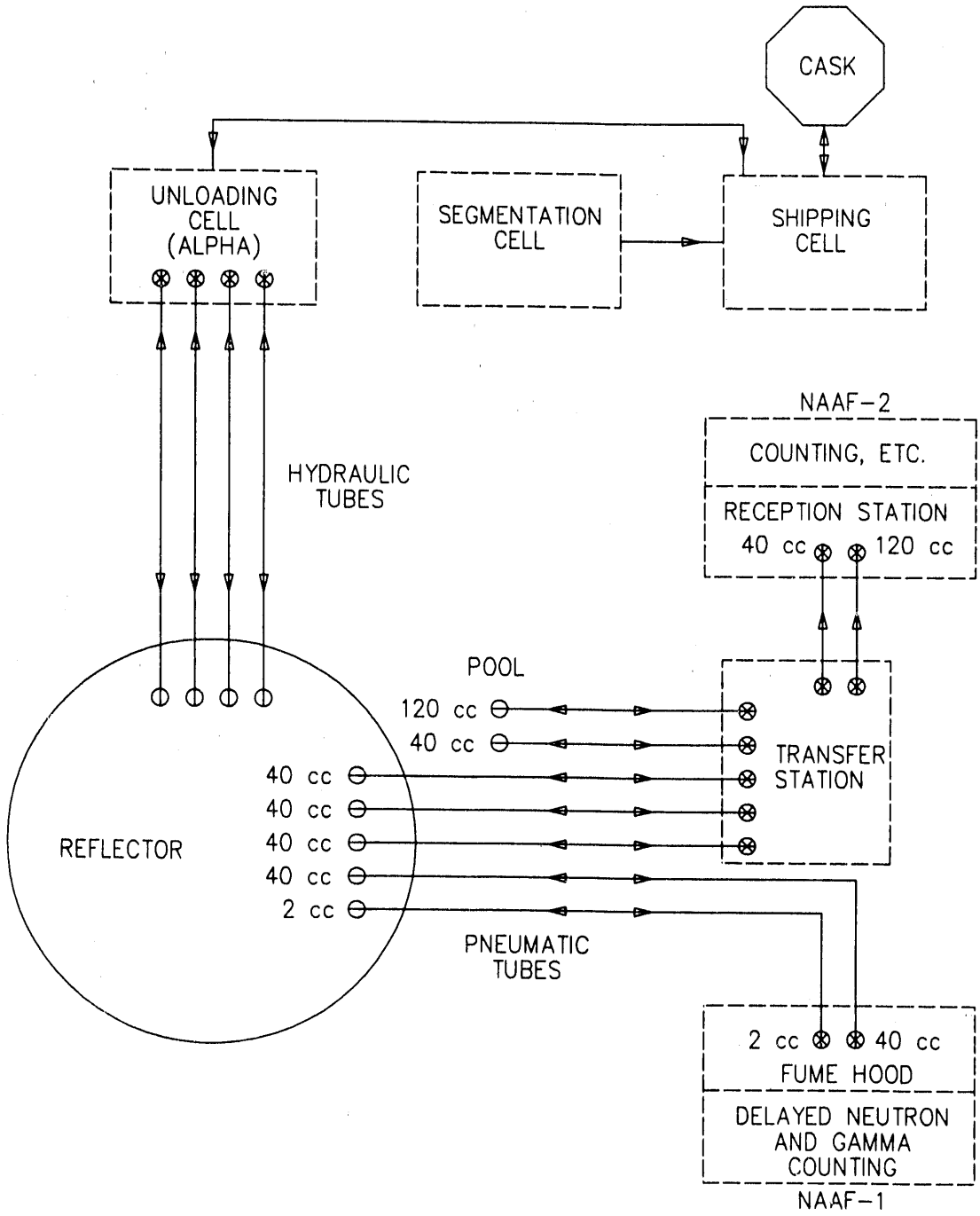


**Fig. 3.6. Schematic diagram of the pneumatic and hydraulic tube systems.**

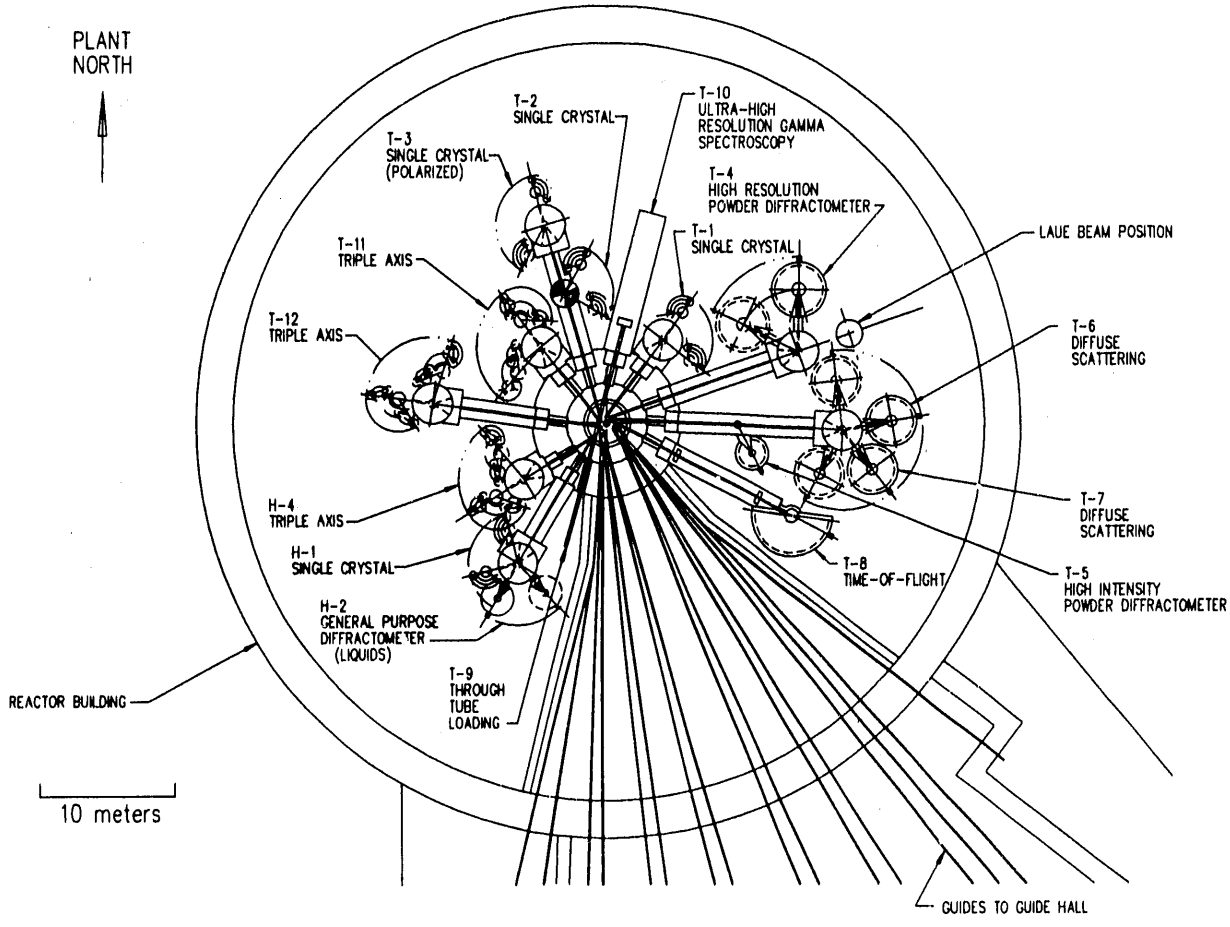


**Fig. 3.7. Ground-floor beam-room instrument layout plan view.**

## 3.4 SITE AND BUILDINGS

### 3.4.1 Site and Facility Design Effort

The end of FY 1991 marked the culmination of an intense effort to understand the best utilization of a preferred ANS site located on the DOE Oak Ridge Reservation (ORR). A proposed site layout, prepared by the team of Gilbert/Commonwealth, Inc., and DRS Architects/Planners, was preceded by a careful analysis and prioritization of numerous criteria that laid the foundation for a user-friendly facility design.

A comprehensive ANS Site and Facility Criteria data base was developed containing a discussion of user needs and requirements of the ANS as well as an expanded description for each of the targeted functions, spaces, and buildings. The data base provides information on general, architectural, structural, electrical, HVAC, experimental systems, security, safety, ALARA, industrial hygiene, and general support criteria for each of the functions/spaces. It was developed to function as a tool for storing, sorting, and retrieving information as well as for identification of areas of conflict that require further study. The data base, which currently lists more than 400 records, is constantly updated.

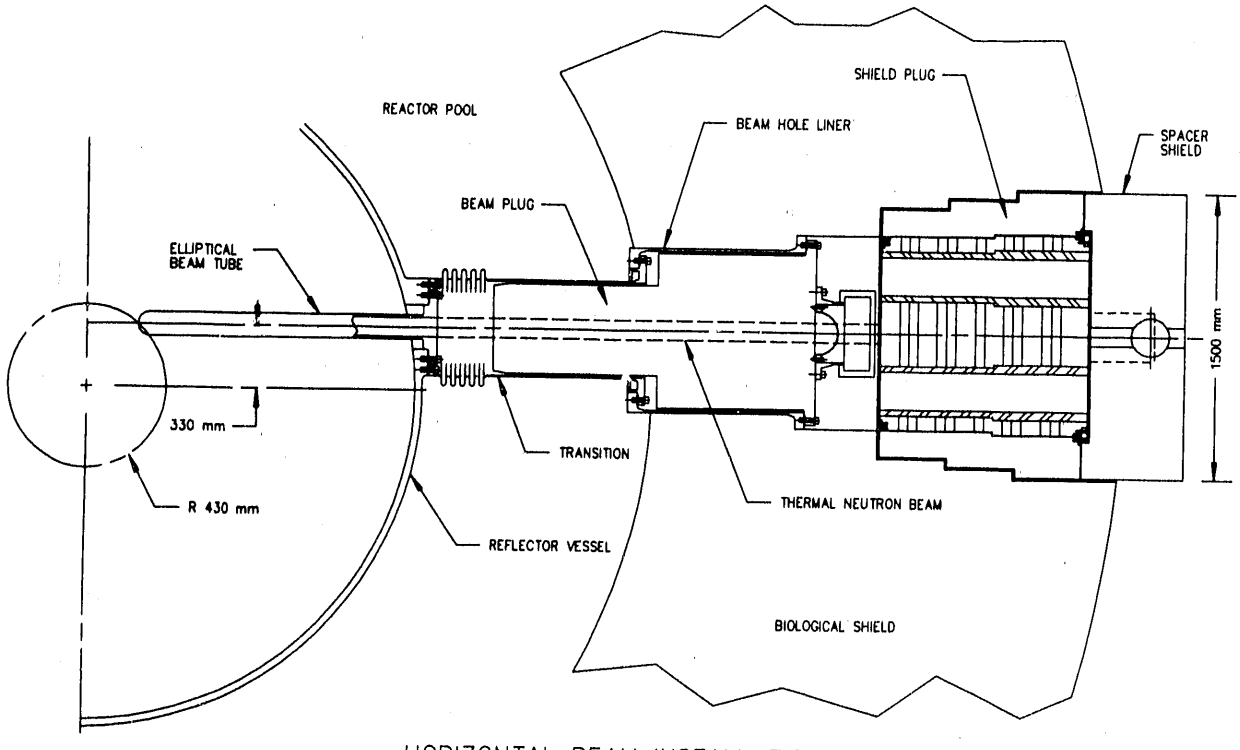


**Fig. 3.8. Conceptual design for a standard beam-tube biological shield penetration.**

Some of the key design requirements identified as important for a user-friendly facility are (1) a design that clearly separates users from security areas and minimizes their exposure and interaction with nuclear-grade security, (2) an arrangement that accommodates zoning and flow patterns including security zones, flow of personnel into and within the complex, flow of neutrons from the reactor, flow of materials, flow of exhaust, and evacuation flow patterns, and (3) a layout with capacity for growth through building expansions and possible additional facilities on the site.

Essential to the user-friendly approach is a design (Fig. 3.12) that divides the facility into three distinct activity zones, each with a different level of security and safety requirements, without sacrificing the close-knit arrangement that minimizes distances and reduces confusion and disorientation in a large facility. This approach also facilitates possible expansion of each of the facility's buildings without encroaching on the other buildings or limiting their capacity for future growth. The main entrance to the building for all personnel (Fig. 3.13) is located in the lowest security zone (Zone I), which is comprised mainly of the office building for the scientists, their visitors, and program personnel, and as such, will also be readily open to visitors. This zone includes an observation gallery and an exhibit area that will be open for tours. Access from Zone I to Zones II (experiments) and III (reactor operations) is

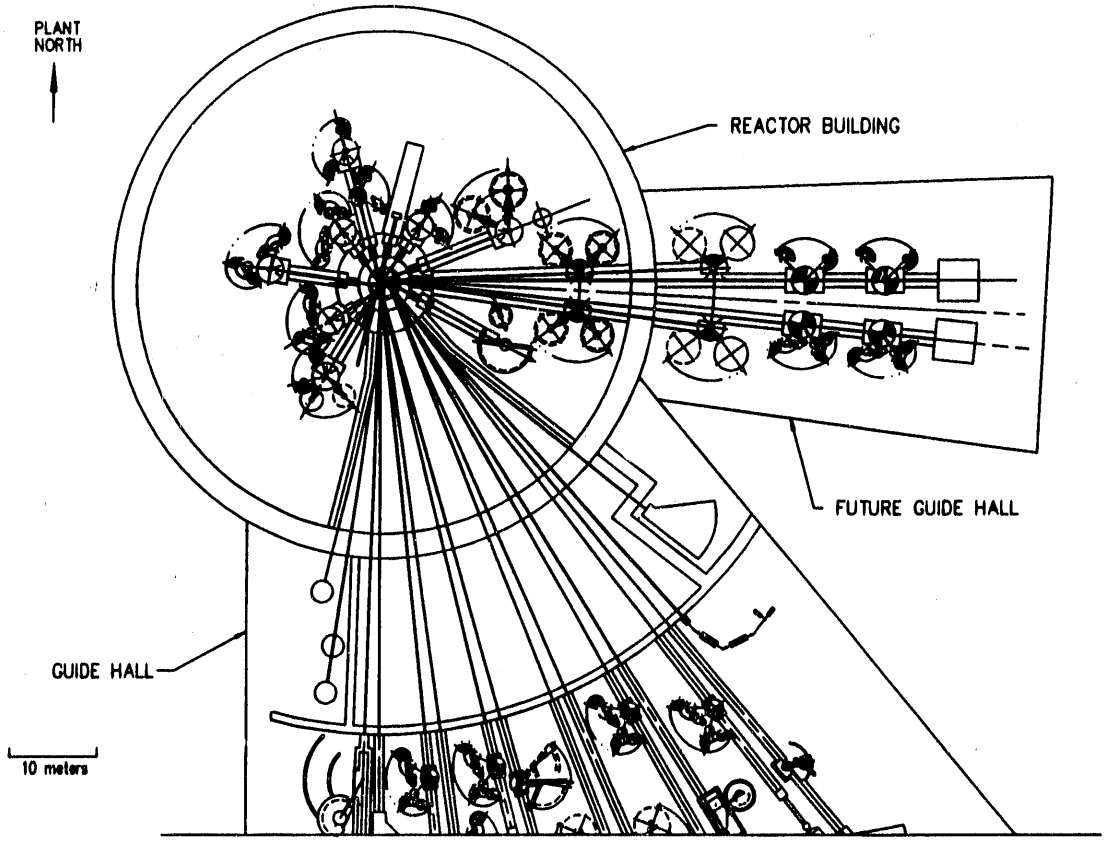


**Fig. 3.9. Future guide-hall expansion conceptual layout plan view.**

limited and is controlled in the interface building (corridor) that provides the central security checkpoint as well as the health and safety buffer. Zone II includes the research support shops and laboratories, a guide-hall building, and the beam rooms in the reactor building. Zone III is comprised of the facilities dedicated to the operation of the reactor, including the operations areas of the reactor building, the reactor-support building, and the operation-support building. Safety and security requirements mandate that this zone be accessible only to people assigned to these areas, and therefore additional security is required to prevent entry to this zone from the other two zones.

In the development of the site plan, there was considerable discussion of zoning requirements, access control, and security requirements. The visual appearance of the facility, including the field of view upon the initial approach to the facility, was also addressed. Work with structural and geotechnical engineers led to the understanding that a saddle of land, rising off low drainage areas in the valleys, offered the potential to locate the ANS facilities above wet areas and provided the elevation changes necessary for implementation of passive cooling concepts. An architectural theme based on a beam-line array was used to establish a discipline throughout the planning process. Estimates of the

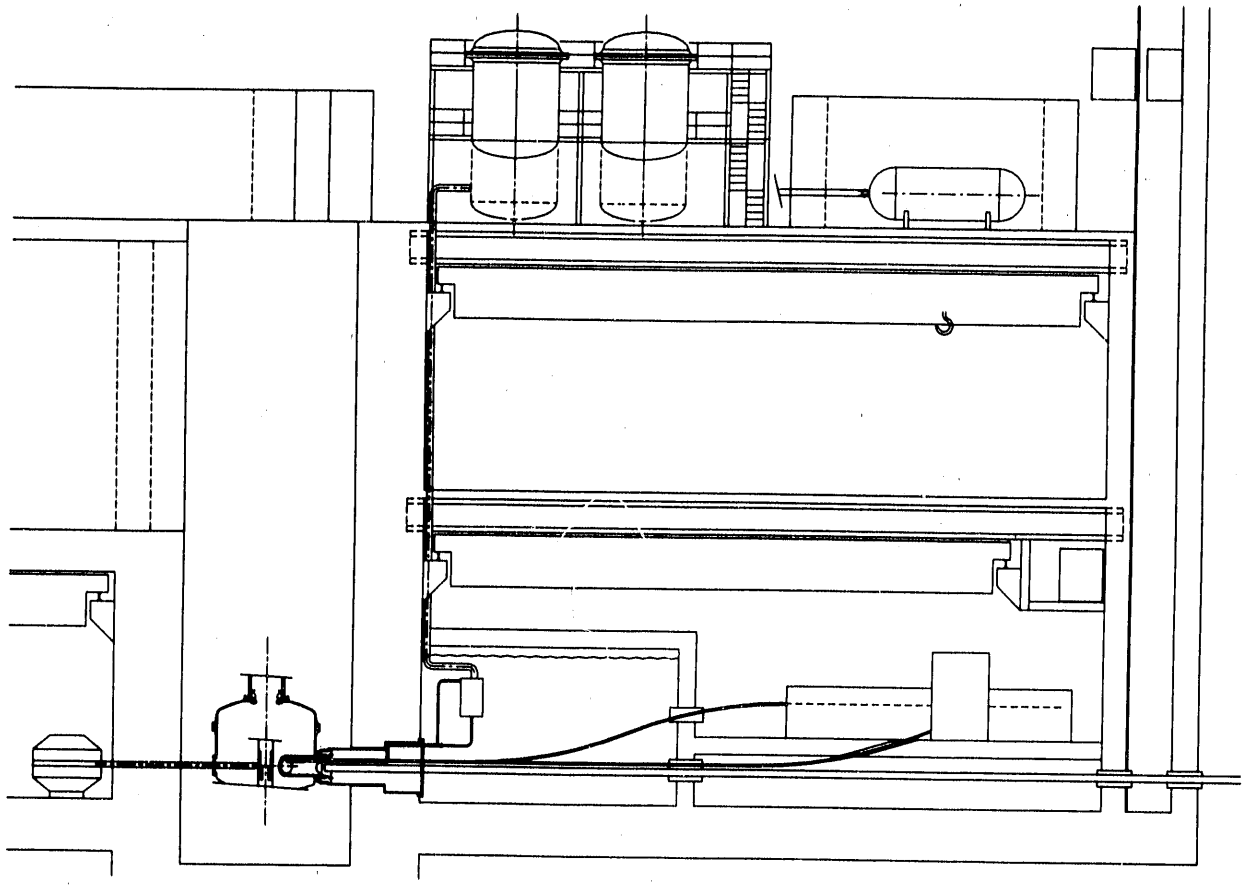

**Fig. 3.10. Horizontal cold-source arrangement and instrument layout section view.**

depth to competent rock, based on preliminary site characterization activities, were used to select the elevations of the complex. The general orientation and elevation of the facility was also influenced by the need to lay out the beam-room floor and guide-hall floor on solid footings (the reactor building would be supported entirely on bedrock). Since the horizontal as well as the vertical relationship among the reactor building, guide hall, and research-support building have been very carefully worked out to meet both the beam layout and equipment flow (including overhead crane coverage and location of a truck-unloading bay in the guide hall adjacent to the research-support building), preserving this relationship posed additional constraints on the selection of elevation. The orientation of the reactor-support functions provides for the necessary elevation changes (particularly for the secondary-reactor cooling basin pools and tower structures) as well as for access to utility corridors in an efficient manner.

The resulting site plan attests that a general understanding of the overall design approach to major systems locations and site utilization and the general arrangement of major buildings, structures (including the cooling towers, electrical substations, and stack), utility corridors, roads, and fencing has been achieved.

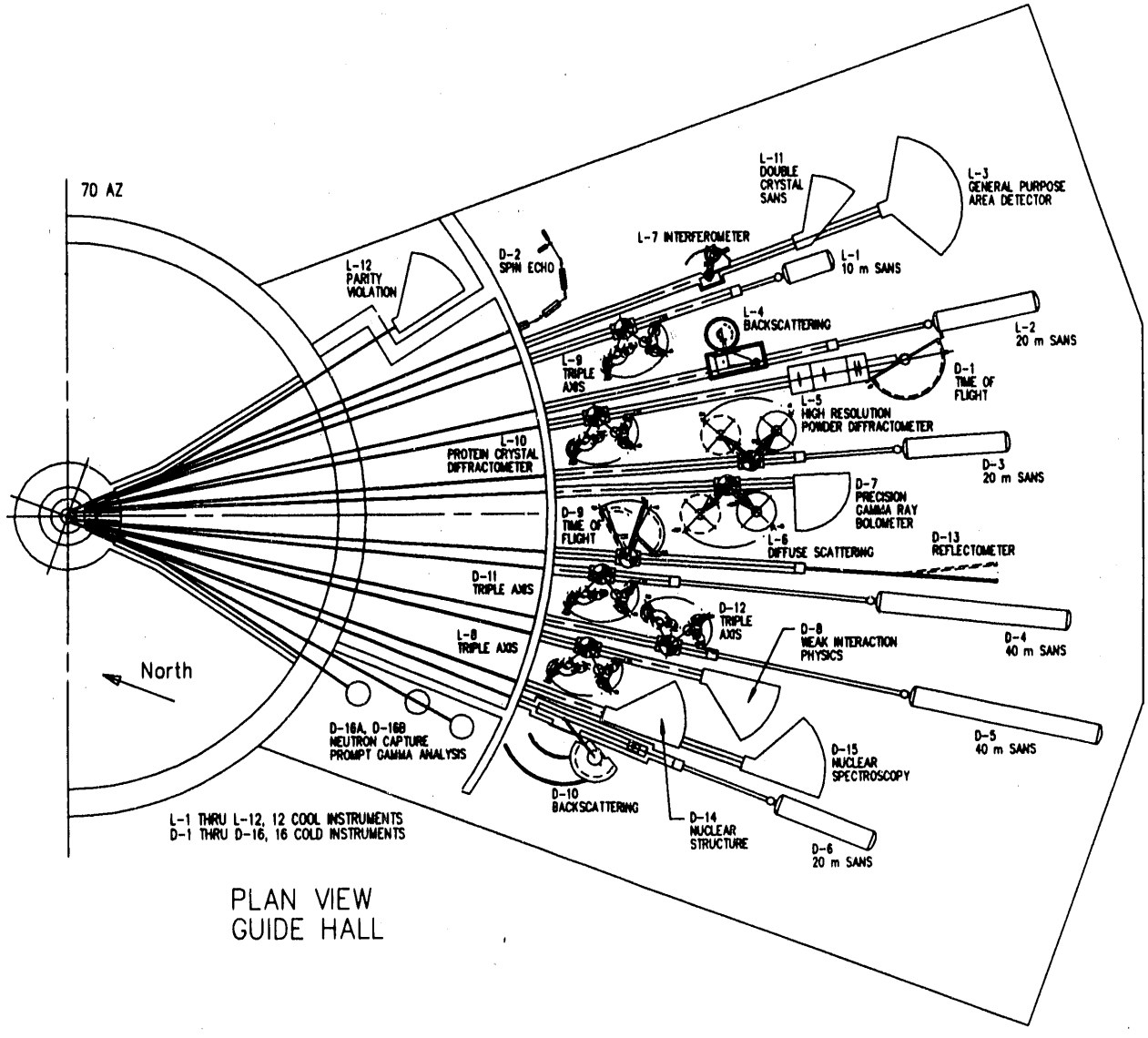


**Fig. 3.11. Guide-hall instrument layout plan view.**

### 3.4.2 Reactor Secondary-Cooling System

Definition of the conceptual design for the reactor secondary-cooling system (RSCS) was one of the first tasks initiated by the A/E team. This effort has been accomplished with the A/E team building upon the work that had been completed by the ANS Project team in 1990. The focus of the work has been to understand and strengthen the concept of passive cooling. Results from recent studies include moving the elevated cooling-water basins as close to the reactor building as feasible, simplifying the geometry of safety-related piping, and eliminating the need for safety-related pumps. Cooling systems associated with the reflector tank are also provided with the location of reflector-tank heat exchangers in parallel with the main heat exchangers. The present concept retains the ability to provide emergency short-term cooling (up to 72 h) through

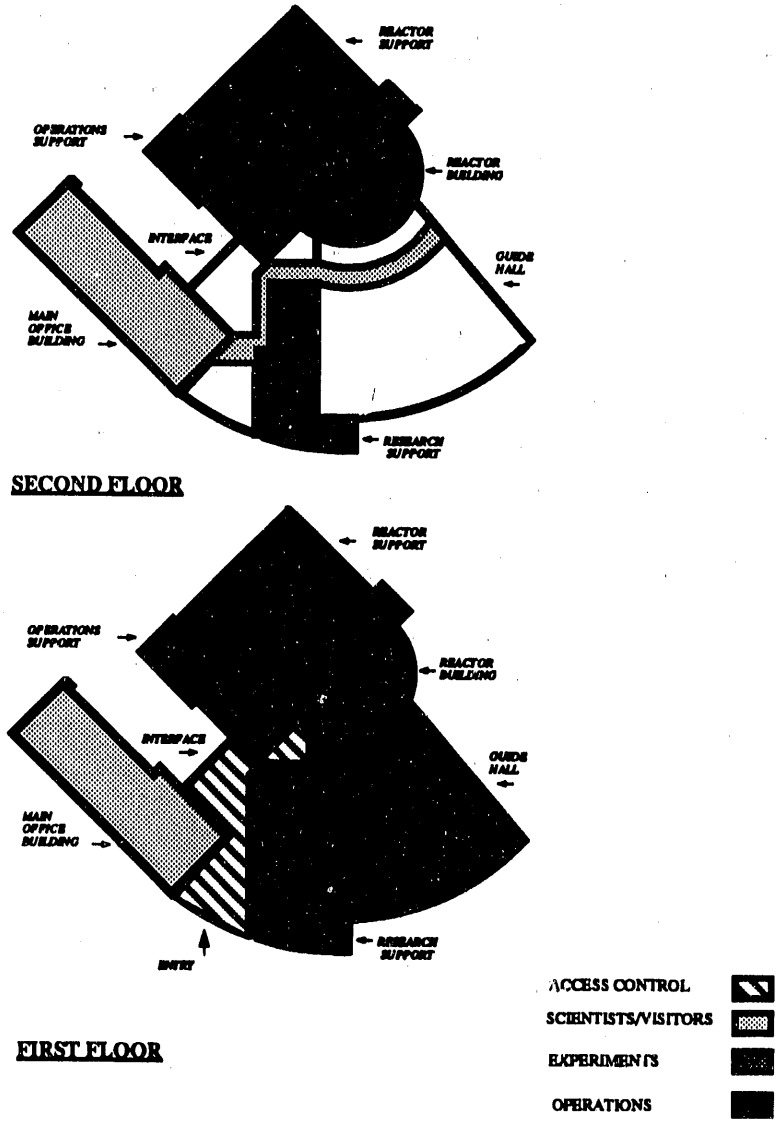


**3.12. Facility layout schematic showing activity/security areas.**

the use of emergency heat exchangers and the heat capacity of flooded equipment cells.

The RSCS, as shown in Fig. 3.14, provides for the removal of both fission and decay heat from the reactor primary-cooling system and the reflector tank-cooling system to the atmosphere for all modes of operation while the fuel element is in the reactor. The system operates in forced circulation modes during normal reactor operations and in either forced or natural circulation modes during shutdown and emergency operating modes.

The RSCS is comprised of four separate and independent loops, each containing a main heat exchanger, an emergency heat exchanger, a reflector-tank heat exchanger, a main circulating pump, a strainer, a mechanical draft-cooling tower, a seismically qualified basin, a flooded equipment cell, containment isolation valves, and the piping, valves, and instrumentation necessary to meet all design-basis operating events. A side-stream filter, a pump, and a blowdown line are provided to control the quality of the water.

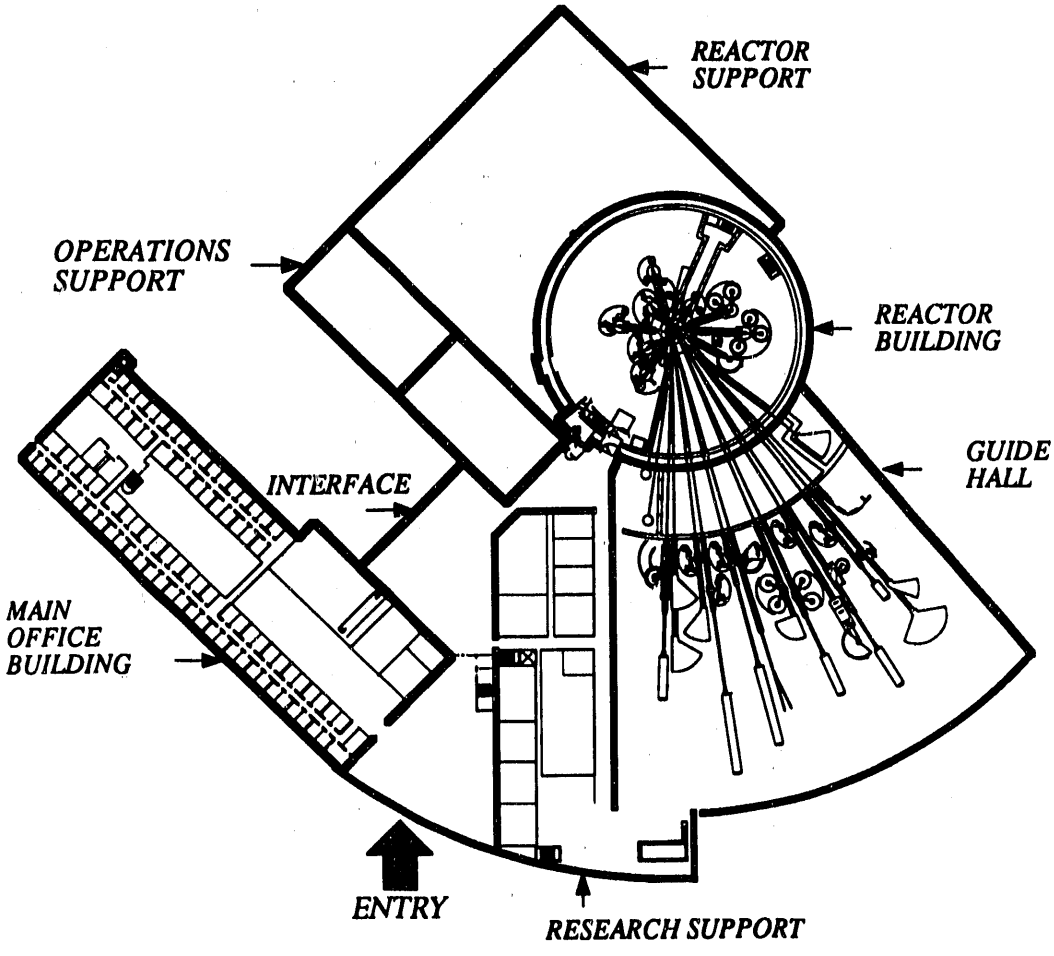


**Fig. 3.13. Facility plan view showing primary buildings and functions.**

During normal full-power operations, three of the four loops are required. Water is pumped from the safety-class basin through the main and reflector-tank heat exchangers to mechanical draft-cooling towers where it is cooled and returned by gravity to the basins. The cooling tower fans are speed-controlled to maintain constant basin water temperature as heat loads and ambient conditions vary. This mode of operation maintains relatively constant basin temperatures, thus simplifying reactor control, and provides lower life-cycle costs. Startup and shutdown operations are enhanced by designing the RSCS pumps to pump water to the cooling towers while operating at reduced speed.

For normal and emergency decay heat removal, only one of the four loops is required. Following shutdown of the reactor, the main RSCS pumps may continue to operate at reduced speed until the pumps can be tripped and natural circulation alone utilized to remove decay heat. If normal ac power is not available (station blackout), the basin temperature will gradually increase, but each basin is sized so that three of them can provide cooling for a period of 30 d.

### 3.4.3 Electrical Off-Site Power

The off-site power supply system includes the structures, equipment, and components that

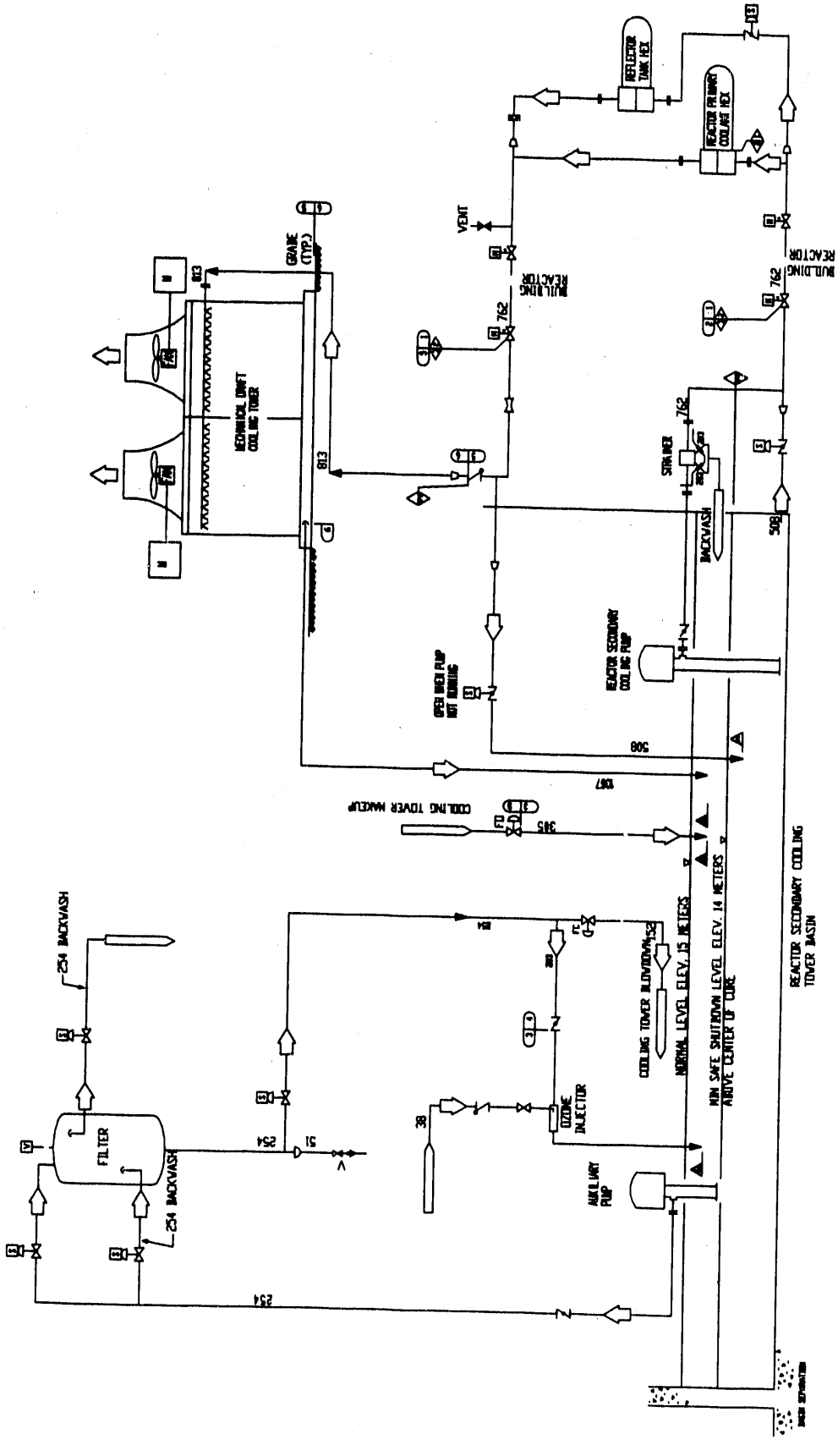


**Fig. 3.14. Flowsheet of the reactor secondary-cooling system.**

deliver the estimated 20 to 30 MW of bulk electrical power to the ANS. Routing of off-site power systems include consideration of the potential exposure to the power lines from on-site structures and utilities (e.g., potential damage to the power lines from a falling ventilation stack) and the potential damage to other ANS support structures should power lines break or their supporting structures fail.

The preferred off-site power supply provides electrical power during normal startup and operating modes and is also the preferred electrical source during accident and postaccident conditions. Preferred off-site power can be provided from the existing Ft. Loudon Dam to the Elza Gate Substation 161-kV transmission line, which is presently owned and operated by the Tennessee Valley Authority (TVA). This transmission line, which passes within approximately one km of the ANS site, would be rerouted to the ANS primary substation.

The transmission line routing provides for two separate points of entry to the ANS primary substation. This routing will allow acceptable separation of the incoming feeders in accordance with *NRC Regulatory Guide 1.155, Station Blackout*, for reliability of preferred power systems. Specific design routing will take advantage of site topography to shield the support towers and right-of-way corridors from view when entering the ANS site.

The ANS primary substation will include suitable circuit breaker arrangements to assure a reliable power supply for ANS while providing continuity of service for the TVA transmission line. The 161-kV power system will be installed above ground because of the prohibitively high cost of underground installation of systems in this voltage range. The ANS primary substation transformers will step the 161 kV down to 4.16 kV for distribution to ANS facilities. At least two transformers will be provided, with the transformers sized so that any one transformer can handle the entire ANS electrical load.

Reserve off-site power would be provided by a new 13.8-kV distribution circuit derived from ORNL's existing Substation 0901. The reserve power supply will be sized to handle only Class 1E loads during periods when the preferred power supply is unavailable. The on-site portion of the 13.8-kV line most likely will be installed below ground.

### 3.4.4 I&C Architecture

A concept defining the architecture to be used for electrical power, instrumentation and controls, and information management systems has been developed, including the connection of equipment to electric power systems; the arrangement of signal cabling systems that carry signals between field equipment, computer hosts, and control-system processors; the interconnection of computer hosts and control-system processors to allow proper data communication between systems throughout the plant; and a highly integrated control-room concept that minimizes dedicated displays and controls.

The major issues driving the conceptual design of this architecture are related to:

1. Licensability—the ANS must conform to the codes and standards used for comparable licensed reactors with the intent that the design would be certified as operable by an organization yet to be determined.
2. Flexibility—the architecture should allow use of the most technologically advanced, commercially proven equipment, systems, operator displays, human factors techniques, and data handling techniques while allowing for possible changes in operation techniques because of advanced technologies.
3. Reactor shutdown and power-control response times—the response times needed for reactor shutdown in response to some accident events and for reactor power control are much faster than those presently used in commercial reactors.
4. Single failure criteria and signal segregation requirements—NRC guidelines, safeguards and security requirements, plant availability requirements, and other sources define numerous signal cabling and equipment separation requirements.
5. Safeguards and security requirements—both DOE Order and NRC requirements must be met.

6. **Multiple reactor shutdown channels and cooling loops—the architecture must provide a reliable, maintainable, highly available, and cost effective way to support four primary reactor shutdown system (PRSS) channels, four secondary reactor shutdown system (SRSS) channels, and four primary-cooling water loops.**

As required by *10 CFR 50* and recommended by NRC guidelines and IEEE Standards, separate Class 1E (reactor safety related) and non-Class 1E systems are provided. The electrical power and signal cabling architecture for these systems is shown in Fig. 3.15 and Fig. 3.16. These components of the system architecture provide the following features:

1. two Class 1E power divisions (designated 1 and 2);
2. eight separate Class 1E signal cable systems—four for PRSS channels and four for SRSS channels;
3. four separate Class 1E Plant Control and Data Acquisition System (PCDAS) channels (signal cabling for the Class 1E PCDAS will be run in the cabling system used for the SRSS);
4. four separate and isolated computer rooms to house the reactor shutdown system and Class1E PCDAS electronics equipment;
5. two non-Class 1E power divisions (designated A and B);
6. two separate signal cabling systems for plant security systems to support redundant plant security hosts;
7. two non-Class 1E PCDAS channels to provide redundancy needed to support plant availability goals;
8. two separate non-Class 1E facility signal cabling systems to provide process control,

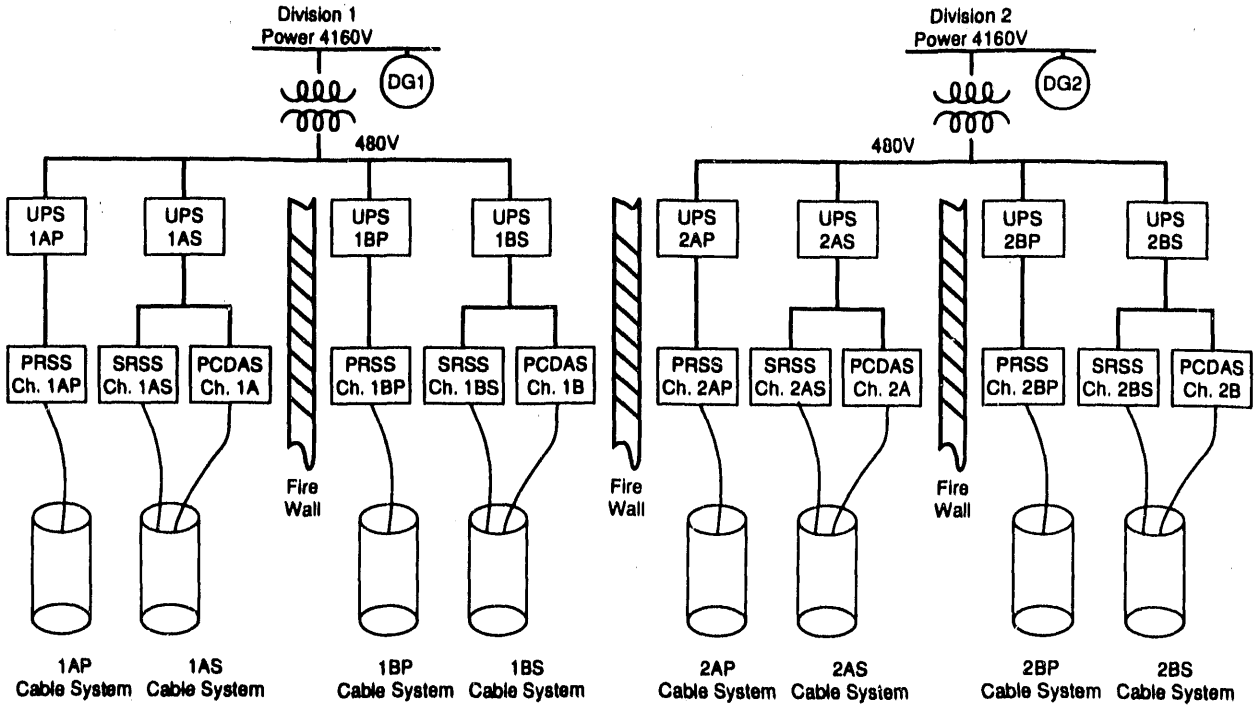


**Fig. 3.15. Class 1E power and signal cabling systems.**

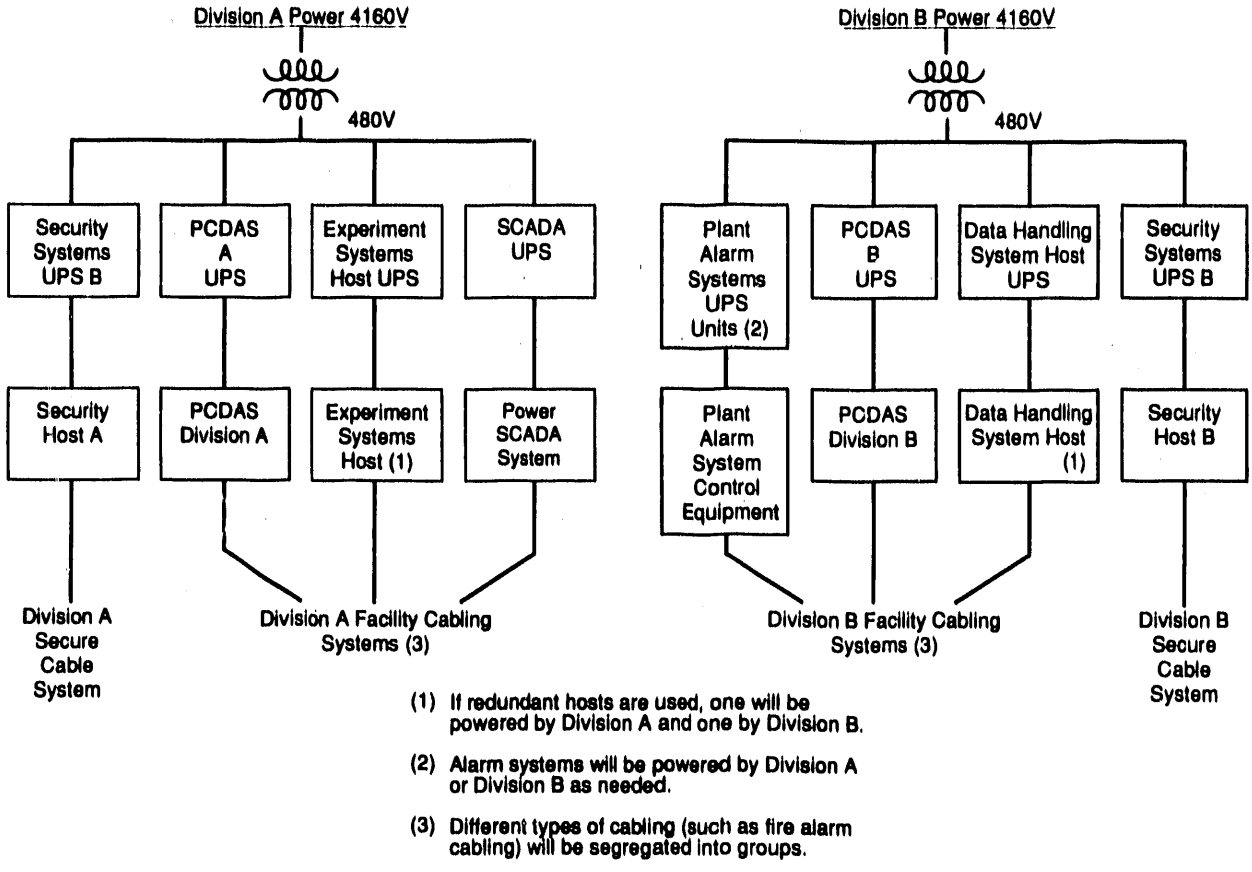


**Fig. 3.16. Non-Class 1E power and signal cabling systems.**

data handling, experiment systems data, plant alarm, and other signal cabling in a manner that supports plant availability goals; and

9. separate uninterruptable power supplies for reactor shutdown system channels, PCDAS channels, security, data handling, experiment system hosts, electric-power Supervisor Control and Data Acquisition Systems (SCADA), and plant alarm systems as needed.

The interconnection of instrumentation, control, and data management hosts is shown in Fig. 3.17, which illustrates several major features including (1) a high-speed, fiber-optic backbone providing capability of file transfer and task-to-task communication between plant data management and control systems with filtering and/or isolation devices to provide appropriate separation of data and (2) separate communicatio systems for instrumentation and control, plant security, business data, experiment data, and other information management systems that allow a graded approach to configuration control, to prevent systems from adversely impacting each other, and to tailor communication techniques used on each system to its particular needs.

The major architectural issues remaining to be resolved include the interconnection of the reactor protection system, PCDAS, and operator display equipment to provide a highly integrated,

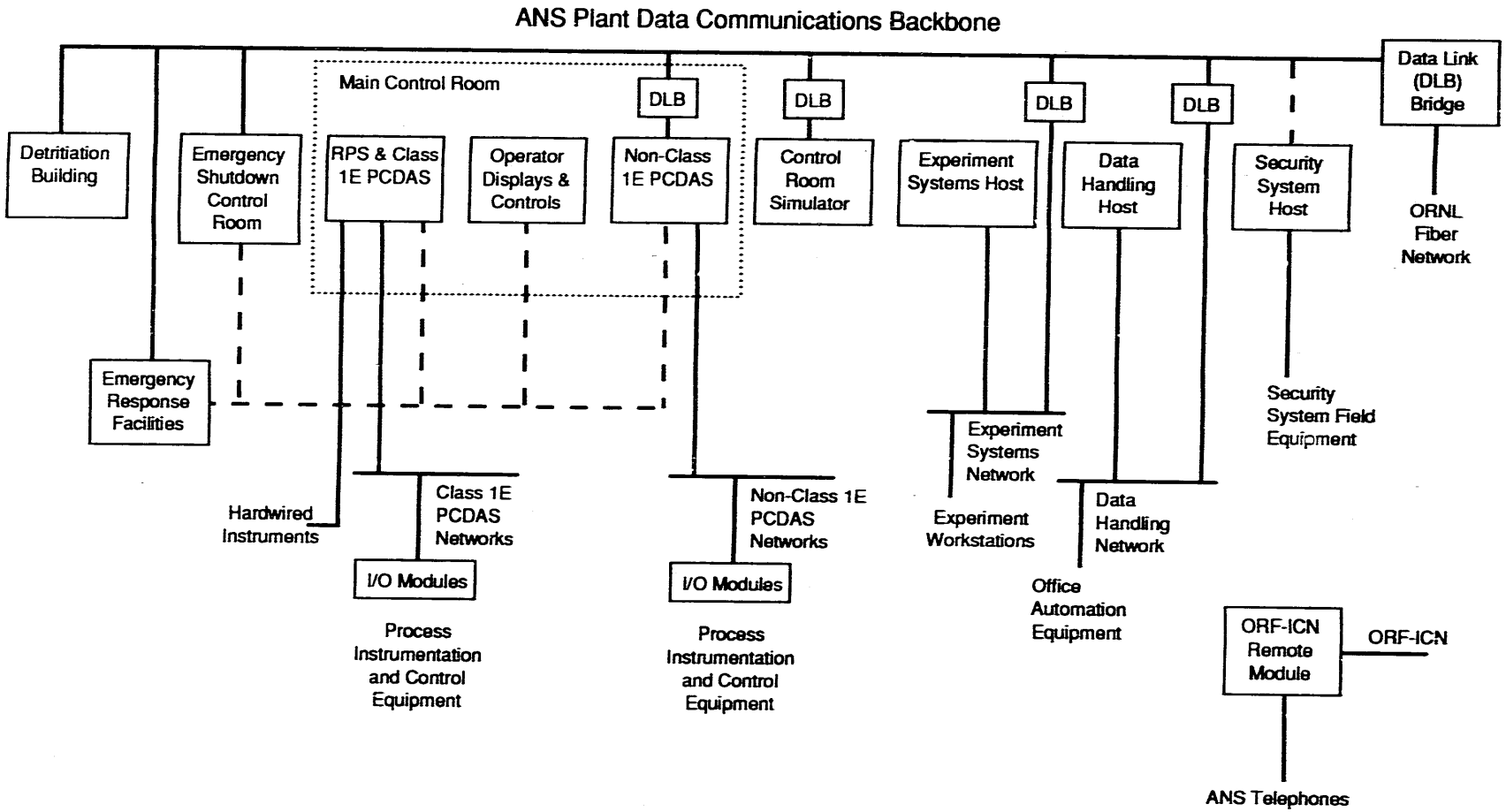


**Fig. 3.17. Data communications interconnection of instrumentation, control, and data management.**

technologically advanced, licensable design with the needed response times for reactor shutdown and reactor power control. An architecture using very few dedicated displays, controls, and data communication techniques to connect equipment is new to commercial reactors in the United States; however, similar architectures have been proposed by several reactor manufacturers for advanced reactor designs and are currently used in other industries. This issue will probably not be resolved until the licensing/certifying agent is known and available for consultation. Other issues are related to the interconnection and cabling method that will allow four shutdown system channels to drive two out of four coincidence logics and subsequently cause insertion of control rods; to the extent to which digital systems can be used to meet licensability and response time requirements; and to determining a graded approach to the Software Quality Assurance program, simplified software in safety-related areas, and hardwired and/or analog circuitry that will meet licensability requirements without overburdening software procurement, development, or verification and validation activities.

### 3.4.5 Environmental Report

Before detailed design can begin, an environmental impact statement (EIS) must be completed and the secretary of energy must sign a record of decision authorizing construction and operation of the ANS. The EIS will be prepared by ANL. ORNL's Energy Division is preparing an environmental report (ER) to facilitate ANL's preparation of the EIS and to assist the design process by identifying impacts that may be avoidable.

Work on the ER began with preparation of a plan, *Preliminary Environmental Impact Statement Implementation Plan for the Advanced Neutron Source*. This plan laid out the relationships among the ER, the EIS, the conceptual design, and the associated safety-analysis report, and delineated the scope of the ER. The ER assesses the impact of the ANS while it is being designed. This allows the design to be modified early in the project, while it is relatively easy to make changes and to avoid or minimize impacts. Similarly, design changes that would minimize the potential of accidents can be made. Finally, by assessing the impacts of the ANS and assembling source materials for use by ANL, the ER will support preparation of the EIS.

In support of collection of geotechnical information for design purposes, the ER team prepared an assessment of environmental impacts from preliminary site characterization activities for the ANS Project. The environmental assessment examined the potential for the characterization activities to have significant impacts to terrestrial and aquatic ecology, cultural resources, and worker health and safety.

The ER is being prepared in two phases. Phase 1 is focused on those data and analyses that are needed to support preparation of the EIS. Phase 2, which will begin after completion of Phase 1, includes those additional data and analyses that would be included in an ER providing a total data package equivalent to that submitted with a license application to the NRC. An annotated outline of the Phase 1 ER was developed, and most analyses were initiated this fiscal year. The remainder of the analyses will be completed by February 1992.

A significant part of the effort has been committed to assisting ANL staff in their efforts on the EIS. ER team members have explained the scope of the ER and described the conditions that exist on the ORR to ANL staff.

# SAFETY 4

Safety analysis activities conducted during the current reporting period included investigation and identification of applicable regulatory requirements, thermal-hydraulic accident analysis, severe accident analysis, and PRA. The planning basis for all safety activities is dictated by the end of the currently defined conceptual-design period in June 1992. Investigators in each safety analysis area have been active members of the design team, providing safety-related advice and calculations. In addition, the major burden of providing accident analysis for and integrating the Conceptual Safety Analysis Report (CSAR), to be issued in June 1992 with the CDR, will fall in the safety area.

The first phase of the Level I PRA will be completed several months after the CSAR, the better to utilize system-design description information developed for the CDR and accident analyses produced for the CSAR.

## 4.1 PROBABILISTIC RISK ASSESSMENT

PRA is one of the many methods used to evaluate design concepts for ANS. The determination of the risk presented by any aspect of a plant requires models of the operation, identifications of failure, estimates of the probability of failure, and evaluation of the consequences to the public and to the plant of the failure. Various aspects of PRA have been applied as the design progressed: to provide a current estimate of risk, to prioritize the need for design improvements, and to identify to the designers aspects of the design that contribute significantly to the risk. The work that began last year using failure modes effects and criticality analysis (FMECA) for the identification of comparative design weaknesses has identified issues, which are now being addressed by the designers, in the following systems.

### 4.1.1 Reactivity Control and Scram

The reference design, on which the FMECA was based, controls reactivity by two independent systems of neutron absorbers. The inner system consists of three absorbers capable of continuous position control, hence continuous reactivity control for normal reactor operation. But it also is capable of a fast insertion for reactor scram. The outer system consists of eight independent neutron absorbers. Full insertion of either of the systems will scram the reactor. Both control-rod drive mechanisms use mechanical designs similar to those proven in the HFIR operation. The principal concerns identified by the FMECA were:

- The two systems are not diverse. While the HFIR-like design has proven reliability, the

proximity of the systems at the bottom of the reactor in the subpile room has the potential for common-cause failure that violates the presumed independence of the systems. Presently, mechanical inner mechanisms and hydraulic outer mechanisms have been selected for further design in order to incorporate more diversity into the reactor protection system.

- The control-rod drive mechanism design that was analyzed used a sliding seal on the rod that actuates scram has a potential for particulate binding. The current design replaces this seal with a bellows that, unfortunately, increases the force required of the magnetic release mechanism. Alternatives are being investigated.
- Beneath the reactor is the subpile room in which the control-rod drive mechanisms are located. The reactor pool is excluded from the region through which the control-rod drives pass. Thus, the reactor pool is reduced in effectiveness for mitigating the descent of a molten core in a severe core-melt accident. The subpile room must be a limited volume cell to limit the loss in case of a loss-of-coolant accident (LOCA). Further investigation is needed to assess the risk contribution of this configuration.

### 4.1.2 Flow Degradation

The ANS reference design uses four submerged pumps, each powered by an ac main motor, a dc pony motor, and possibly a flywheel operating in air. The FMECA identified the following concerns:

- If a pump were to seize, there is a possibility that the inertial forces could cause a break in the pipe to which the pump is attached. Such a problem could be eliminated by a shear pin in the drive shaft to limit the torque.
- A literature review of pump problems identified vibration as a major cause (it is a cause of pipe failure also and detrimental to the experimental environment). One cause is the fluid centroid not coinciding with the mechanical centroid. This suggests that a sleeve be located about the pump drive shafts so the pump shafts operate in air even though the pump is submerged.
- The power system for ANS was analyzed by FMECA, but no significant weakness was found at the current stage of design.

### 4.1.3 Beam Tube Rupture

Neutrons will be delivered to many of the experiments at ANS through beam or guide tubes. Beam tubes are evacuated or gas-filled pipes providing low attenuation neutron passage. Guide tubes are highly polished rectangular tubes down which very low energy neutrons may pass by multiple reflection from the walls. The very low energy neutrons are produced by two cold, vacuum-insulated, liquid-deuterium neutron sources. The most efficient shape for the cold source is an ellipsoid of revolution with a reentrant cavity. The FMECA identified the following concerns:

- An overpressure in the reflector tank will have a tendency to collapse the nonspherical envelope about the cold target. If this occurs, rapid heating of the liquid deuterium would result, which would challenge the deuterium dump/catch system. Deuterium must be prevented from mixing with air because of the accident potential. The strength of the vacuum envelope is limited by the need for minimizing neutron absorption. The suggestion offered is the possible ribbing of the envelope to provide additional stiffness.
- Double valves will be required on the guides that penetrate the containment to comply with NRC requirements.

### 4.1.4 Pressurizer

Operating pressure for ANS is provided by two pressurizer pumps. In case of a LOCA, the pumps do not have sufficient flow to maintain the pressure necessary to avoid a critical heat-flux condition, and the additional flow needed is

provided by large, gas-pressurized accumulators on each of the four primary legs.

In normal ANS operation, primary flow is discharged through a letdown valve to a letdown tank for coolant cleanup and detritiation to be returned by the pressurizer pumps. The FMECA identified the following concerns:

- Excessive gas pressure in the pressurizers could result in gas injection into the primary system, causing pump cavitation. Design and procedures should eliminate this problem.
- Proper selection of pressurizer pumps according to their pump curve should allow constant speed operation of the pressurizer pumps and eliminate the runaway pressurizer problem that contributes to the HFIR risk.
- The large accumulators present seismic restraint problems. If the line to one pressurizer fails, only two pressurizers will be available to mitigate the depressurization.

### 4.1.5 Refueling

The PRA for HFIR assesses foreign objects that enter the primary-coolant system during refueling to be the largest risk contributor. The refueling design of ANS has not advanced to the point that an FMECA can be performed; nevertheless, a conceptual innovative refueling approach for ANS was conducted to determine if, in principle, refueling can be conducted while controlling the entrance of foreign objects. From this it was concluded:

- It is possible, through refueling automation, to prevent foreign object entry.
- Dropping a spent or fresh core from its neutron poison rods has severe accident potential.
- An accidental criticality in the spent-fuel storage pool would also be a severe accident.

### 4.1.6 Containment Isolation System

The ANS conceptual design houses the reactor in an essentially leak-tight containment building. In the event of a severe accident, fission products would be released from the fuel, but release to the environment would be controlled by the containment-design leak rate of 0.5% of the containment free volume per day. The containment may be pictured as a leak-tight dome completely enveloping the reactor, but a realistic evaluation of containment reliability must consider the possibility of failure of one or more of the many penetrations that pass through containment: penetrations for electrical supply lines, for coolant lines, and for ventilation system lines, and for the personnel access airlocks that are themselves the largest containment penetrations. The secondary containment building surrounds the primary containment; ventilation fans maintain a negative pressure inside the secondary containment building and direct any leakage from the primary containment through charcoal and absolute air filters prior to release to the environment.

The ANS Project has established probabilistic safety goals to ensure that the ANS reactor presents a negligible health risk to individuals in the vicinity of the reactor. Proper functioning of containment is essential to meet the risk goals. Therefore, an auxiliary containment-reliability goal has been established: given the occurrence of a severe accident, the probability of containment failure should be less than $10^{-2}$.

Probabilistic calculations were undertaken during the current reporting period to gain a preliminary idea of how difficult it will be to meet the containment-reliability goals. The following failures were considered: isolation valve failure, penetration failure, airlock failure, and secondary containment ventilation system failures. For the case of isolation valves or ventilation system blowers, the failure modes were clear—failure to close and failure to run. For the airlocks and penetrations, actual failure data were used,[23] but the severity and modes of failure were not readily obtainable during the short period of the study. It was not defined for this study whether the available failure data represents gross failure of the containment pressure boundary at the penetration or simply failure to meet a strict containment leak-testing requirement. In this respect, it is possible

that the results discussed below are very conservative.

The IRRAS code, developed at INEL, was used to quantify the combined containment failure probabilities. The results, in terms of the top five contributors to containment, may be summarized as follows:

| Containment element | Failure probability *per demand* |
|---|---|
| Airlocks | $3.9\ (10)^{-2}$ |
| Mechanical penetrations through primary containment | $3.1\ (10)^{-3}$ |
| Electrical penetrations through primary containment | $5.4\ (10)^{-3}$ |
| Mechanical penetrations through secondary containment | $3.1\ (10)^{-3}$ |
| Electrical penetrations through secondary containment | $5.4\ (10)^{-3}$ |
| Secondary containment blowers | $7.6\ (10)^{-4}$ |

From these results, it is apparent that the total failure probability exceeds the containment failure goal of $10^{-2}$/demand. The largest single contributor is the airlocks, and other penetrations are well below the desired limit. This shows that careful attention to airlock design will be very important during the remainder of conceptual design. In addition, further effort will be necessary in order to define more closely the failure modes for penetration and airlock failure.

## 4.2 TRANSIENT THERMAL HYDRAULICS

Significant changes in the ANSR design during the current reporting period made the development of an updated RELAP model necessary. These design changes include reorientation of the emergency heat exchangers to allow for natural circulation cooling from the reactor pool; the inclusion of four separate inlet piping legs; and other changes in dimensions, elevations, and specifications of the various components. A major task during FY 1991 has been to update the RELAP model to reflect these changes. This new model has been used to analyze several accident scenarios, including a series of LOCAs as well as locked-rotor and station-blackout transients. LOCA events studied included break sizes ranging from 51 mm to 203 mm at the pump exit, 76 mm to 152 mm at the CPBT inlet, and 51 mm and 152 mm at the CPBT outlet. In addition, a task was initiated to benchmark RELAP and the ANSR RELAP model with the ANS dynamic model and the ANS steady-state code.

Since RELAP5/MOD3 will be the only RELAP version continuing to get INEL technical support in the future, a decision was also made to convert from using RELAP5/MOD2.5 and MOD4B1 to RELAP5/MOD3. Tasks were initiated at INEL during this fiscal year to incorporate the ANS updates (described in the February 1991 ANS progress report) in the MOD3 version of RELAP and to install this version of the code on the IBM RISC/6000 platform at ORNL. Modifications made to the code allow a flag to be set in the input deck that triggers the ANS thin-channel structures. An additional task was initiated at INEL to improve the RELAP accumulator model, allowing backflow into the accumulator during transients.

The RELAP verification and validation effort initiated during FY 1990 continued and expanded this fiscal year. Efforts included continuation of experimental planning, convening a group of thermal-hydraulic experts to develop a phenomena identification and ranking (PIR) table, and initiation of analysis to examine core flow-blockage issues.

A new task was initiated to develop the use of statistical uncertainty techniques for safety analysis. This task includes the identification of appropriate uncertainty levels for transient analysis, developing appropriate methodology for using these uncertainties, and some initial scoping studies using this technique.

### 4.2.1 Planning for RELAP5 Experimental Validation

#### 4.2.1.1 Development of the Phenomena Identification and Ranking Table

A process developed by the NRC called the code scaling applicability and uncertainty (CSAU) process has been used to quantify the performance of best estimate simulation tools used for power reactor safety analysis. The CSAU methodology has been developed to examine a prescribed power reactor design and a prescribed transient. The analysis begins with the construction of a PIR table, which is developed using an analytical hierarchy process (AHP). The PIR table lists all of the system components and associated phenomena that are involved in the transient and ranks these phenomena and components according to their importance in predicting the transient response accurately.

The information in a PIR table can be used to establish priorities for the development of experiments supporting the verification and validation of transient simulation tools such as RELAP5/MOD3, used for ANSR analysis. Therefore, a team of experts was assembled to prepare a PIR for a LOCA located at the inlet of the CPBT. The ANSR PIR will accomplish the following:

1. rank phenomena important to safety-related transients,
2. establish if the important phenomena are (or can be) adequately modeled in RELAP5/MOD3, and
3. establish which of the important phenomena require experimental investigation before reliable models can be formulated.

The design of the ANSR was fixed for the purposes of the ANSR PIR team as that represented by the RELAP model shown in Sect. 4.2.2 of this report. The first two meetings of the ANSR PIR team have taken place as of this writing, with two more scheduled before the process is complete in December 1991.

#### 4.2.1.2 Flow Blockage

Fuel assembly inlet flow blockage has continued to surface as a leading cause for potential damage in the ANSR fuel assembly. Therefore, a combined experimental and analytical program has been initiated to establish the size of blockage the fuel assembly inlet can withstand without sustaining damage.

Two phenomena can be identified as important: the effect of a blockage on the channel's average flow characteristics (e.g., the blockage can "starve" flow to the channel) and the local effects downstream of the blockage. An initial set of scoping calculations was performed analyzing the variation in channel average mass flux and flow excursion limit (as predicted using the Costa correlation, 1967) as a function of the size of the inlet flow blockage. This analysis indicated that for a flow blockage of 50%, both the channel mass flux and the limiting power are reduced approximately 20% from nominal values.

In order to examine the local effects, a computational fluid dynamics (CFD) analysis of the inlet flow blockage is being conducted using a computer code called FLUENT. This analysis will be tuned and validated using the results of the experimental effort described below. The CFD model of the flow channel with inlet flow blockage provides a flexible tool for evaluating a broad range of inlet flow blockage positions and sizes. Only a few bounding blockage situations will then need to be evaluated experimentally.

A finite-element structural-analysis model of the fuel plate will be developed to translate the thermal stresses and mechanical stresses associated with the inlet flow blockage to fuel-plate deflections. The fuel-plate deflections can further perturb the flow field, the pressure field, and the heat transfer downstream of the blockage.

The experimental portion of the effort will use a single flat, narrow, rectangular channel with dimensions prototypic of an ANSR fuel cooling

channel. Flow will be forced through the cooling channel at the ANSR nominal flow velocity. The channel will be heated on one side using a low-power heater. The side of the heater away from the flow will be covered with a thermochromic film. A flow blockage will be positioned at the channel inlet, and the variation in the temperature field downstream of the blockage will be measured on the back side of the heater using the thermochromic film and image processing techniques. This information will describe the spatial distribution of the heat transfer coefficient since the heater power is not sufficient to affect the fluid bulk temperature. Local static fluid pressure measurements will also be taken in the channel downstream of the blockage.

The three efforts evaluating flow blockage will combine to establish the blockage size and position range that will result in fuel damage. This information may be used to design fuel-assembly inlet flow straining devices and to guide the design of components likely to contribute to a fuel inlet-blockage event.

## 4.2.2 RELAP5 Transient Calculations

### 4.2.2.1 RELAP Model

A RELAP5 ANSR system model based on the conceptual design has been developed to perform LOCA analyses. A standard procedure in developing the model was followed. An initial model review was conducted on September 27, 1990, that included evaluation of the modeling assumptions and nodalization scheme. The model input and calculation document was independently reviewed at INEL, and a review of RELAP5-calculated results was performed in February 1991. The RELAP5 model was based on reactor conceptual-design information available at the time (first quarter of CY 1991).

The model (Fig. 4.1) consists of three major regions: the core region, the heat-exchanger loop, and the pressurizing/letdown system. The core model consists of two fuel elements, bypasses, and a central control-rod region. The core is surrounded by the CPBT, which separates the high-pressure primary system from the low-pressure moderator tank. Core power is calculated using a point kinetics model with reactivity feedback from both coolant-density change and control-rod movement. Relative axial power profiles are based on the I3 fuel-loading design (an internal designation representing a particular radial and axial distribution of fissile material within the active fuel region) at the end of the cycle.

The loop model contains four independent heat-exchanger loops, three active and one standby. Each loop further consists of an isolation valve, a hot leg, a horizontal U-tube main heat exchanger, a horizontal U-tube emergency heat exchanger, a cold leg, an accumulator, a centrifugal main circulation pump, and a check valve. The heat exchangers were adjusted to provide correct flow rates and pressure drop characteristics at design conditions. The single-phase homologous curve of the pumps was developed from the manufacturer's (Byron Jackson's) three-quadrant design curves.

An open-loop representation of the letdown and pressurizing system is included in the model. Primary system pressure is controlled through modulation of the letdown valves using a specified letdown flow velocity. The accumulator, installed upstream of the primary-coolant-pump suction side, was assumed to be 5 $m^3$ filled with 4.875 $m^3$ of heavy water and a 0.125 $m^3$ nitrogen bubble, initially at the pool water temperature.

### 4.2.2.2 Pipe-Break Analysis

Analysis of a pipe break between the cold leg distribution header and the core inlet is a typical example of results obtained thus far. This location results in rapid system depressurization because of the break's location in the primary-coolant-pump discharge piping. Three break sizes were studied: small- (76-mm), medium- (152-mm), and large- (203-mm) diam. In the model, the break was assumed to open instantaneously to obtain the most conservative margin to fuel damage.

The sequence of events is as follows. When the break opened at 10 s, a depressurization wave propagated around the primary-coolant system

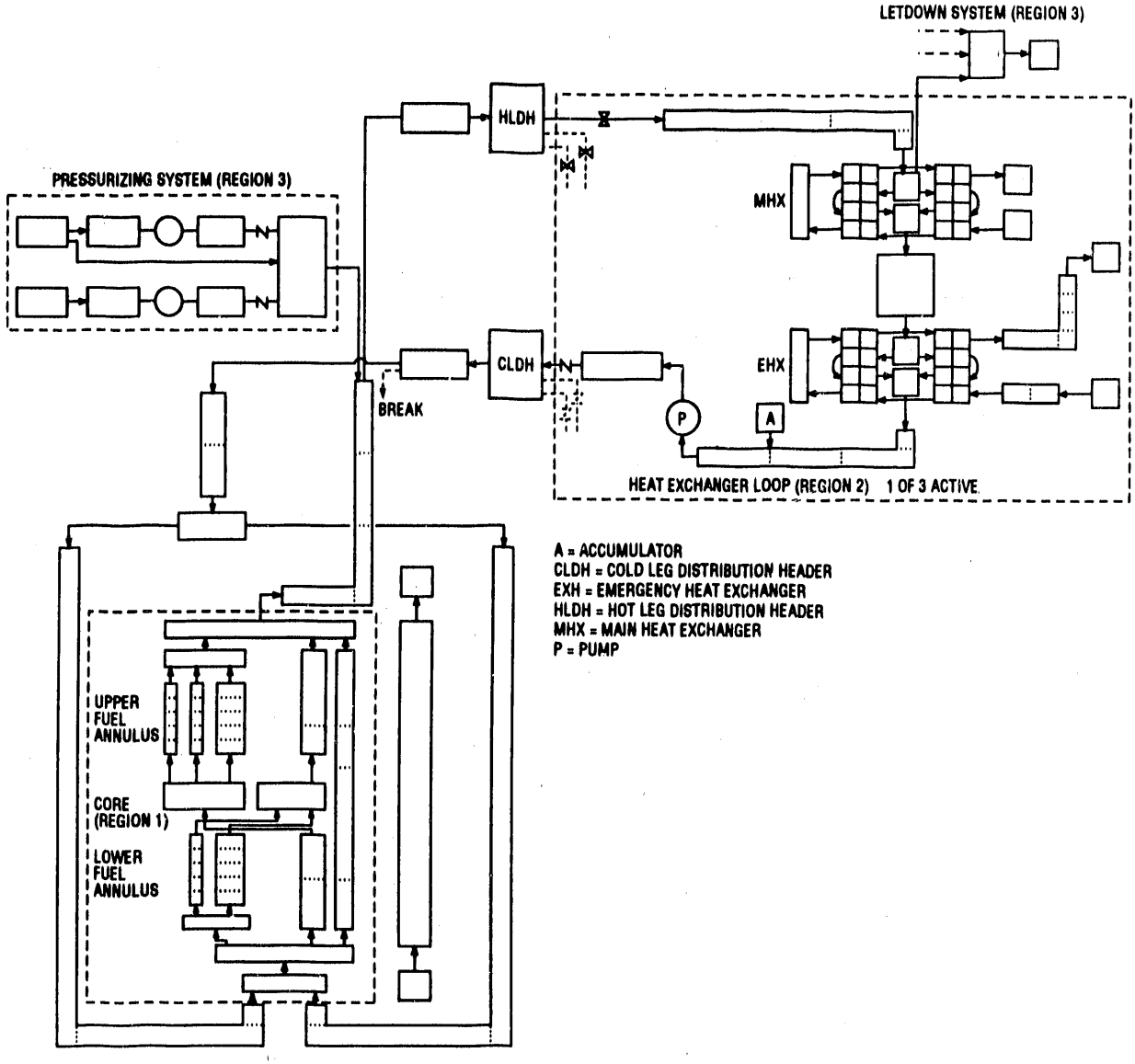


**Fig. 4.1. Nodalization of the RELAP5 ANSR conceptual-design system model.**

from the break location. The depressurization wave reached the accumulator about 14 ms after the break (this is independent of break size) and initiated accumulator injection flow. For the 203-mm break, the flow excursion limit was exceeded at about 26 ms. A reactor trip signal on low core exit pressure was generated at about 20 ms, but scram rod insertion did not start until 80 ms because of a 60 ms delay caused by sensor and mechanical factors.

Figure 4.2 shows the hot-spot heat flux normalized by the predicted values of the Costa flow excursion limit vs time. Flow excursion between parallel flow channels can initiate fuel damage as the flow in a hotter channel oscillates between normal flow and lower values. For the 76-mm break, the fraction is calculated to be about 0.25 (i.e., hot-spot heat flux does not exceed approximately 25% of the critical heat flux). For the 152-mm break, two peaks were observed with much closer approach to the Costa limit. These peaks are controlled by the core outlet-pressure minima. For the 203-mm break, the Costa limit was exceeded at about 26 ms. Thus, it is seen that

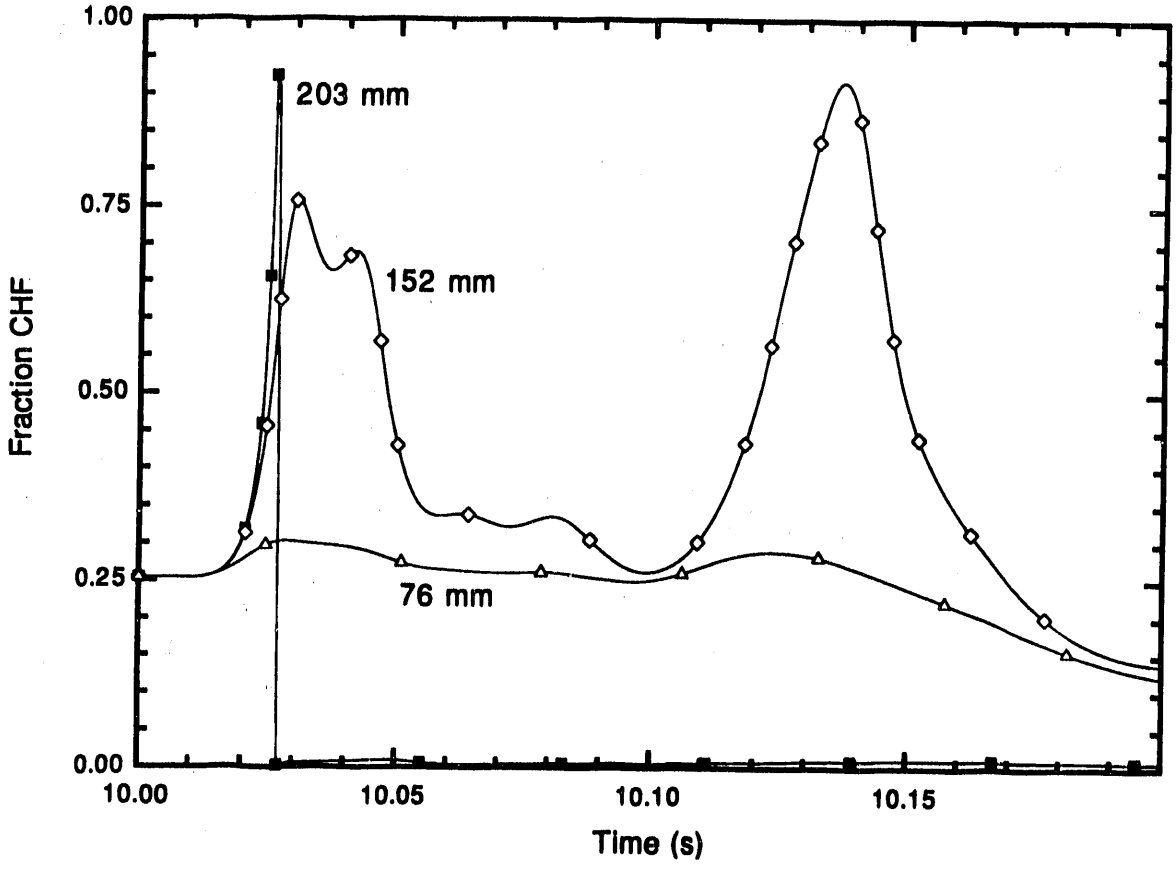


**Fig. 4.2. Local heat flux normalized by the Costa critical heat flux at the hot spot.**

the core can withstand up to a 152-mm break without exceeding the Costa flow-excursion limit, but this particular design is susceptible to early fuel damage for the large break (203-mm) size.

Design modifications to accelerate scram rod insertion or to slow the depressurization to eliminate early fuel damage have been adopted. These include elimination of the cold leg distribution header, addition of preferred-direction flow orifices at the cold leg connection to the CPBT, and relocation or resizing of accumulators. An extensive and systematic LOCA study has begun for piping breaks near the core region, such as at the CPBT inlet and outlet, and for double-ended guillotine breaks located upstream and at the midsection of the preferred-direction flow orifice. Furthermore, the assumption of an instantaneous break-opening time is presently being evaluated to see if a finite-opening time can be justified.

#### 4.2.2.3 Locked-Rotor Event

During the transition to the conceptual-design model, a series of calculations was performed at INEL investigating a locked-rotor event in one of the primary circulation loops, using the preconceptual-design RELAP model (see February 1991 ANS progress report). Results of these calculations indicate that the ANS design can withstand, without fuel damage, the instantaneous locking of the rotor of one main coolant pump. The locked rotor resulted in minor pressure oscillations within the primary-coolant system that were damped out within approximately 1 s (Fig. 4.3). A reactor scram resulted from a low core inlet-pressure condition and became fully effective by about 0.5 s. Cooldown of the primary system coolant caused declining pressures over the first 4 s because of

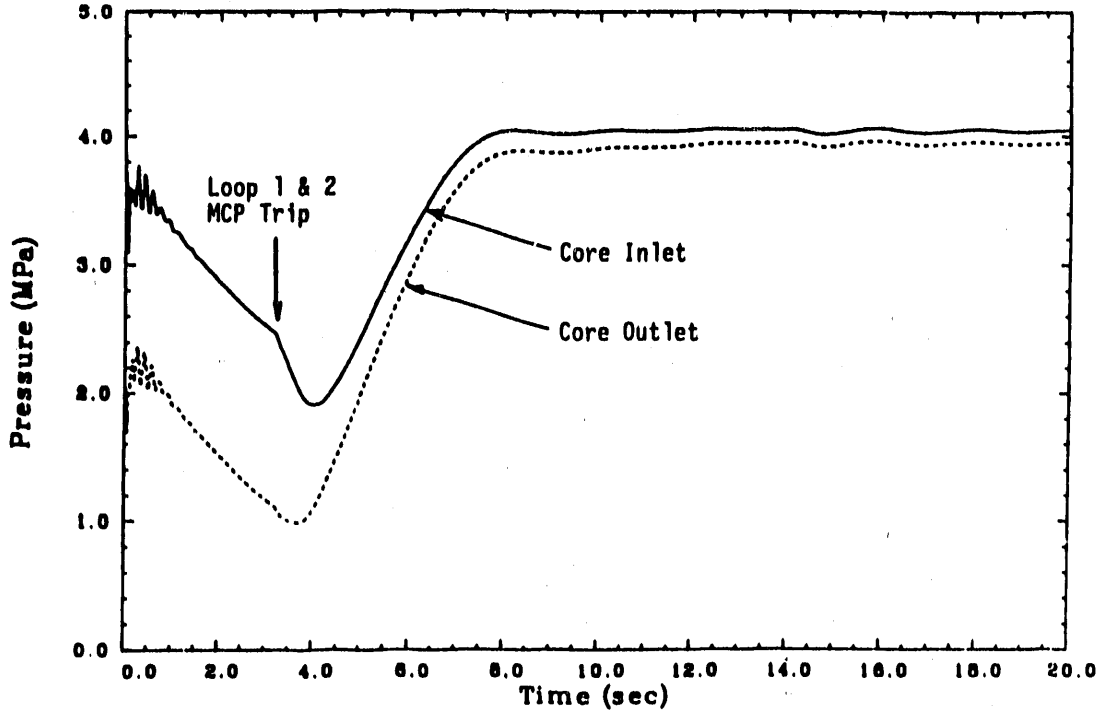


**Fig. 4.3. Locked-rotor run 1, core inlet and outlet pressures.**

coolant shrinkage. Flow in the locked-rotor loop was disrupted almost immediately; however, the pressure disturbance caused a rapid flow increase in the two active flow loops, thus partially compensating for the total loss of flow in the locked-rotor loop. As a result, the initial decrease in core flow amounted to only about 12% of nominal flow.

The declining coolant-system pressure resulted in an increased pressurizing system flow. This flow further increased dramatically after about 3 s, when the standby pressurizing pump was coming up to speed. At about 4 s, the coolant-volume-addition rate from the pressurizing system exceeded the coolant-shrinkage rate, and the system repressurized.

At the end of the calculation, the primary-coolant system had been stabilized at high pressure with steady core flow. The stabilized pressure was determined by the balance between the volumetric inflow from the pressurizing-system pumps and the coolant volumetric-shrinkage rate because of system cooldown. This end state indicates that the core will continue to be cooled. No core fuel-plate heatup was indicated during this transient. A minimum fluid subcooling of 42 K was calculated at the exit of the lower-core hot channel during the initial depressurization.

### 4.2.3 Statistical Uncertainty Analysis

The goal of statistical uncertainty analysis is to express the exceedance probability at a known confidence level for any given reactor condition and governing limit. Reactor conditions can range from steady-state operation to rapidly developing accidents; governing limits range from incipient boiling to fuel temperature limits. A typical statistical uncertainty criterion is that the nonexceedance probability for critical heat flux at the hot spot should be at least 95%, at a confidence level of 95%. A comprehensive uncertainty analysis must consider uncertainties in fuel-plate manufacturing parameters, operating

parameters such as coolant pressure and temperature, and uncertainties in analytical models or constitutive relationships such as the CHF correlations.

In order to achieve an optimum balance between maximum operating power and the necessary safety margins, a program was initiated in FY 1991 to quantify the appropriate uncertainty levels. In concert with the design effort, this task has included:

1. a sensitivity study to determine most important parameters and correlations,
2. evaluation and selection of the input parameters and analytical models (correlations) to be used,
3. quantification of the uncertainties involved by determining the error probability distributions for each of the key parameters and correlations,
4. evaluation and selection of a cost-effective statistical approach for both steady-state and transient uncertainty analysis, and
5. a preliminary analysis determining the maximum power possible consistent with various acceptable risk criteria.

The major uncertainty analysis activities that were completed during the reporting period are described below. A more detailed description on the related R&D activities, including the thermal-hydraulic experiments and models determination, is given in Sect. 4.1 of the thermal-hydraulic R&D program.

### 4.2.3.1 Statistical Methods and Uncertainty Data Development

Several tasks have been completed that led to the initial identification and quantification of significant uncertainty contributors as well as uncertainty combination techniques. Thus far, this effort has centered around the ANS steady-state thermal-hydraulics code described in the R&D section of this report. An initial sensitivity study was conducted with this code to determine the important uncertainty factors. Of many parameters involved in the analysis, eleven factors have been identified for preliminary study (Table 4.1) and are used in the remainder of the analysis presented here. Several other important parameters (such as channel gap width) are recognized, but uncertainties are not assigned to them yet.

**Table 4.1. Probability distributions used in Monte Carlo uncertainty analysis**

| Parameter | U factor[a] | Probability distribution | Mean $\overline{U}$ | Standard deviation |
|---|---|---|---|---|
| CHF correlation | U22 | Normal | 1.098 | 0.262 |
| Local fuel segregation | U18 | Log-normal | 1.3 | 0.0980 |
| Power density distribution | U3 | Normal | 1.0 | 0.10 |
| Hot streak—entrance[b] | U24 | Log-normal | 1.119 | 0.0171 |
| Hot streak—exit[c] | U24 | Log-normal | 1.027 | 0.00380 |
| Forced conv. H.T. correlation | U8 | Normal | 1.006 | 0.0283 |
| Friction factor correlation | U7 | Normal | 1.0 | 0.05 |
| Reactor power | U1 | Normal | 1.0 | 0.02 |
| Total fuel plate H.T. area | U2 | Normal | 1.0 | 0.029 |
| IB correlation | U3 | Normal | 1.0 | 0.05 |
| Inlet coolant temperature | U6 | Normal | 1.0 | 0.01 |

[a]HFIR U factor designation.
[b]Hot streak distribution for lower or entrance region of fuel elements.
[c]Hot streak distribution for upper or exit region of fuel elements.

In order to quantify uncertainty levels associated with correlations used in the thermal-hydraulic analysis, a task was initiated to develop a data base for the significant thermal-hydraulic phenomena. These included the single-phase heat-transfer coefficient and friction factor, the incipient boiling point, the critical heat-flux point, and the flow-excursion limit. An evaluation of several correlations for each of these factors has led to selection of correlations best suited for ANS thermal-hydraulic analysis. Uncertainty levels for each correlation were also determined during this process.[24] In addition, correlations for heavy-water and light-water properties were developed and their errors quantified. An extension of this effort to transient conditions is presently under way. This includes modifications of correlations applied for very fast transient conditions and correlations for the quasi-steady-state, off-nominal conditions encountered in transient analysis. For the case of an extremely rapid reactivity excursion accident, the expected critical heat-flux limit (transient CHF correlation) can be two to three times higher than the comparable steady-state value for the reactor power-surge exponential period of 5 to 10 ms. It was determined that the worst-case ANS reactivity excursion would be unlikely to have a period less than about 90 to 150 ms, which is slow enough to justify the use of the normal steady-state CHF correlation.

#### 4.2.3.2 Maximum Power Calculations

During normal reactor operation, the automatic control system holds the reactor very close to 100% power by making small control-rod adjustments in response to fuel depletion and minor fluctuations in coolant temperature. If power exceeds 100% by a sufficient margin, an automatic setback will insert control rods until the reactor reaches a preset lower power level. If the setback fails and the power continues to climb to 115% power, the reactor protection system will initiate a scram to insert all control rods rapidly and to shut down the reactor completely. The 15% margin between operating power and the scram set point is necessary to prevent spurious scrams. Considering heat balance error and instrument drift or error, the scram might not be initiated until power reaches 119%, even though the nominal set point is 115%.

If an anticipated operational occurrence takes the reactor into an overpower situation, the reactor fuel must, per the *NRC General Design Criteria*, remain within acceptable fuel design limits.[25] Anticipated operational occurrences would not be severe enough, i.e., rapid enough, to lead to significant overshoot of the scram set point. The probability of an event that could bring the power to 119% is low—on the order of $10^{-3}$ per year.

During the current reporting period, statistical uncertainty analysis techniques were applied to define the maximum allowable operating power level with respect to a variety of thermal limits. Since the reactor design parameters, such as fuel grading, were changing rapidly during this period, this exercise is considered only as a demonstration of a practical way to apply statistical techniques to set design parameters. The safe power levels thus derived should be considered very much subject to change as the design and analysis techniques are refined.

Two statistical acceptance criteria were considered—95% nonexceedance probability at 95% confidence and 99.9% nonexceedance probability at 50% confidence. The 95/95 criterion comes from the NRC standard review plan[26] and might be regarded as a minimum requirement. The 99.9/50 criterion is a best-estimate of a more stringent nonexceedance probability. Considering the rarity of severe protection system challenges, meeting the 99.9/50 criterion would ensure a very low frequency—on the order of $10^{-6}$/year—of exceeding the specified limit. These two criteria were applied at the 119% overpower condition. Uncertainties were combined mathematically by a special Monte Carlo program to yield uncertainty factors for input to the ANS steady-state code. The actual thermal-hydraulic calculations were performed on the ANS steady-state computer code.

Two sets of conditions were examined, the first combining the overpower condition with nominal coolant pressure and temperature, and the second combining the overpower condition with

the highest inlet temperature and lowest inlet pressure allowed by the protection system. The first set of operating conditions will be more appropriate if the reactor protection system is designed to prevent simultaneous overpower and underpressure. The second set is more appropriate to protection system designs that do not prevent such simultaneous conditions.

Some parametric uncertainties were treated with distributions, while others were taken at worst-case values. The former were used in hot-spot and hot-channel Monte Carlo analysis to define power-peaking factors at desired probability/confidence levels for use in the thermal code. The latter could not be simply combined in separate Monte Carlo analysis. The current treatment of parameter uncertainties that are included in this analysis is conservative; however, it is recognized that other parameter uncertainties will have to be considered in future analysis. To the extent that this conservatism balances unaccounted-for parameter uncertainties, the preliminary estimates provided here will be representative.

Thermal limits included in the analysis are:

1. CHF at the hot spot,
2. flow excursion along the hot streak (based on the Costa correlation),
3. incipient boiling (IB),
4. fuel centerline temperature less than 400°C,
5. fuel oxide temperature drop less than 119°C, and
6. fuel surface temperature less than the saturation temperature ($T_{wall} < T_{sat}$).

Results of calculations of the ANSR maximum fission power level (fission power = 1.12 times the heat power transferred to the primary coolant flowing through the core) are provided in Table 4.2. Power levels reported include a 19% margin to account for measurement and set point uncertainty and for scram set point margin. As indicated, the limiting power level and cycle time step at which the limiting condition occurs is given for probability levels of 95 and 99.9%.

Maximum power levels, based on CHF, IB, and $T_{wall} = T_{sat}$ with reactor power, coolant pressure, and temperature simultaneously at the reactor protection system set point limits, drop by about 10% from those based on nominal pressure and temperature. Maximum power levels drop most significantly, ~16%, in the case of flow excursion. The drop is enough in the 95% probability case that flow excursion becomes more limiting than CHF. Centerline temperature and oxide temperature drop-based maximum power levels are not as significantly affected. Extended operation at worst-case temperature and pressure conditions is not likely. Thus, oxide growth, which depends on integral cycle conditions, will be overpredicted when the worst-case operating conditions are used. As a result, the centerline temperature and oxide temperature drop will be overpredicted. Thus, for these limiting phenomena, the results calculated at the set point limits are conservative. Results calculated at nominal temperature and pressure could be nonconservative if the reactor operates near the scram set point limits for most of the fuel cycle, but extended operation very near scram set points is not considered credible. Remember, these examples are only an early demonstration of the output from the statistical method; they are not our present actual estimates, which are continually evolving.

## 4.3 SEVERE ACCIDENT ANALYSIS

A severe accident is defined as one that proceeds beyond the design basis and therefore has the potential for releasing significant quantities of fission products out of the fuel-cladding matrix. For the ANS, considerable efforts have been made to introduce various safety features in order to make the event of severe accident occurrences a low probability. Notably, the ANS reactor cooling and protective systems are being designed to achieve a severe core-damage risk limitation goal of 1/100,000 core-damage events per year (applicable to internal events). A defense-in-depth philosophy has been adopted.

**Table 4.2. Examples of statistically calculated maximum ANSR steady-state core fission power at nominal operating conditions**
(including a 19% set point uncertainty and scram set point margin)

| Phenomena | Nominal operating conditions 95% probability level | | Nominal operating conditions 99.9% probability level | |
|---|---|---|---|---|
| | Limit | | Limit | |
| | P(MW) | Time step | P(MW) | Time step |
| CHF | 393 | 5 | 336 | 5 |
| Flow excursion | 414 | 5 | 372 | 5 |
| IB | 295 | 5 | 277 | 5 |
| Centerline temperature or oxide temperature drop | 299 | 4 | 278 | 4 |
| $T_{wall} = T_{sat}$ | 266 | 5 | 250 | 5 |

| Phenomena | Low-pressure, high-temperature set point conditions 95% probability level | | Low-pressure, high-temperature set point conditions 99.9% probability level | |
|---|---|---|---|---|
| | Limit | | Limit | |
| | P(MW) | Time step | P(MW) | Time step |
| CHF | 360 | 5 | 307 | 5 |
| Flow excursion | 355 | 5 | 319 | 5 |
| IB | 267 | 5 | 251 | 5 |
| Centerline temperature or oxide temperature drop | 291 | 4 | 271 | 4 |
| $T_{wall} = T_{sat}$ | 235 | 5 | 221 | 5 |

In response to this commitment, severe accident analysis and related technology development efforts have been introduced early in the design phase. This was done to aid in designing a sufficiently robust containment for the retention and planned release of radionuclides in the event of a severe accident, providing a means for satisfying on-site and off-site regulatory

requirements on accident-related dose exposures, providing containment response and source-term best-estimate analyses for the Level-2 and -3 probabilistic risk assessments that will be produced, providing the best possible understanding of the ANS under severe accident conditions, and finally, providing insights for the development of strategies and design philosophies for accident mitigation, management, and emergency preparation efforts.

The goals mentioned above are being achieved through the following combination of efforts:

1. scoping studies on conventional power reactor severe accident issues to evaluate applicability to the ANS and the need for further research and development into resolving key phenomenological aspects;
2. implementation of lessons learned from past commercial reactor safety research and insights gained from scoping analyses into the design at an early stage of development; and
3. application of state-of-the-art analysis tools and methods, suitably modified and validated against appropriate experiments for application to ANS conditions.

Past activities in the area of severe accident analysis included scoping studies on hydrogen explosion loadings, fuel-coolant-interaction (FCI), debris-recriticality safety analyses, preliminary CONTAIN and MELCOR code evaluations for containment pressurization during postulated severe accidents, core-melt progression and fission-product release, and molten-core-concrete-interactions (MCCI). The results of these studies have been reported in previous ANS Project progress reports. Several follow-up efforts have been made to assist in resolving issues highlighted from these studies. For example, a task team has been organized at the national level to resolve jointly FCI and other severe accident issues for U-Al-fueled reactors. We have supplemented this effort by initiating experimental efforts investigating the triggerability and energy conversion aspects of silicide fuel for best-estimate FCI analysis. The task team consists of participants from other DOE laboratories with U-Al-fueled research, test, or production reactors. Several meetings have taken place, and plans are being formulated for the definition and development of appropriate analyses. A containment-design team, formed at ORNL, organized a workshop wherein participants from various external organizations provided valuable suggestions for improvements. In addition, cooperative efforts that were initiated with Japan Atomic Energy Research Institute (JAERI) researchers in the general areas of safety research for U-Al-fueled reactors (specifically those using silicide fuel) were further strengthened.

During the current reporting period, scoping studies on core-melt progression, fission-product release, and debris recriticality were conducted. Work was initiated with ANS designers to identify and implement design-fixes and mitigative strategies for preventing and managing severe accidents early in the design process. Containment response evaluations (from several hypothetical severe accidents including radionuclide transport) using the MELCOR code and off-site response and consequence modeling using the MACCS code were initiated for providing the necessary information for the forthcoming ANS EIS. The results of these activities are summarized below.

### 4.3.1 Core Debris Recriticality

The study of recriticality represents an important phase of any hypothetical severe accident that has progressed to the point of core-debris relocation outside of the control-rod region. This section provides a synopsis of the work in this area.

The KENO5A and DORT codes were used to examine several different postulated configurations for ANS core debris after it relocated from the control region in the core to a large steel pipe filled with $D_2O$ and surrounded on the outside with $H_2O$. Predictions from these codes were first validated against critical experiment data where good agreement was

observed. KENO5 and DORT code predictions for various postulated ANS core-debris configurations indicated that lumped configurations would remain substantially subcritical, but that dispersed configurations could become supercritical with $k_{eff}$ values up to 1.09 for the cases tested.

During FY 1991, the results of analyses for ANS debris recriticality were reexamined and modified to account for more realistic configurations and also because the $^{235}U$ fuel loading in the ANS core has been substantially reduced (from about 25 kg to about 15 kg). Furthermore, previous analyses for dispersed configurations were made assuming that the aluminum in the fuel plates would completely separate from the $U_3Si_2$ fuel. While this is clearly conservative, physical reality dictates that the $U_3Si_2$ will bond upon melting with the cladding and form a eutectic (with the aluminum). Hence, the presence of aluminum should be accounted for in dispersed configurations.

The KENO5A code was introduced on the IBM RISC/6000 platform (referred to here as KENO5A/WS) and verified for quality assurance. Checks were made against sample problems and against previous computations using KENO5 on the mainframe (referred to as KENO5A/MF). KENO5A/WS is essentially the same as KENO5A/MF with the exception of the cross-section libraries used. KENO5A/WS utilizes the Hansen-Roach 16-group cross-section library, whereas with KENO5A/MF Slater used a 39-group cross-section set.

Several calculations were conducted using KENO5A/WS to evaluate $k_{eff}$ values for a variety of situations. Some of these results are summarized in Table 4.3. As noted from Table 4.3, KENO5A/WS predicts $k_{eff}$ values that are generally lower by about 2 to 4% (with appropriate accounting for shielding effects) compared with predictions made by KENO5A/MF. For the lumped sphere configuration (Case 1), KENO5A/WS predicted a $k_{eff}$ of 0.85 compared to 0.87 by KENO5A/MF. Again, for the dispersed fuel ($U_3Si_2$ only) condition (Case 2), KENO5A/WS predicted a $k_{eff}$ of 1.03 compared to 1.07 calculated using KENO5A/MF. Cases 3 and 4 were evaluated for dispersion conditions where aluminum from the fuel plates would also be available in the mixture. For Case 3, 40 kg of aluminum (representing the aluminum from the fuel meat section) was added to the mixture. This condition reduced the value of $k_{eff}$ from 1.03 (a supercritical configuration) to 0.977 (a somewhat subcritical configuration). For Case 4, 85 kg of aluminum representing all of the

**Table 4.3. Predictions of $k_{eff}$ by KENO5A/WS and KENO5A/MF**

| Case | $k_{eff}$ | | Description |
|---|---|---|---|
| | KENO5A/WS | KENO5A/MF | |
| 1 | 0.85 | 0.87 | Lumped $U_3Si_2$-Al sphere of radium 11.005 cm in a pipe of diam 48.8 cm filled with $D_2O$ and surrounded with $H_2O$. |
| 2 | 1.03 | 1.07 | $U_3Si_2$ (15 kg U-235) dispersed in a pipe of diam 48.8 cm (over a 1-m length) filled with $D_2O$ and surrounded with $H_2O$. |
| 3 | 0.97 | | $U_3Si_2$-Al (15 kg U-235) dispersed in a pipe of diam 48.8 cm (over a 1-m length) filled with $D_2O$ and surrounded with $H_2O$. Mass of Al = 40 kg. |
| 4 | 0.91 | | $U_3Si_2$-Al (15 kg U-235) dispersed in a pipe of diam 48.8 cm (over a 1-m length) filled with $D_2O$ and surrounded with $H_2O$. Mass of Al = 85 kg. |

aluminum in the fuel plates was added to the mixture. This condition reduced the value of $k_{eff}$ from 1.03 to 0.91 (a significantly subcritical configuration).

These scoping calculations were conducted under room temperature conditions, and as such, incorporate a degree of conservatism in the estimates of recriticality under severe accident conditions. They do indicate that dispersed configurations have the potential for introducing a supercritical condition. The key to deciding whether a recriticality event will occur clearly depends upon adequately delineating realistic configurations, based upon core-melt progression studies, and conducting KENO calculations with temperature-adjusted cross-sections. Work is planned towards developing a test matrix of calculations depicting realistic configurations of the ANS core debris during various hypothetical severe accidents. Areas to be investigated are debris dispersion upon fuel melting in a flowing medium, upper-core relocation downwards before scram initiation, and other core-melt relocation cases relating to severe accidents. Results of these investigations will be given in the next reporting period.

### 4.3.2 Core-Melt Progression and Fission-Product Release Considerations for the ANS

The study of core-melt progression and fission-product release addresses the most fundamental aspects of severe accident analysis. It pertains to the issues that relate to core heatup, melting, and relocation, with simultaneous release and transport of the available radionuclide inventory. The core-region construction and operation for the ANS are radically different from that of power reactors. Such radical differences make it prudent to conduct a scoping study in order to judge which aspects of the heatup and melting processes require further attention and methods-development efforts and also to investigate safety concerns that can be addressed by proper system design. Work on this scoping study was initiated during FY 1990 and continued during FY 1991. In the following paragraphs, we present salient aspects of work conducted during FY 1991 and documented in detail in a yet-to-be-published report on core-melt progression and fission-product release considerations for the ANS.[27]

Work during FY 1991 concentrated upon modeling and analysis of data obtained by researchers at JAERI relating to fission-product release under high burnup conditions and $U_3Si_2$-Al fuel performance under reactivity excursion conditions. Both sets of data were shared by JAERI with ORNL for use in ANS safety-technology development.

The data obtained by JAERI for fission-product release under high burnup conditions (i.e., 66 at. %) were jointly analyzed with JAERI staff for evaluating release amounts and form (i.e., aerosol vs vapor). The analysis and modeling of release amounts for the volatile species (including ruthenium) has been completed, and a paper[28] has been submitted for publication to *Nuclear Safety*. Overall, it was found that silicide fuels release volatile fission products to a much lesser extent than U-Al alloy fuels. Interestingly, this was found to be the case even for noble gas releases, which for other U-Al fuels is essentially complete upon melting of aluminum cladding. For example, at 23 at. % burnup and at 660°C (the melting temperature of aluminum), only 30% of the noble gas inventory escapes from silicide fuels. Not until the fuel temperature reaches 1110°C does more than 90% of the inventory escape. This was also found to be the case for the important iodine species. These are important results from the standpoint of minimizing on-site and off-site radiological doses during hypothetical severe accidents and attest to the potential benefits of using silicide fuel for the ANS. Development work was completed for a library of correlations for various U-Al fuel types to predict release rates (for each individual volatile species) that may vary with time, ambient environment, burnup, and temperature. This work was based upon analysis of characteristic trends, phenomenological aspects, and regression analysis. A comparison of suggested correlation predictions against measurements is shown in Fig. 4.4. An overall mean value and standard deviation of 1.02 and

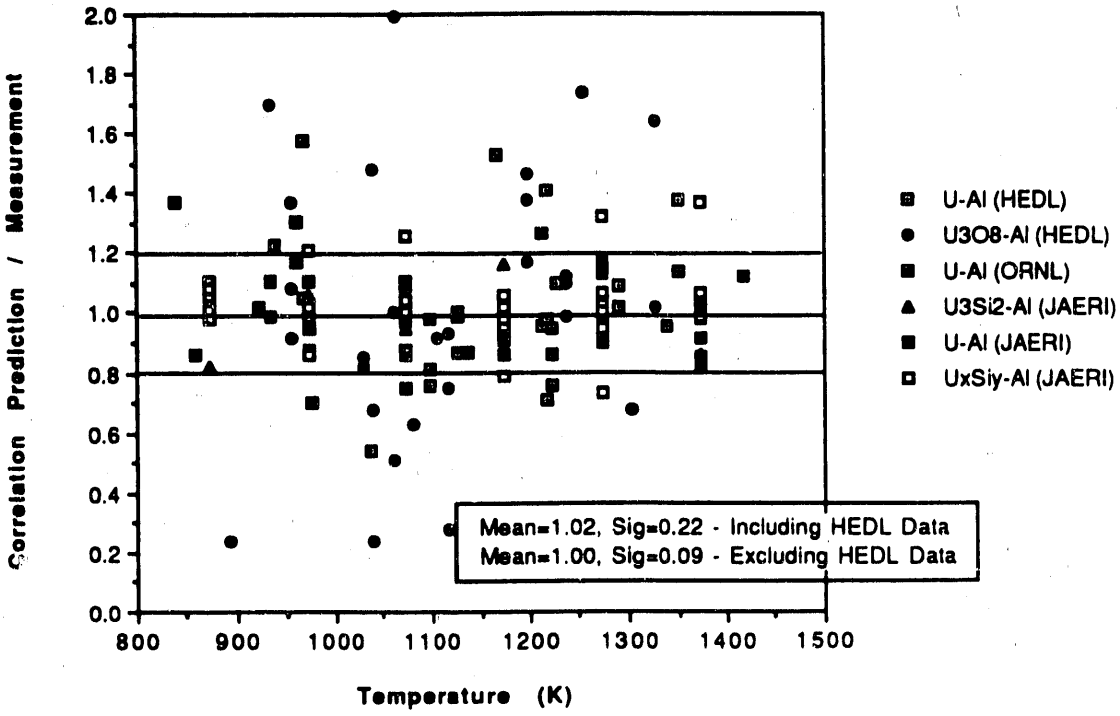


**Fig. 4.4 Relation of suggested correlation predictions to measurements vs temperature.**

0.22 are obtained over the temperature range investigated. Overall, statistics improve significantly (mean = 1.0, standard deviation = .09) if the Hanford Engineering and Development Laboratory (HEDL) data (which displayed considerable data scatter) are excluded.

Work was also begun on modeling and analysis of silicide fuel performance data taken in JAERI's Nuclear Safety Research Reactor (NSRR). In these tests, small $U_3Si_2$-Al fuel-plate samples (encapsulated with water) were subjected to rapid bursts of neutrons. The energy deposition levels varied from low to high. At low level, phenomena such as onset of blistering and structural deformation information were obtained. At the higher level, enough energy was deposited to cause fuel-plate melting (i.e., of aluminum). Promisingly, the fuel plates retained their structural shapes reasonably well all the way up to melting conditions. Even upon aluminum melting, the plates did not collapse. Material dispersion also did not occur (to cause steam explosions). These data were shared by JAERI researchers with ORNL for joint analyses and modeling that are ongoing. Data obtained so far will prove valuable in core-melt progression modeling for Level-2 PRA applications and for improving the safety performance of the ANS.

Further data acquisition is planned by JAERI with higher levels of energy deposition. Results of analysis and modeling of this data and other aspects dealing with core-melt progression will be discussed in future progress reports.

### 4.3.3 Design Features for Severe Accident Prevention and Mitigation in the ANS

A short-term scoping study was undertaken to facilitate the process of considering severe accidents in the ANS design, with the goal of providing key ANS-relevant severe accident information in a form that is immediately useful to the designers. This attests to the recognition by the ANS Project that it is better to introduce a design modification early in the design cycle that will

address an issue than to engage in an extensive research program that may solve the problem.

A scoping study of ways to design for severe accident risk reduction was performed. In addition to providing a review of relevant severe accident phenomena, discussions were included to suggest a number of mitigative strategies or design features that could make the ANS less vulnerable to severe accidents than if the designs did not incorporate such concepts. Possible design features or mitigation strategies conceived in this scoping study are summarized in Table 4.4. Currently, recommendations from this study are being used by the plant designers interactively with severe accident researchers to help evaluate severe accident issues in the context of all the other considerations that need to go into a realistic design.

### 4.3.4 ANS Source Term and Off-Site Consequence Evaluations for the EIS

During FY 1991, work was begun towards developing preliminary models of the ANS for determination of source terms and off-site consequences to support the needs of the ANS ER. The MELCOR and MACCS severe accident codes are being utilized for generating the necessary input for the ANS ER. This section describes the salient aspects of work performed so far.

Due to the preliminary stage of severe accident technology development for the ANS, it is not appropriate to develop mechanistic tools for capturing core-melt progression phenomena. In the absence of such information, two different severe accident scenarios are postulated with a view to evaluating conservative source terms. The first scenario evaluates maximum possible steaming loads and associated radionuclide transport, whereas the second is geared towards evaluating conservative containment loads from releases of radionuclide vapors and aerosols with associated generation of combustible gases. Scenario 1 is modeled based on guidance provided in the Atomic Energy Commission's (AEC's) report TID-14844, which stipulates that 100% of the noble gases and 50% of the halogen inventory should be sourced into the containment atmosphere and remaining radionuclides sourced into the reactor pool to cause steaming loads. Scenario 2 models an MCCI event, under the assumption that all of the volatile fission-product elements get released into the subpile room upon molten-fuel relocation there, with the balance of the fission-product elements retained within core debris, interacting with the subpile room concrete floor. These two postulates are based upon a fundamental assumption that specific aspects of explosive conditions are absent (shock wave generation and missile penetration) or are not important to model mechanistically. But the possible effects of containment failure from explosive phenomena such as steam explosion will be accounted for by providing a direct release path to the environment to provide results in the early containment-failure release category.

The MELCOR severe accident analysis code was used to develop an overall representation of the ANS containment (subject to several assumptions that are too numerous to mention here). Significant additional coding was also done to develop so-called control functions that enable the definition or control of various aspects of the simulation, such as opening and closing of valves, specification of pump characteristics, and specification of heat structure boundary conditions. The preliminary model consists of 11 control volumes, 15 flow paths, and 21 heat structures (that represent structural components such as walls, ceilings, shells, and miscellaneous materials) of various shapes. A fan model has also been included to account for flow through the large annulus gap between the steel shell and outer containment structure. Aerosol and vapor filtration processes are also modeled, as are various complex aerosol and vapor transport phenomena.

It should be noted that because of the preliminary stage of severe accident technology development for the ANS, it was not possible to model specific aspects of core melt progression. From this perspective, the MELCOR evaluations performed for the ANS ER will lack a sense of physical realism because various important physical phenomena related to fuel and

**Table 4.4. Summary of possible design fixes to mitigate severe accidents**

| Recommendation | Notes on recommendation |
|---|---|
| Employ an ANS design that retards or traps fission-product vapors and aerosols for minimization of the source-term. | Fundamental safety prescription. |
| Design against selective overpressurization in containment compartments. | Carefully engineered venting paths with selective compartmentalization without overpressurization is desirable to provide more time for evacuation. |
| Carefully consider a more robust reflector tank material than aluminum. | Containment of steam explosion pressure pulses and also radionuclide dispersion. |
| Consider incorporation of a missile shield or other energy-absorbing mechanism. | If evaluations indicate a high probability of energetic missile generation from explosive events. |
| Alter the design and operation to minimize possibilities for molten-core debris coming in contact with large amounts of water in the subpile room. Employ strategic flooding or timed sprays for subpile room. | Improves quenching, prevents explosive fuel-coolant-interactions, and prevents core-concrete-interactions. |
| Consider use of additives to increase viscosity of water used for flooding strategies. | Minimizes triggering potential; can be used in conjunction with an appropriate surfactant. |
| Find a mechanism that prevents uniform dispersion of core debris in reactor coolant system to prevent recriticality. Another consideration would use borated water injection system as in power reactors. | Recriticality prevention via design and operation. |
| Adopt in-depth measures to prevent and mitigate combustible gas detonation. | Includes igniters (e.g., in subpile room) to burn combustible gases as they evolve and before detonation concentrations are reached. |
| Consider either confining debris (using a core catcher) or dispersing it to avoid non-coolability and unacceptable structural ablation. | Iterate with severe accident researchers to determine location and validity of the installed mechanism. |
| Line the subpile room floor with alumina concrete and provide for strategic flooding to minimize structural ablation and production of combustible gases. | Unless operational considerations dictate otherwise. |
| Make every effort to design flow paths to ensure that released fission products are transported via passage through a water pool. | Iterate between designers and severe accident researchers to optimize the scrubbing potential of the water pool. |
| Design to ensure that the radionuclides in the production target rods do not escape from the reactor cooling system. | Work needs to be done iteratively between designers and severe accident researchers. |
| Address phenomena such as combustible gas stratification, via mixing mechanisms. | For prevention of detonable gas formation. |

radionuclide material relocation, entrapment, and transport have not been accounted for. Additionally, the effects of explosions and rapid energy generation have not been included explicitly. However, by allowing a direct flow path for radionuclide transport to the environment from the high-bay area volume, and employing the postulates for accident scenarios outlined above, it is felt that results of source-term evaluations will be appropriately conservative, if not bounding, and hence will be appropriate for the purposes of inclusion in the ANS ER.

It is expected that inclusion of mechanistic core-melt progression modeling will considerably reduce the source terms predicted with the MELCOR model described above because of various natural and designed retention and entrapment processes and fixtures. Such a capability is also called for to provide best-estimate information critical to the Level-2 PRA and accident management. It is thus planned that modeling and simulation efforts will be initiated during FY 1992. Results of this effort, along with impacts on MELCOR source-term predictions, will be reported in next year's progress report.

In addition to the MELCOR model for source-term evaluation, efforts have also been initiated to develop a MACCS code model for the prediction of off-site dose consequences. MACCS input will include effects of site meteorology, population density, emergency preparation, and MELCOR source-term output. Results of this effort will be reported in next year's progress report.

# PUBLICATIONS FY 1991

# 5


D. J. Alexander, "Materials for Cold Neutron Sources: Cryogenic and Irradiation Effects," *International Workshop on Cold Neutron Sources*, Los Alamos Natl. Lab., LA-12146-C, VC-413 (August 1991).

R. C. Birtcher, M. H. Mueller, and J. W. Richardson, "Neutron Irradiated Uranium Silicides Studied by Neutron Diffraction and Rietveld Analysis," *Materials Research Society*, Boston, Massachusetts, November 1990.

R. S. Booth et al., *Plant Design Requirements, Rev. 2*, ORNL/TM-11625 (August 1991).

R. R. Fullwood, *Large LOCA Assessment of an Early Preconceptual Design for the Advanced Neutron Source Reactor*, ORNL/M-1064 (March 1991).

M. L. Gildner, *ANS Project Quality Assurance Plan*, ORNL/TM-11446/R1 (August 1991).

A. N. Goland, *Review of the Advanced Neutron Source (ANS) Materials Irradiation Facilities*, CONF-901276 (March 1991).

R. M. Harrington, "Designing for Safety in the Conceptual Design of the ANS," *Nucl. Safety*, April 1991.

J. B. Hayter, "SANS Studies of Ferrofluids," *Neutron News* **1**, No. 4 (1990).

J. B. Hayter, "Status of the Advanced Neutron Source," p. 75 in *Proceedings XI International Conference on Advanced Neutron Sources*, KEK, 1991.

J. B. Hayter, "Determination of Structures in Ferrofluids by Small-Angle Neutron Scattering," *J. Chem. Soc. Faraday Trans.* **87**, 403 (1991).

J. B. Hayter, "Advanced Neutron Source—The User's Perspective," *Trans. Am. Nuc. Soc.* **62**, 139–40, TANSAO 62 1-722, ISSN: 0003-018X (November 1990).

M. Ibn-Khayat, J. March-Leuba, and H. L. Dodds, "On-Line Thermal Power Estimation for Control and Protection of the Advanced Neutron Source Reactor," Trans. *Am. Nuc. Soc.* **62**, 564–65, TANSAO 62 1-722, ISSN: 0003-018X (November 1990).

B. S. Maxon, R. Miller, and G. R. McNutt, "Practical Application of Passive Safety Features for the Advanced Neutron Source Cooling System," *Trans. Am. Nuc. Soc.* **62**, 379–80, TANSAO 62 1-722, ISSN: 0003-018X (November 1990).

M. R. McBee, ed., *ANS News Source, No. 2, October 1990* (newsletter), ORNL/M-1313 (November 1990).

B. W. Patton and R. P. Taleyarkhan, "Thermal-Hydraulic Response of ANS Containment During Hypothetical Severe Accidents," *Proceedings of the 1991 Summer Annual American Nuclear Society Conference*, Orlando, Florida, June 1991.

R. E. Pawel et al., "The Corrosion of 6061 Aluminum under Heat Transfer Conditions in the ANS Corrosion Test Loop," *Oxid. Met.* **36**, Nos. 1/2 (1991).

F. J. Peretz, et al., *Plant Design Requirements, Rev. 1*, ORNL/TM-11625 (April 1991).

F. J. Peretz, "Advanced Neutron Source—The Designer's Perspective," *Trans. Am. Nuc. Soc.* **62**, 138–39, TANSAO 62 1-722, ISSN: 0003-018X (November 1990).

R. T. Primm III, "Fabrication Constraints Applied to the Reactor Physics Design of the Advanced Neutron Source," *Trans. Am. Nucl. Soc.* **63**, 443–45 (June 1991).

S. Raman and J. B. Hayter, "The Advanced Neutron Source," p. 923 in *Proceedings Seventh International Conference on Capture Gamma-Ray Spectroscopy* **238**, AIP Conference Proceedings, 1991.

E. L. Redmond II and J. M. Ryskamp, "Monte Carlo Methods, Models, and Applications to the Advanced Neutron Source," *Nucl. Tech.* **95** (September 1991).

G. J. Russell (LANL) and C. D. West (ORNL), comps., *Proceedings of the International Workshop on Cold Neutron Sources*, Los Alamos Natl. Lab., August 1991.

J. M. Ryskamp, D. L. Selby, and C. D. Fletcher, "Reactivity Studies on the Advanced Neutron Source Preconceptual Reactor Design," *Proceedings of the Topical Meeting on the Safety, Status, and Future of Non-Commercial Reactors and Irradiation Facilities*, Vol. I, 337, Boise, Idaho, October 1990.

J. M. Ryskamp, D. L. Selby, and R. T. Primm III, "Reactor Design of the Advanced Neutron Source," *Nucl. Tech.* **93**, 330 (March 1991).

D. L. Selby, R. M. Harrington, and F. J. Peretz, "The Advanced Neutron Source Project Progress Report," ORNL-6656 (February 1991).

R. C. Thayer, E. L. Redmond II, and J. M. Ryskamp, "A Monte Carlo Method of Evaluating Heterogeneous Effects in Plate-Fueled Reactors," *Trans. Am. Nucl. Soc.* **63**, 445 (June 1991).

C. D. West, "An Overview of the Planned Advanced Neutron Source Facility," *Proceedings of International Conference on Neutron Scattering*, Bombay, India, January 1991.

C. D. West, ed., *IGORR News, Issue No. 2, July 1991* (newsletter).

# REFERENCES


1. J. F. Briesmeister, ed., *MCNP—A General Monte Carlo Code for Neutron and Photon Transport*, LA-7396-M, Rev. 2, Los Alamos Natl. Lab., 1986.

2. J. Rest and G. L. Hofman, "Mechanistic Interpretation of an Observed Rate Dependence of Low Temperature Swelling of Irradiated Uranium Silicide Dispersion Fuels," *Proceedings of the 15th ASTM Symposium on Effects of Irradiation on Materials*, Nashville, Tenn., June 17–21, 1990.

3. B. H. Montgomery, R. E. Pawel, and G. L. Yoder, "The Advanced Neutron Source Test Loop Facility," *Trans. Am. Nuc. Soc.* **57**, 300 (1988).

4. D. L. Selby, R. M. Harrington, and F. J. Peretz, *Advanced Neutron Source (ANS) Project Annual Report (April 1987–March 1988)*, ORNL/TM-10860, Martin Marietta Energy Systems, Inc., Oak Ridge Natl. Lab., February 1989.

5. D. L. Selby, R. M. Harrington, and F. J. Peretz, *Advanced Neutron Source (ANS) Project Progress Report*, ORNL-6574, Martin Marietta Energy Systems, Inc., Oak Ridge Natl. Lab., April 1990.

6. D. L. Selby, R. M. Harrington, and F. J. Peretz, *Advanced Neutron Source (ANS) Project Progress Report*, ORNL-6656, Martin Marietta Energy Systems, Inc., Oak Ridge Natl. Lab., February 1991.

7. R. E. Pawel et al., "Fuel Cladding Corrosion Studies for the Advanced Neutron Source," *Trans. Am. Nuc. Soc.* **61**, 388 (1990).

8. R. E. Pawel et al., *The Development of a Preliminary Correlation of Data on Oxide Growth on 6061 Aluminum under ANS Thermal-Hydraulic Conditions*, ORNL/TM-11517, Martin Marietta Energy Systems, Inc., Oak Ridge Natl. Lab., June 1990.

9. R. E. Pawel et al., "The Corrosion of 6061 Aluminum under Heat Transfer Conditions in the ANS Corrosion Test Loop," *Oxid. Met.* **36** (1/2), 175 (1991).

10. J. C. Griess et al., *Effect of Heat Flux on the Corrosion of Aluminum by Water. Part III. Final Report on Tests Relative to the High-Flux Isotope Reactor*, ORNL-3230, Martin Marietta Energy Systems, Inc., Oak Ridge Natl. Lab., December 1961.

11. J. C. Griess, H. C. Savage, and J. L. English, *Effect of Heat Flux on the Corrosion of Aluminum by Water. Part IV. Tests Relative to the Advanced Test Reactor and Correlation with Previous Results*, ORNL-3541, Martin Marietta Energy Systems, Inc., Oak Ridge Natl. Lab., February 1964.

12. W. K. Sartory, *Analysis of Hydraulic Instability of ANS Involute Fuel Plates*, ORNL/TM-11580, Martin Marietta Energy Systems, Inc., Oak Ridge Natl. Lab., November 1991.

13. W. F. Swinson and G. T. Yahr, "Dynamic Pressure Approach to Analysis of Reactor Fuel Plate Stability," *Trans. Am. Nuc. Soc.* **61**, 390, June 1990.

14. J. H. Schemel, *ASTM Manual on Zirconium and Hafnium*, ASTM STP 639, p. 33 (1977).

15. W. D. Wilkinson and W. F. Murphy, *Nuclear Reactor Metallurgy*, D. Van Nostrand, p. 312 (1958).

16. G. J. Salvggio et al., *Properties of a Hafnium Control Rod After Exposure During Three Seed Lives in PWR Core 1*, Bettis Atomic Power Laboratory Report, WAPD-TM-457, p. 10, June 1965.

17. R. A. Livingston, *ATR Hafnium Fluence Limits*, TRTSB-ATR-093, Rev. 1, EG&G Idaho, Inc., September 6, 1984.

18. J. D. Durney and D. W. Croucher, "Replacement of Core Components in the Advanced Reactor," *Proceedings of the International Symposium on Research Reactor Safety, Operations, and Modifications*, pp. 421–431, Chalk River, Ont., Canada, October 1989.

19. O. W. Hermann and R. M. Westfall, "Scale—A Modular Code System for Performing Standardized Computer Analyses for Licensing Evaluation," Book II, *NUREG/CR-0200*, Vol. 2, ORNL/NUREG/CSD-2/R1, December 1984.

20. T. R. England, R. Wilczynski, and N. L. Whittemore, *CINDER-7: An Interim Report for Users*, LA-5885-MS, Los Alamos Natl. Lab., 1975.

21. W. B. Wilson et al., *DKPOWR: A Code for Calculating Decay Power, Energy, Activity, and $\beta + \gamma$ Spectra in LWR Fuel Using Fission Pulse Sanctions*, LA-UR-85-157, Los Alamos Natl. Lab., 1985.

22. *Advanced Neutron Source Plant Design Requirements*, ORNL/TM-11625, Martin Marietta Energy Systems, Inc., Oak Ridge Natl. Lab., August 1991.

23. *IEEE Guide to the Collection and Presentation of Electrical, Electronic, Sensing Component, and Mechanical Hardware Reliability Data for Nuclear Power Generating Stations*, ANSI/IEEE Standard 500-1984, The IEEE, Inc., New York, December 13, 1983.

24. M. Siman-Tov et al., "Thermal-Hydraulic Correlations for the Advanced Neutron Source Reactor Fuel Element Design and Analysis," *Proceedings of the 1991 ASME Winter Annual Meeting*, Atlanta, December 1991.

25. 10 CFR 50

26. U.S. Nuclear Regulatory Commission, *Standard Review Plan for the Review of Safety Analysis Reports for Nuclear Power Plants*, NUREG-0800 (June 1987).

27. R. P. Taleyarkhan, *Core Melt Progression and Fission Product Release Considerations for the Advanced Neutron Source Reactor at ORNL*, ORNL/TM-12022, Martin Marietta Energy Systems, Inc., Oak Ridge Natl. Lab., to be published.

28. R. P. Taleyarkhan, "Analysis and Modeling of Fission Product Release from Uranium-Aluminum Plate-Type Reactor Fuels," *Proceedings of the International Topical Meeting on the Safety, Status, and Future of Non-Commercial Reactors and Irradiation Facilities*, Boise, Idaho, October 1990.

## INTERNAL DISTRIBUTION

1. C. W. Alexander
2. D. J. Alexander
3. R. G. Alsmiller
4. J. L. Anderson
5. B. R. Appleton
6. J. W. Baker
7. R. E. Battle
8. R. M. Beckers
9. R. S. Booth
10. W. W. Bowman
11. R. A. Brown
12. G. J. Bunick
13–14. J. H. Campbell
15. R. M. Canon
16. N. C. J. Chen
17. R. D. Cheverton
18. K. K. Chipley
19. J. E. Cleaves
20. J. T. Cleveland
21. G. L. Copeland
22. B. L. Corbett
23. W. G. Craddick
24. B. Damiano
25. J. R. Dixon
26. H. L. Dodds
27. F. F. Dyer
28. W. W. Engle
29. S. R. Ervin
30. D. K. Felde
31. R. E. Fenstermaker
32. G. F. Flanagan
33. C. P. Frew
34. R. K. Genung
35–36. M. L. Gildner
37. R. W. Glass
38. H. A. Glovier
39. F. J. Graziano
40. J. E. Hardy
41–42. R. M. Harrington
43–44. J. B. Hayter
45. W. R. Hendrich
46. D. R. Hicks
47. R. W. Hobbs
48. M. Z. Ibn-Khayat
49. D. T. Ingersoll
50–51. J. A. Johnson
52. R. L. Johnson
53. J. E. Jones, Jr.
54. H. T. Kerr
55. R. A. Lillie
56. M. A. Linn
57. A. W. Longest
58. C. R. Luttrell
59. M. F. Marchbanks
60–61. J. A. March-Leuba
62–63. B. S. Maxon
64. L. N. McCold
65. M. T. McFee
66. T. J. McManamy
67. G. S. McNeilly
68. G. R. McNutt
69. P. E. Melroy
70–71. B. H. Montgomery
72. R. M. Moon
73. D. G. Morris
74. J. A. Mullens
75. J. A. Murray
76. R. K. Nanstad
77. T. F. Orlin
78. F. S. Patton
79. R. E. Pawel
80–81. F. J. Peretz
82. R. T. Primm, III
83. C. C. Queen
84. S. Raman
85. J. S. Rayside
86. J. B. Richard
87. A. E. Ruggles
88. T. L. Ryan
89. W. K. Sartory
90–91. D. L. Selby
92. H. B. Shapira
93. W. D. Shults
94. M. Siman-Tov
95. K. D. St. Onge
96. J. O. Stiegler

97. W. F. Swinson
98. R. P. Taleyarkhan
99–100. P. B. Thompson
101. K. R. Thoms
102. A. W. Trivelpiece
103. D. B. Trauger
104. B. D. Warnick
105–106. C. D. West
107. J. L. Westbrook
108. B. A. Worley
109. G. T. Yahr
110. G. L. Yoder
111. A. Zucker
112. ORNL Patent Office
113. Central Research Library
114. Document Reference Section
115. [illegible]-12 Technical Library
116–117. Laboratory Records Department
118. Laboratory Records (RC)

## EXTERNAL DISTRIBUTION

119. A. Adams, U.S. Nuclear Regulatory Commission, MS-10-0-21, Washington, DC 20555
120. R. Avery, Argonne National Laboratory, 9700 S. Cass Avenue, Argonne, IL 60439
121. R. Awan, Division of Energy Research Reactors, Office of Nuclear Energy, Department of Energy, NE-473, Washington, DC 20585
122. P. Ageron, Institut Laue Langevin, 156X 38042, Grenoble Cedex, France
123. J. Ahlf, Joint Research Center, Institute for Advanced Materials, 1755 ZG Petten, P.O. Box 2, The Netherlands
124. P. Armbruster, Institut Laue Langevin, 156X 38042, Grenoble Cedex, France
125. T. Asaoka, Deputy Director General, Tokai Research Establishment, Japan Atomic Energy Research Institute, Tokai-mura, Naka-gun, Ibaraki-ken, Tokyo 319-11, Japan
126. J. Axe, Brookhaven National Laboratory, Building 510A, Upton, NY 19973
127. A. Axmann, Hahn-Meitner Institute Berlin, N3, Glienicker Str. 100, D-1000 Berlin 39, Germany
128. F. Bates, Department of Chemical Engineering and Material Science, University of Minnesota, 151 Amundson Hall, 421 Washington Avenue, SE, Minneapolis, MN 55455
129. G. S. Bauer, Paul Scherrer Institute, CH-5234 Villigen, Switzerland
130. J. M. Baugnet, Nuclear Services Program, S.C.K./C.E.N., Boeretang 200, B2400 Mol, Belgium
131. R. C. Birtcher, Argonne National Laboratory, 9700 S. Cass Avenue, Argonne, IL 60439
132. K. Böning, Fakultät für Physik E21, Technische Universität München, D-8046 Garching, West Germany
133. P. Breant, CEN Saclay, SPS ORPHEE, 91191 Gif-sur-Yvette Cedex, France
134. R. Burns, Gilbert/Commonwealth, Inc., GH2-3597, P.O. Box 1498, Reading, PA 19603-1498
135. H. A. Capote, Burns & Roe, 800 Kinderkamack Road, Oradell, NJ 07649
136. G. K. Carlough, DRS Hundley Kling Gmitter, Architects-Planners, One Gateway Center, Pittsburgh, PA 15222
137. D. Chung, Division of Energy Research Reactors, Office of Nuclear Energy, Department of Energy, NE-473, Washington, DC 20585
138. K. N. Clausen, RISO National Laboratory, Physics Department Postbox 49, DK-4000 Roskilde, Denmark
139. M. F. Collins, Nuclear Reactor, McMaster University, Hamilton, Ontario, L8S 4K1, Canada
140. R. A. Cordani, Babcock & Wilcox, Mt. Athens Road, P.O. Box 785, Lynchburg, VA 24505-0785
141. R. S. Denning, Sr. Research Leader for Nuclear Safety, Battelle Memorial Institute, 505 King Avenue, Columbus, OH 43201

142. C. Desandre, Technicatome, Centre d'Etudes Nucleaires de Saclay, BP17, 92291 Gif-sur-Yvette Cedex, France
143. Y. Fanjas MTR Fuel Technical and Project Manager, CERCA, BP 1114, 26104 Romans Cedex, France
144. B. Farnoux, CEN Saclay, Laboratoire Leon Brillouin, 91191 Gif-sur-Yvette Cedex, France
145. C. D. Fletcher, Idaho National Engineering Laboratory, P.O. Box 1625, Idaho Falls, ID 83415
146. R. R. Fullwood, Building 130, Brookhaven National Laboratory, Upton, NY 11973
147. W. R. Gambill, Route 5, Box 220, Clinton, TN 37716
148. W. Glaser, Fakultät für Physik, Technische Universität München, D-8046 Garching, West Germany
149. H. N. Goldstein, Gilbert/Commonwealth, Inc., P.O. Box 1498, Reading, PA 19603-1498
150. B. Gupta, AECL Technologies, 1155 Metcalfe Street, 8th Floor, Montreal, Quebec, H3B 2V6 Canada
151. O. K. Harling, Massachusetts Institute of Technology, 77 Massachusetts Avenue, Cambridge, MA 02139
152. J. R. Harries, Embassy of Australia, 1601 Massachusetts Avenue, NW, Washington, DC 20036
153. D. Henderson, University of Wisconsin - Madison, Nuclear Engineering and Engineering Physics Department, 1500 Johnson Drive, Madison, WI 53706
154. A. F. Henry, Professor, Department of Nuclear Engineering, Massachusetts Institute of Technology, 77 Massachusetts Avenue, Cambridge, MA 02139
155. G. L. Hofman, Argonne National Laboratory, 9700 S. Cass Avenue, Argonne, IL 60439
156. R. A. Hunter, Director, Office of Facilities, Fuel Cycle/Test Programs, Department of Energy, NE-47, Washington, DC 20585
157. L. C. Ianniello, Acting Associate Director, Office of Basic Energy Sciences, Office of Energy Research, U.S. Department of Energy, ER-10, Washington, DC 20585
158. M. Iizumi, Japan Atomic Energy Research Institute, Tokai Research Establishment, Tokai-mura, Naka-gun, Ibaraki-ken 319-11, Tokyo, Japan
159. S. N. Jahshan, Idaho National Engineering Laboratory, P.O. Box 1625, Idaho Falls, ID 83415
160. K. Kanda, Research Reactor Institute, Kyoto University, Kumatori-cho, Sennan-gun, Osaka 590-04, Japan
161. T. L. Kerlin, University of Tennessee, College of Engineering, 315 Pasqua Engineering Building, Knoxville, TN 37996-2300
162. J. D. Kling, DRS/Hundley Kling Gmitter, Architects/Planners, One Gateway Center, Pittsburgh, PA 15222
163. N. Kunitomi, Osaka University, 1-1 Yamadaoka, Fuita-Shi, Osaka 565, Japan
164. W. Krull, GKSS, Postfach 1160, D-2054 Geesthacht, Germany
165. R. T. Lahey, Jr., Department of Nuclear Engineering and Engineering Physics, Jonsson Engineering Center, Rensselaer Polytechnic Institute, Troy, NY 12180-3590
166. J. A. Lake, Manager, Nuclear Engineering and Reactor Design, Idaho National Engineering Laboratory, P.O. Box 1625, Idaho Falls, ID 83415
167. D. Lancaster, Georgia Institute of Technology, Atlanta, GA 30332
168. A. G. Lee, Atomic Energy of Canada, Ltd., Whiteshell Nuclear Research Establishment, Pinawa, Manitoba, ROE 1L0, Canada
169. L. LeSage, Argonne National Laboratory, 9700 South Cass Avenue, Argonne, IL 60439
170. R. F. Lidstone, Atomic Energy of Canada, Ltd., Whiteshell Nuclear Research Establishment, Pinawa, Manitoba, ROE 1L0, Canada

171. W. F. Manning, U.S. Department of Energy, Oak Ridge Field Office, FEDC, MS-8218, P.O. Box 2009, Oak Ridge, TN 37831-8218
172. S. Matsuura, Japan Atomic Energy Research Institute, Tokai Research Establishment, Tokai-mura, Naka-gun, Ibaraki-ken 319-11, Tokyo, Japan
173. J. McKibben, Research Reactor Facility, University of Missouri-Columbia, Research Park, Columbia, MO 65211
174. W. E. Meek, Project Manager, Gilbert/Commonwealth, Inc., P.O. Box 1498, Reading, PA 19603-1498
175. A. I. Miller, Manager Chemical Engineering, AECL Research, Chalk River Laboratory, Ontario, K0J 1J0, Canada
176. R. Miller, Lucas Heights Research Laboratories, New Illawarra Road, Lucas Heights, NSW, Australia
177. H. Nakata, Project Engineering Division, Department of JMTR Project, Japan Atomic Energy Research Institute, Oarai Ibaraki-ken, Tokyo, Japan
178. W. T. Oosterhuis, Materials Science Division, Office of Basic Energy Sciences, Office of Energy Research, U.S. Department of Energy, ER-132, Washington, DC 20585
179. S. L. Ostrow, Ebasco Services, Inc., 2 World Trade Center, 89th Floor, New York, NY 10048
180. Y. V. Petrov, Leningrad Nuclear Physics Institute, Academy of Science of USSR, 188350 Gatchina, Leningrad District, USSR
181. H. J. Prask, National Institute for Standards & Technology, A-106 Reactor, Gaithersburg, MD 20899
182. H. E. Preble, Babcock & Wilcox, Inc., P.O. Box 785, Lynchburg, VA 24505-0785
183. T. J. Raney, Ebasco Services, Inc., 2 World Trade Center, 89th Floor, New York, NY 10048
184. J. Rest, Argonne National Laboratory, 9700 S. Cass Avenue, Argonne, IL 60439
185. H.-J. Roegler, Interatom GmbH, Friedrich-Ebert-Strasse, D-5060 Bergish-Gladbach 1, West Germany
186. M. Rowe, National Institute of Standards and Technology, Washington, DC 20234
187. J. J. Rush, National Bureau of Standards, Washington, DC 20234
188. J. M. Ryskamp, Idaho National Engineering Laboratory, P.O. Box 1625, Idaho Falls, ID 83415
189. T. Shibata, Japan Atomic Energy Research Institute, Kinki University, Kowakae, Higashi-Osaka, Osaka 577, Japan
190. P. J. Shipper, Gilbert/Commonwealth, Inc., P.O. Box 1498, Reading, PA 19603-1498
191. E. Shirai, Department of Research Reactor Operations, Japan Atomic Energy Research Institute, Tokai-mura, Naka-gun, Ibaraki-ken 319-11, Tokyo, Japan
192. J. B. Slater, Atomic Energy of Canada, Ltd., Research Company, Chalk River Nuclear Laboratories, Chalk River, Ontario, K0J 1J0, Canada
193. J. L. Snelgrove, Coordinator, Engineering Applications, RERTR Program, Argonne National Laboratory, 9700 S. Cass Avenue, Argonne, IL 60439
194. E. Steichele, Physik-Department, der Technische Universität München, D 8046 Garching München, West Germany
195. P. T. Talarico, Gilbert/Commonwealth, Inc., P.O. Box 1498, Reading, PA 19603-1498
196. T. G. Theofanous, Theofanous & Company, Inc., 857 Sea Ranch Drive, Santa Barbara, CA 93109
197. I. L. Thomas, Director, Materials Science Division, Office of Energy Research, U.S. Department of Energy, ER-13, Washington, DC 20585
198. H. R. Thresh, Argonne National Laboratory, 9700 S. Cass Avenue, Argonne, IL 60439
199. V. Tschinkel, Landers & Parsons, 310 W. College Ave., Tallahasse, FL 32301

200. M. Utsuro, Research Reactor Institute, Kyoto University, Kumatori-cho, Sennan-gun, Osaka 590-04, Japan
201. J. Verdier, Centre d'Etudes Nucleaires, SBT, 85X, 38041 Grenoble Cedex, France
202. R. P. Wadkins, Idaho National Engineering Laboratory, P.O. Box 1625, Idaho Falls, ID 84515
203. J. M. Warren, Gilbert/Commonwealth, Inc., 1055 Commerce Park Drive, Suite 200, Oak Ridge, TN 37830
204. C. A. Wemple, Idaho National Engineering Laboratory, P.O. Box 1625, Idaho Falls, ID 83415
205. R. F. Wichman, Atomic Energy of Canada Ltd., Research Company, Chalk River Nuclear Laboratories, Chalk River, Ontario, K0J 1J0, Canada
206. T. C. Wiencek, Argonne National Laboratory, 9700 S. Cass Avenue, Argonne, IL 60439
207. D. K. Wilfert, Energy Programs, U.S. Department of Energy, Oak Ridge Field Office, FEDC, MS-8218, P.O. Box 2009, Oak Ridge, TN 37831-8218
208. R. J. Willard, U.S. Department of Energy, Oak Ridge Field Office, P.O. Box 2001, Oak Ridge, TN 37831-2001
209. R. Wilson, Department of Physics, Harvard University, Cambridge, MA 02138
210. P. W. Winkler, Air Products and Chemicals, Inc., 7201 Hamilton Boulevard, Allentown, PA 18195-1501
211. H. G. Wood, III, Associate Professor, Department of Mechanical and Aerospace Engineering, Thornton Hall, University of Virginia, Charlottesville, VA 22901
212. Office of Assistant Manager for Energy Research and Development, U.S. Department of Energy, Oak Ridge Field Office, P.O. Box 2001, Oak Ridge, TN 37831-2001
213. Office of Honors and Awards, P. King, P.O. Box 2008, Building 2518, MS-6324, Oak Ridge, TN 37831-6324
214–226. Office of Scientific and Technical Information, P.O. Box 62, Oak Ridge, TN 37831

# END

# DATE FILMED

3/24/92